High-frequency EEG activity

from different perspectives

UMC Utrecht Brain Center

Anne H. Mooij

High-frequency EEG activity

from different perspectives

Anne H. Mooij

High-frequency EEG activity from different perspectives

ISBN: 978-90-393-7236-4

Cover design and layout: Anne Mooij and Loes Kema
Cover image: Piet Mondriaan: Avond; De rode boom. A high-resolution image of this painting was provided by the Kunstmuseum Den Haag
Printing: GVO drukkers & vormgevers B.V.

The research presented in this thesis and the printing of this thesis were supported by the Dutch Epilepsy Foundation (grant number 15-09).

High-frequency EEG activity
from different perspectives

Hoogfrequente EEG activiteit
vanuit verschillende perspectieven
(met een samenvatting in het Nederlands)

Proefschrift

ter verkrijging van de graad van doctor aan de Universiteit Utrecht
op gezag van de rector magnificus, prof. dr. H.R.B.M. Kummeling,
ingevolge het besluit van het college voor promoties
in het openbaar te verdedigen op

dinsdag 14 januari 2020 des middags te 2.30 uur

door

Anne Henriëtte Mooij

geboren op 11 november 1983
te Middelburg

Promotoren:
Prof. dr. K.P.J. Braun
Prof. dr. J. Gotman

Copromotoren:
Dr. G.J.M. Zijlmans
Dr. G.J.M. Huiskamp

Table of contents

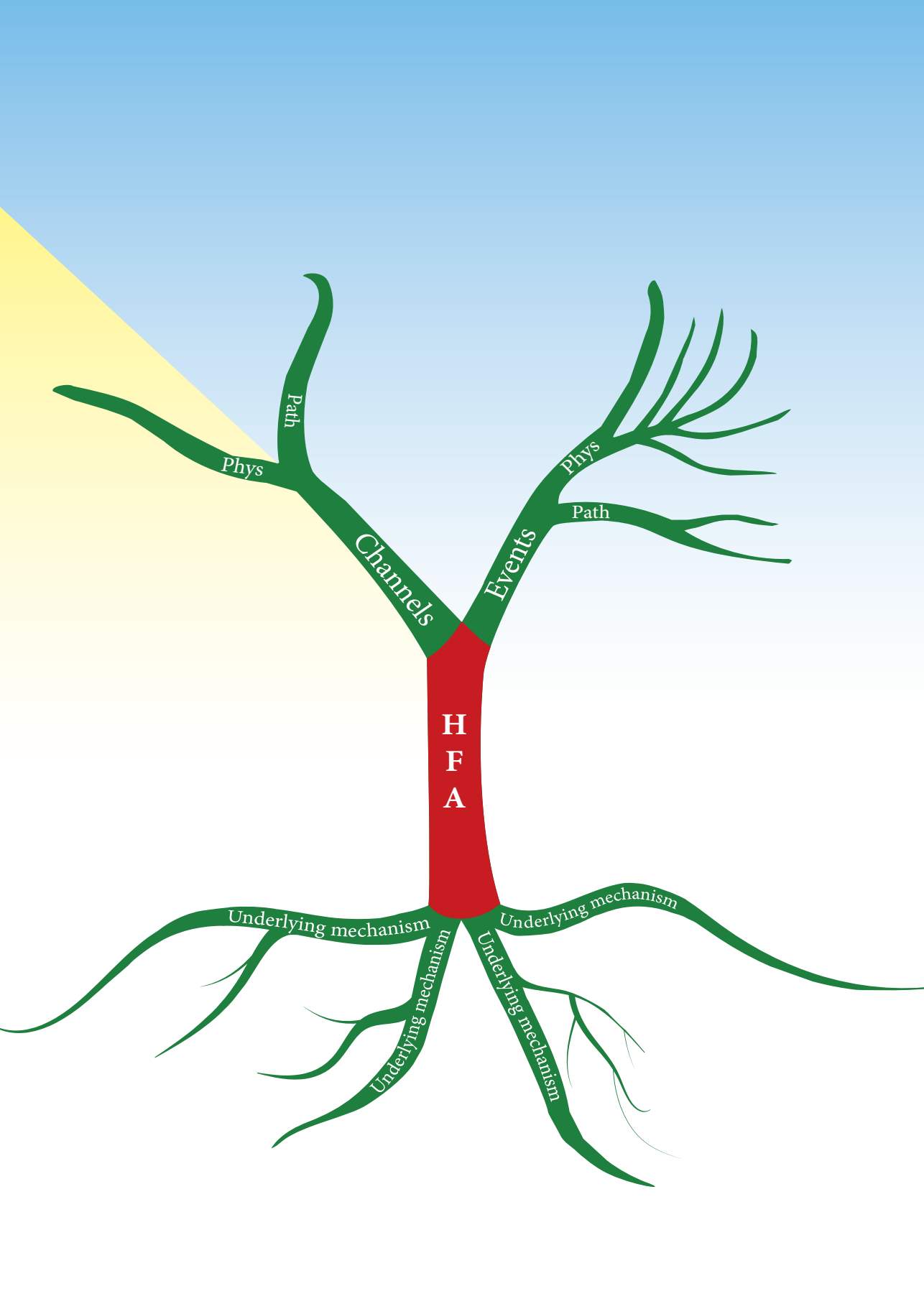
H
F
A
Channels
Phys
Path
Events
Phys
Path
Underlying mechanism
Underlying mechanism
Underlying mechanism
Underlying mechanism

Chapter 1
General introduction

Introducing electroencephalography (EEG)

Electrical activity generated by brain tissue can be recorded with EEG. The first report of a human EEG recording appeared in 1929. In this report, Hans Berger described the alpha (α) rhythm: sinusoidal activity with a frequency of 8-13 Hz that was recorded over the occipital regions when the eyes were closed and that was attenuated when eyes were open. Following Berger's example, other EEG rhythms were also named with Greek letters: the beta (β, 14-40 Hz), gamma (γ, > 40 Hz), delta (δ, < 4 Hz) and theta (θ, 4-7.5 Hz) rhythms, which occur during different levels of vigilance: delta activity during sleep, theta activity during drowsiness, alpha activity during quiet wakefulness with eyes closed, beta activity during wakefulness, perhaps especially when there is a need to maintain the 'current' behavioral state, and gamma activity during higher cognitive processes. All of these EEG rhythms can occur in the EEG of healthy people. The normal background activity of the EEG of adults during wakefulness usually consists of low amplitude activity, mostly of alpha and beta frequencies, without the rhythmicity of the alpha activity that occurs when eyes are closed.[1]

In clinical practice, EEG is most often used to help diagnose epilepsy. Epilepsy is "a disorder of the brain characterized by an enduring predisposition to generate epileptic seizures" that affects about 70 million people worldwide.[2,3] The first report of ictal EEG activity (i.e., recorded during a seizure) appeared in 1935.[1] Epileptic activity can also be recorded in between seizures (i.e., interictal), in the form of interictal epileptiform discharges (IEDs): spikes, with durations of 20-70 ms, or sharp waves, with durations of 70-200 ms. Both types of IEDs are multiphasic transients that stand out from the background EEG signal. The background activity itself can also change in people with epilepsy, for example when it becomes asymmetrical or when slow activity predominates in a recording during normal wakefulness.[1]

High-frequency EEG activity

All of the above mentioned rhythms and transients occur in the frequency range of 0-70 Hz. From the ninety-nineties, technical advances in EEG equipment made it possible to study activity above 70 Hz as well. This so-called high-frequency activity (HFA) includes different types of activity. This thesis is about activity in the high-gamma band and high-frequency oscillations (HFOs) (Figure 1.1).

The frequency borders of activity in the high-gamma band differ between studies but are usually between 60 Hz and 200 Hz.[4] In this thesis, we studied high-gamma band activity of 65-95 Hz. HFOs can be divided in ripples and fast ripples, which have also been defined using varying frequency bands.[5] In this thesis, ripples are oscillations with frequencies between 80 and 250 Hz, and fast ripples have frequencies between 250 and 500 Hz.

HFA can be physiological or pathological. Physiological high-gamma activity can, for example, be recorded during motor or language tasks.[4] Physiological

ripples have been related to cognitive functioning such as memory consolidation and retrieval.[6,7] Pathological HFOs are considered biomarkers for epilepsy.[8,9]

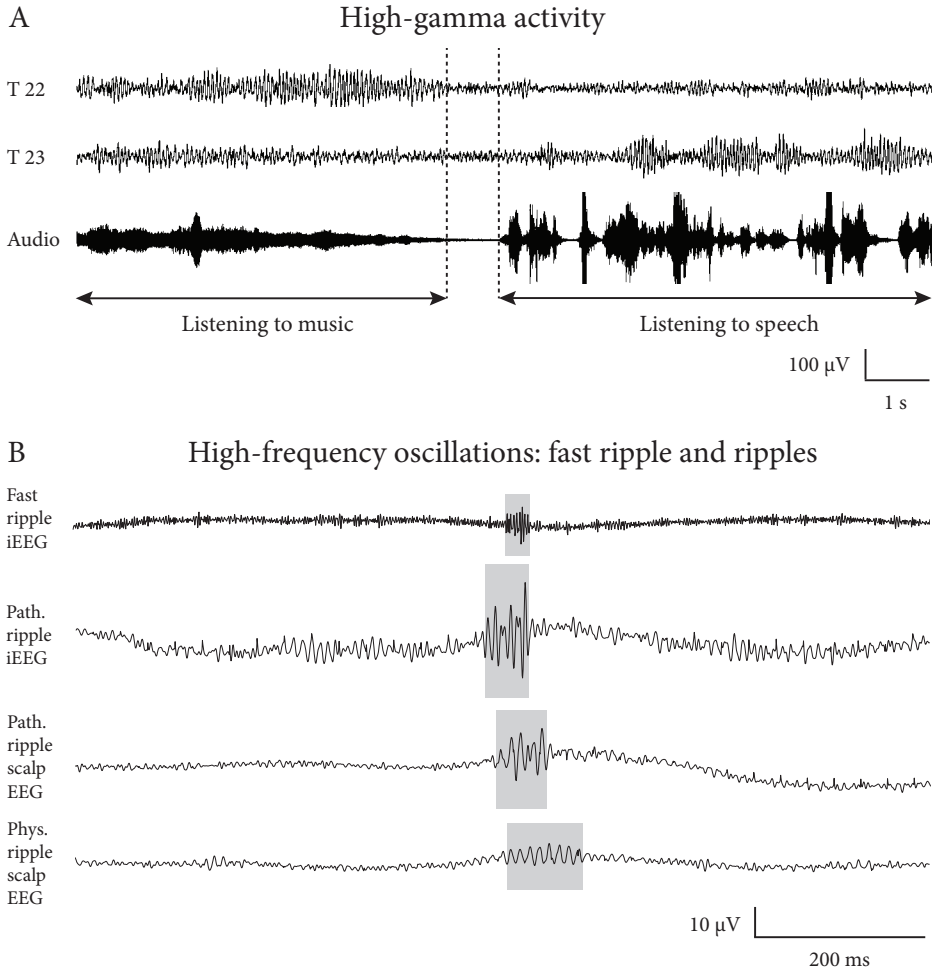

Figure 1.1 A) High-gamma activity recorded with electrocorticography (ECoG) in two electrodes placed on the superior temporal (T) gyrus while listening to music or speech. Note that electrode T22 shows high-gamma activity during the music fragment, while T23 shows high-gamma activity during the speech fragment. B) From upper line to lower line: example of a fast ripple and a pathological (path.) ripple recorded with intracerebral (i)EEG, and a pathological and a physiological (phys.) ripple recorded with scalp EEG. The trace containing a fast ripple was filtered between 250 and 500 Hz, traces containing ripples were filtered between 80 and 250 Hz. The two iEEG examples come from the same patient, the two scalp-EEG recorded ripples come from two other patients.

Different perspectives

In this thesis, I view physiological and pathological HFA from different perspectives. The different perspectives reflect three main topics:
1. Clinical utility versus basic neurophysiology;
2. Recording method: invasive versus non-invasive;
3. Wake versus sleep.

1. Clinical utility

Twenty-five to 40% of people with epilepsy do not sufficiently respond to treatment with anti-epileptic drugs.[10] Some of these patients are candidates for epilepsy surgery.[11] Before epilepsy surgery can be performed, two things must become clear: what does the neurosurgeon need to preserve, and what needs to be removed?

What to preserve?

The goal is to preserve areas that would result in major functional deficits if they were removed, so called eloquent areas. Examples of eloquent areas are primary motor areas and language areas. I will focus on locating language areas, as this is the topic investigated in this thesis.

The gold standard for locating language areas is electrocortical stimulation mapping (ESM).[12] ESM is based on the idea that local electrical stimulation of the cortex results in a temporary block of function, which is thought to reflect the functional deficit that would occur if the stimulated area would be removed.[12] Thus, if stimulating certain brain areas results in temporary loss of language function, the conclusion is drawn that these areas should be spared in order to preserve language function after surgery. ESM has for many years been the gold standard for language mapping, but it has several disadvantages: the electrical currents can induce seizures or after-discharges, which often hinder further functional mapping, and ESM is a time consuming (usually over one hour) and demanding procedure that requires good patient cooperation.[12,13] Researchers have therefore sought alternative methods for localizing eloquent areas. High-gamma seems to be task-specific activity, i.e. it is thought to reflect activity of neurons involved in a task.[4] Locating high-gamma activity that is induced by a language task ('high-gamma mapping') could therefore be an alternative method for locating language areas. High-gamma mapping is not the only potential alternative, however: functional magnetic resonance imaging (fMRI) is also used, but this is not a topic in this thesis.

Several research groups have evaluated the performance of high-gamma mapping by comparing its outcome to the results of ESM. Almost twenty years since the first report of auditory task-induced high-gamma activity[14] there are many papers claiming promising results, but it is still not clear if high-gamma mapping can safely be used as alternative for ESM.

What to remove?
The goal of epilepsy surgery is to remove the epileptogenic zone. The epileptogenic zone is defined as the "area that needs to be removed to obtain seizure freedom".[15] The hypothesis for the presumed epileptogenic zone is based on the results of several diagnostic techniques, including MRI and other imaging techniques,[15] but in this thesis, I focus on interictal epileptic events that are recorded with EEG. Identifying the area containing interictal spikes was already a standard step in the pre-surgical work-up of patients with epilepsy. Pathological ripples and fast ripples are now increasingly recognized as additional biomarkers for the epileptogenic zone.[16,17] However, identifying spikes and HFOs in an electrographic recording, either with automatic detectors or by visually scanning the recording, can be challenging.[18]

2. Recording method: invasive versus non-invasive
Invasive recording techniques measure brain activity from inside the skull. Two invasive techniques are used in the studies reported in this thesis: electrocorticography (ECoG), during which electrodes are placed directly on the cortical surface, and intracerebral EEG (iEEG, or stereo EEG (sEEG)), where electrodes are inserted within the brain tissue. These invasive methods are applied when eloquent areas or the presumed epileptogenic zone need to be located with a better spatial resolution than non-invasive recording techniques can provide. For example, locating deep sources of epilepsy, such as in mesiotemporal lobe epilepsy, often requires recording with depth electrodes.

Such invasive methods were for several years thought to be the only option for recording HFOs. The history of recording HFOs started with intracerebral microelectrodes in rodents (1992) and humans (1999).[19,20] The next step was the discovery that recording HFOs with intracranial macroelectrodes was also possible (2006).[21,22] Against all expectations, it turned out that pathological ripples (2010) and even fast ripples (2018) could also be recorded with scalp EEG.[23–25] This discovery meant that HFO research was no longer limited to people who are expected to undergo surgery. HFOs could now be studied in all people with epilepsy, and even in people without epilepsy.

3. Wake versus sleep
The EEG recorded during sleep displays several characteristics that are not present in an EEG recorded during wakefulness and that therefore require further introduction. Normal sleep consists of cycles in which different sleep stages alternate. These sleep stages are non-rapid eye movement (NREM) sleep stage 1, 2, and 3, and rapid eye movement (REM) sleep. NREM 1 is characterized by a slowing of the background activity compared to wakefulness, attenuation of alpha activity even though eyes are closed, and appearance of sleep-specific transients such as vertex waves, (which are sharply contoured events with a duration of less than 0.5 seconds), and in children, hypnagogic hypersynchrony, (which are bursts of 3-3.5 Hz waves with high amplitude and widespread distribution). NREM 2

is characterized by the appearance of the sleep-specific transients K-complexes (multiphasic, large EEG transients with durations of more than 0.5 seconds) and sleep spindles (trains of 11-16 Hz oscillations with durations of more than 0.5 seconds). NREM 3 is also called slow-wave sleep, because its most prominent feature is the occurrence of waves with large amplitude and frequencies of 0.5-2 Hz. Finally, the characteristic feature of REM sleep is the occurrence of an electrical signal that is generated by rapid movements of the eyes. None of the above-mentioned sleep-specific transients is present in REM sleep, and the background EEG is more like the background activity that is recorded during wakefulness than the background activity recorded during other sleep stages.[26]

HFOs can occur during sleep. For example, the previously mentioned physiological ripples that are involved in the process of memory consolidation occur during sleep.[27] Sleep is also interesting for both clinical and research purposes because it influences the occurrence of epileptiform EEG activity, such as epileptic spikes and pathological HFOs. Both types of pathological EEG transients were reported to occur more often during NREM sleep.[28]

Outline of this thesis

The above introduction shows that HFA is thought to be relevant for the understanding of cognitive functioning and, in the case of pathological HFOs, as biomarkers for epilepsy. The aim of this thesis is to further explore the different aspects of these relatively new EEG phenomena by viewing them from the perspectives that were mentioned earlier.

The outline of this thesis is depicted in Figure 1.2. Parts 1 and 2, represented in the main left branch in Figure 1.2, both aim at clinical utility and describe findings from invasive EEG recordings. The results are presented on the level of ECoG or iEEG channels. The contents of parts 3 and 4, represented in the main right branch, are of basic neurophysiological interest, make use of scalp EEG recordings, and provide more detailed information on the events that were recorded. The third perspective is not equally divided over the parts of the thesis: parts 2, 3 and 4 describe findings from sleep recordings, while part 1 is about recordings made while patients were awake.

Each main branch is divided in two subbranches. One subbranch of the left main branch concerns *physiological activity* (chapters 2 and 3). Specifically, part 1, chapter 2, provides an example of a study in which high-gamma mapping results are compared to electrocortical stimulation mapping (ESM) results, including a discussion of some of the reasons why the clinical utility of high-gamma mapping is difficult to establish from the available literature. Part 1, chapter 3, discusses one of the difficulties that occur when comparing high-gamma language mapping studies in more depth.

The second subbranch of the left main branch is about *pathological activity*: in part 2, chapter 4, we develop a method that identifies channels with interictal

spikes and HFOs without the need to visually mark or detect these events. In this way, we attempt to obtain the information about the hypothesized epileptogenic zone that these biomarkers can provide, but without the challenges that can arise when trying to identify individual events.

The right main branch is also divided in *physiological* and *pathological* subbranches. In part 3, chapter 5, we report that physiological ripples are also visible on scalp EEG and we provide detailed characteristics of these events. In part 3, chapter 6, we explore the sleep-related properties of these physiological ripples: their occurrence across different (NREM) sleep stages and their co-occurrence with sleep-specific transients.

Finally, in part 4, chapter 7, we compare ripples that co-occur with two sharp EEG transients with similar appearance but different neurophysiological significance: physiological vertex waves and pathological spikes or sharp waves. We compare, for the first time in scalp EEG, characteristics of physiological and pathological ripples.

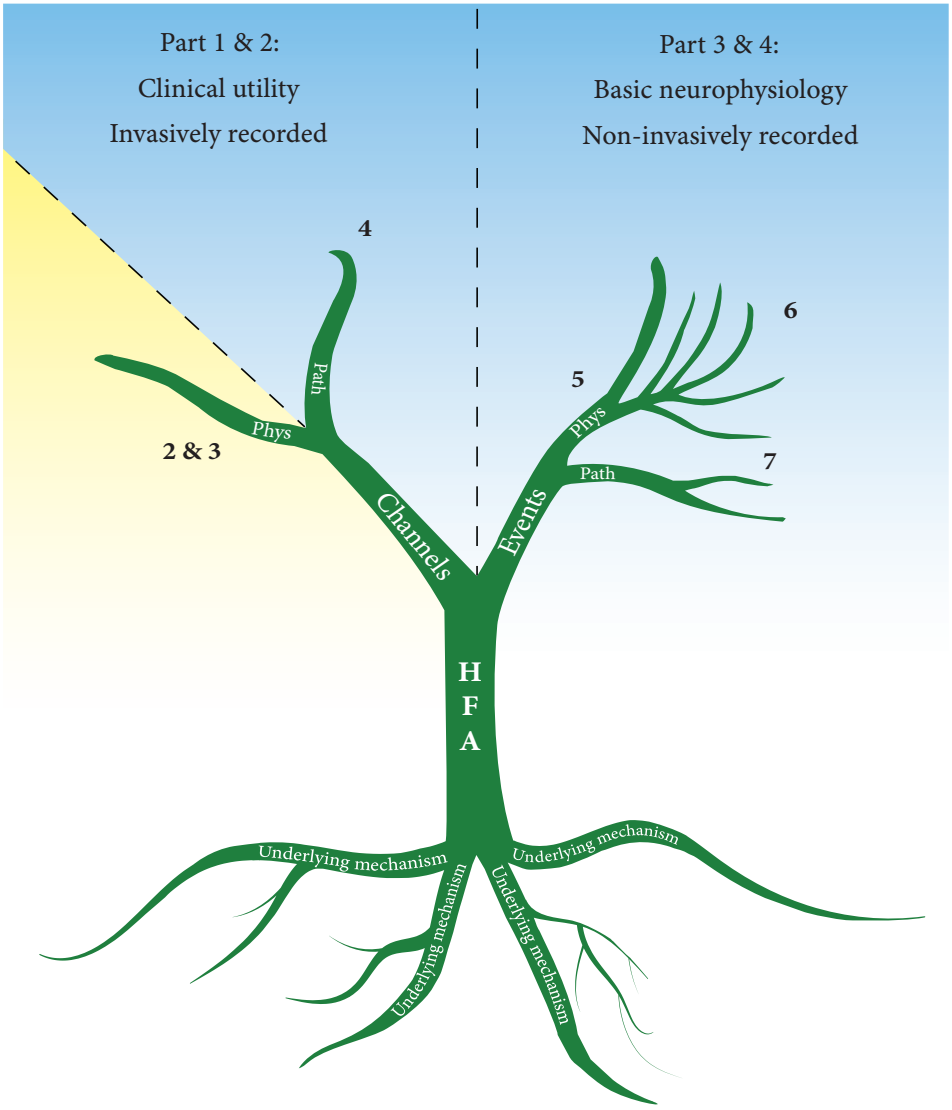

Figure 1.2 Outline of this thesis in different parts and chapters The tree depicts how each of the chapters represents some kind of high-frequency EEG activity. In both parts that aim at clinical utility (parts 1 and 2), the results are presented on the level of ECoG or iEEG channels without detailed information on the high-gamma activity (part 1) or interictal epileptic events (part 2) that were recorded in those channels. In contrast, the basic neurophysiology parts (parts 3 and 4) zoom in on characteristics of physiological (phys) and pathological (path) ripples. The yellow background represents wakefulness, blue represents sleep.

Part 1

Electrocorticographic high-gamma language mapping

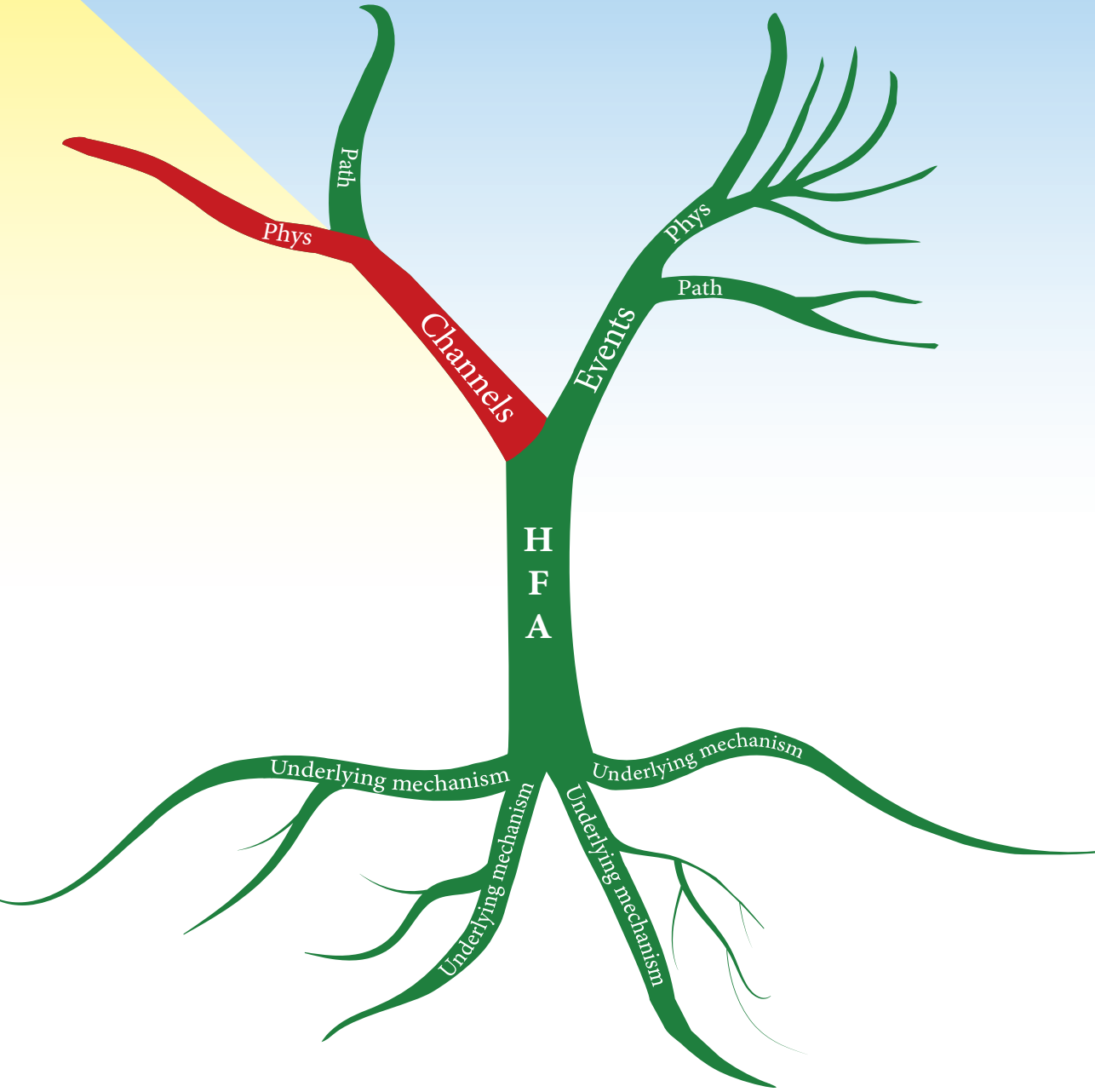

Chapter 2

Electrocorticographic language mapping with a listening task consisting of alternating speech and music phrases

Anne H. Mooij
Geertjan J.M. Huiskamp
Peter H. Gosselaar
Cyrille H. Ferrier

Clinical Neurophysiology 2016; 127:1113-1119

Abstract

Objective
Electrocorticographic (ECoG) mapping of high-gamma activity induced by language tasks has been proposed as a more patient friendly alternative for electrocortical stimulation mapping (ESM), the gold standard in pre-surgical language mapping of epilepsy patients. However, ECoG mapping often reveals more language areas than considered critical with ESM. We investigated if critical language areas can be identified with a listening task consisting of speech and music phrases.

Methods
Nine patients with implanted subdural grid electrodes listened to an audio fragment in which music and speech alternated. We analyzed ECoG power in the 65–95 Hz band and obtained task-related activity patterns in electrodes over language areas. We compared the spatial distribution of sites that discriminated between listening to speech and music to ESM results using sensitivity and specificity calculations.

Results
Our listening task of alternating speech and music phrases had a low sensitivity (0.32) but a high specificity (0.95).

Conclusions
The high specificity indicates that this test does indeed point to areas that are critical to language processing.

Significance
Our test cannot replace ESM, but this short and simple task can give a reliable indication where to find critical language areas, better than ECoG mapping using language tasks alone.

Introduction

The goal in epilepsy surgery is to remove enough epileptogenic tissue to achieve seizure freedom without damaging important functional areas, such as language areas. The current gold standard for localizing critical language areas is electrocortical stimulation mapping (ESM). In ESM, the function in small patches of cortex is determined by running short trains of electrical pulses to temporarily impair execution of an appropriate task. The electrical currents are delivered directly to the cortex, either intraoperatively or through implanted subdural grid- or depth electrodes in pre-surgical monitoring.[12]

A disadvantage of ESM is that the electrical currents can induce seizures or afterdischarges, which often hinder further functional mapping. Moreover, ESM mapping of language is a time consuming (usually over one hour) and demanding procedure that requires good patient cooperation.[12,29,30]

It is therefore important to seek an alternative for ESM. Several studies investigated if recording language task related activity changes with electrocorticography (ECoG) is useful for localizing language areas. Different frequency bands have been explored, but most studies have focused on high-gamma activity between 50 and 200 Hz.[29–36] Activity in this frequency band appears to be the best indicator of task-related cortical activation,[4,14,29–31,34] because timing and spatial localization of high-gamma seem more specific to timing and localization of functional brain activation than task related alpha and beta activity.[4]

So far, ECoG high-gamma analyses were not good enough to replace ESM, because they often reveal more language sites than found with ESM.[29–33,35,36] A suggested explanation for the observed mismatch is that ECoG measures of high-gamma localize regions that are involved in language processing, whereas ESM is thought to only localize critical language areas.[29,33,36]

The aim or our study was to improve the localization of critical language areas with ECoG measures of high-gamma by contrasting language with music. Music and speech are both universal and we can all recognize the many similarities between music and speech. They are streams of sound with a rule-based structure, consisting of basic elements (tones and phonemes) that are built in higher hierarchical structures (melodies and songs, words and sentences).[37,38] But despite the many similarities, there are also obvious differences between speech and music. The contrast between these similar, but at the same time different stimuli might help to 'downsize' the ECoG language sites. This idea resembles the recommendation by Wu et al. who suggest that to discriminate between critical and non-critical language areas, patients need to perform multiple tasks and be presented with stimuli of different modalities.[29]

In this study we addressed the following research question: Can the accuracy of localizing critical language areas with ECoG measures of high-gamma compared to ESM be improved by looking at differences in activity patterns induced by listening to speech and music?

To answer this question, we analyzed the magnitude of high-gamma (65–95 Hz) activity as recorded with implanted subdural grid electrodes while patients listened to an audio fragment in which speech and music phrases alternated. We determined the spatial distribution of the activity patterns in perisylvian electrodes and compared ECoG to ESM by calculating sensitivity and specificity.

Methods

Participants

We retrospectively included nine patients from a consecutive series who fulfilled the following inclusion criteria: 1) patients had medically refractory epilepsy and underwent subdural grid implantation in the University Medical Center in Utrecht for pre-surgical evaluation. Subdural grid electrodes covered completely or partly our region of interest (see Data analysis); 2 patients had undergone ESM language mapping and had listened to the audio fragment during their stay at the intensive epilepsy monitoring unit; 3) patients had confirmed left sided or bilateral language localization with fMRI and/or Wada test. There were no in- or exclusion criteria regarding type of lesion or epilepsy. Approval of the institutional ethical committee was not indicated because of the retrospective character of this study, provided that data were coded and handled anonymously. All patients gave written, informed consent for analyzing and publishing the data.

Listening task

The audio fragment consisted of a story about the life and work of the composer Joseph Haydn (1732–1809). Phrases of speech (male storytelling voice) and music (four different versions of Haydn's 'Die sieben letzten Worte unseres Erlösers am Kreuze') alternated four times. Duration of the speech phrases was 8–43.5–19–29 s (total: 99.5 s), duration of music phrases 27–27.5–28–29 (total: 111.5 s, orchestral, string quartet, piano, and choir respectively). The task was presented using regular PC speakers adjusted to a comfortable hearing level. Patients were relaxed, and were not in an ictal or post-ictal state. They were only asked to listen; the clinical neurophysiologist who performed the test checked that they had paid attention to the test by asking some general questions afterwards.

Data acquisition and pre-processing

ECoG was performed using silastic grids and strips consisting of several rows of eight platinum electrodes, with 2.3 mm exposed diameter per electrode and an inter-electrode distance of 1 cm center to center (Ad-Tech, Racine, USA). Location of electrodes was determined using photographs taken during the implantation and with a post-implantation CT-scan. This CT was co-registered to a pre-implantation 3D MRI. Electrode artifacts were visualized on a rendering of the cortical surface using dedicated software.[39]

Simultaneous ECoG and audio/video was recorded with a 128 channel video-EEG system (Micromed, Treviso, Italy) at a sampling frequency of 512 Hz using a hardware band-pass filter of 0.15–134.4 Hz. Unipolar data were recorded using an extracranial reference electrode (G2) placed on the mastoid contralateral to the implantation. If common artifacts were present, the data were re-referenced to a relatively silent intracranial electrode overlying another silastic grid, remote from the region that was analyzed. In case of remaining artifacts we chose an average reference.

The sound of the audio fragment was extracted from the audio of the video-EEG and added as an additional EEG channel for synchronization of the music and speech onsets. Given the video frame rate of 25 frames/s, this resulted in a synchronization accuracy of at best 40 ms. An example of the synchronized audio and ECoG channels is given in Supplementary Figure 2.1.

Data analysis

For the purpose of our analysis we defined a region of interest in the perisylvian area where language function is expected: the superior temporal gyrus, the frontal operculum, the lower pre- and postcentral gyri and the supramarginal gyrus. Grid placement was guided by clinical information; not every patient had complete electrode coverage of this region of interest.

Data were analyzed using Matlab 7-2012a (The Mathworks, Inc., Massachusetts) and signal processing functions from the EEGlab Matlab suite.[40] We first performed a time-frequency decomposition on the data with a resolution of 100 ms and 2 Hz using Morlet wavelets. Then, we integrated magnitude over the frequency range of interest, 65–95 Hz, thus constructing time signals of gamma band activity in each electrode of the region of interest.

Functional data might show temporal correlations between some electrodes, related to the test, while at the same time uncorrelated interictal epileptic activity can be expected to be present in the same electrodes. Instead of excluding channels with interictal epileptic activity, we applied principal component analysis (PCA) to separate such different components. After removing the baseline in each electrode, PCA resulted in N components, N being equal to the number of electrodes in the region of interest. Of these N components, we considered the first M components that explained 95% of the total variance. Each of these components was specified by its time-function, which represented an uncorrelated time signal present in the data, and a spatial weight distribution that represented how much it was present in the different electrodes.

The PCA time-functions were separated in epochs of the duration of the eight speech and music phrases. We determined if there was significant discrimination between listening to speech and music for each component by comparing the four speech and music epochs using a two-sided t-test ($\alpha < 0.05$) with unequal variances. Next, we used false discovery rate correction to correct for the number M of components considered.

For the components that remained significant after correction we inspected the corresponding time functions to find out if there was more activity during speech compared to music or the other way around. Spatial weight distributions were then used to mark electrodes with dominant contributions as ECoG mapping results (ECoG+ 'speech' or 'music' electrodes). ECoG results were analyzed (by AM) without knowledge of ESM results.

ESM procedure

Electrical stimulation consisted of brief currents (5–10 mA, 50 Hz, 200 μs width, monophasic pulses) that were delivered for several seconds (4–7 s) using an IRES 600 surgical electrical stimulator (Micromed, Treviso, Italy) to pairs of adjacent electrodes. Not all electrodes in the region of interest were stimulated in all patients and the clinical stimulation protocol could include electrodes outside our region of interest that were not included in the analysis.

During stimulation, patients were asked to name pictures that were presented to them on a computer screen. All patients were cooperative and had sufficient baseline language function. Intensity of the stimulations was individually tailored, maximizing the effect size and minimizing the occurrence of afterdischarges. Language errors consisted of speech disruption, naming mistakes or hesitations and were noted by a clinical neurophysiologist and neuropsychologist. If language errors occurred when delivering brief currents to a specific pair of electrodes more than once, that pair of electrodes was labelled 'ESM+'. Otherwise the pair of electrodes was labelled 'ESM−'.

Calculation of sensitivity and specificity

To calculate sensitivity and specificity (Table 2.1), results of ECoG mapping and ESM needed to be compared per electrode. However, as described above, ESM is done in pairs of electrodes. If an electrode pair is considered ESM+, this means that the language area that is temporarily blocked by the electrical pulses could be localized in the cortex between the two electrodes, in the cortex directly underneath one of the electrodes, or in the cortex underneath both electrodes. Because it is unknown what the exact localization is, we decided to use both a 'mild' and a 'strict' rule to translate the pairwise ESM results to ESM results per electrode. With the mild rule, every electrode that is involved in at least one ESM+ electrode pair is considered ESM+. For an electrode to be considered ESM+ with the strict rule, it needed to be involved in two or more ESM+ electrode pairs.

Table 2.1 Calculation of sensitivity and specificity

	ESM+	ESM−
ECoG+	a (TP)	b (FP)
ECoG−	c (FN)	d (TN)

TP: true positive; FP: false positive; FN: false negative; TN: true negative;
Sensitivity: a/(a+c) or TP/(TP+FN); specificity: d/(d+b) or TN/(TN+FP).

Results

Participants

Patient characteristics are given in Table 2.2. All patients were Caucasian, with Dutch as their first language. Patients 6 and 9 had above average total IQ (111–120), patients 1, 3, and 4 had average total IQ (90–110), patients 2, 5, and 8 had below average total IQ (80–89) and patient 7 had total IQ 75. Besides epilepsy and the histopathological diagnosis listed in Table 2.2, patients did not suffer from another active brain disease. All patients underwent preoperative 3T MRI. Patients were admitted between 2009 and 2014, neurological examination at admittance was unremarkable in all patients. They usually stayed at the intensive epilepsy monitoring unit for about a week; antiepileptic drugs were tapered during this period depending on the necessity of occurrence of seizures.

The listening task was performed whenever it fitted in the clinical schedule and when it suited the patient. The listening task and ESM could be done on different days or on the same day; when on the same day, the listening task could be scheduled before or after ESM, or even between ESM sessions. There were no adverse events of the listening task, most patients reported that they had enjoyed it. Afterdischarges during ESM occurred in all patients whereas spontaneous or evoked seizures occurred in some, as is common during this clinical procedure.

Results of analysis of ECoG data

t-test and false discovery rate correction

t-tests yielded one or more significant principal components in all patients. After false discovery rate correction, one component remained significant in patients 1, 3, 4, 5, 7 and 8. Patient 2 had two remaining components, whereas patients 6 and 9 had no significant components remaining.

PCA time functions

The time functions of the components that remained significant after false discovery rate correction showed a clearly visible pattern of higher activity during speech than music, or vice versa (Figure 2.1A).

Table 2.2 Patient characteristics

Patient	Gender	Age	MRI	Surgery	Pathology	Language: Wada	Language: fMRI
1	M	26	Tumor L frontocentral	Lesionectomy L frontal	Ganglioglioma	L	L
2	M	15	Normal	No operation	Not applicable	–	L
3	M	43	MTS L	L temporal lobectomy	MTS	L	L
4	M	45	Gliosis and cavernoma L temporal	Re-resection gliosis L inferior temporal	Gliosis, cavernoma	L	L
5	M	29	Focal gliosis L frontal	L frontal lobectomy	Posttraumatic gliosis	L	L
6	F	23	Cortical dysplasia L temporal	L temporal lobectomy	mMCD and leptomeningeal glioneuronal heteropia	L	L
7	F	33	Cortical dysplasia L frontal	Corticectomy L frontal	FCD 2B	L	L
8	F	42	Subcortical heterotopia L parieto-occipital	L temporal lobectomy	FCD 1B	–	L
9	M	19	Normal	L temporal lobectomy	No abnormalities	L?	L?

fMRI and/or a Wada test clearly established presence of language function in the left hemisphere in all patients except patient 9, who probably had bilateral language representation. M = male, F = female, L = left, MTS = mesotemporal sclerosis, FCD = focal cortical dysplasia, mMCD = mild malformation of cortical development.

PCA weight distributions

The contribution of different electrodes to the activity pattern as shown in Figure 2.1A is depicted in a bar graph of the distribution of the normalized weight factors (Figure 2.1B). We only show the weight bars of the ten electrodes with the biggest contributions to the total weight.

The horizontal lines represent the threshold separating dominant (colored) and non-dominant (white) weights. This threshold was chosen to be the value for a uniform normalized weight distribution (i.e. the square root of 1 divided by the number of electrodes within our region of interest).

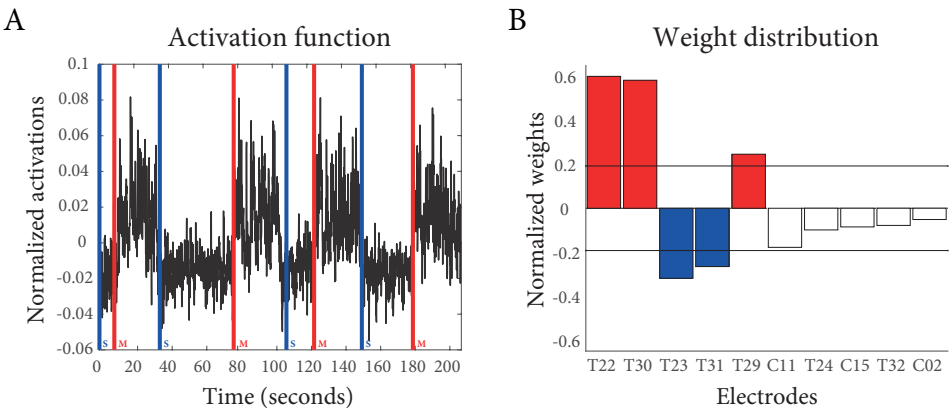

Figure 2.1 A) Example of a PCA time function. This is the time signal of the only component remaining significant after false discovery rate correction in patient 4. On the x-axis time in seconds, on the y-axis a normalized value indicating magnitude of gamma activity within the 65–95 Hz band. Blue and red vertical lines mark the onset of speech and music phrases, respectively. A pattern of higher activity during music than speech is clearly visible. B) PCA weight distribution. An example of a bar graph showing the distribution of weights. This weight distribution corresponds to the time function of Figure 2.1A. Ten electrodes with biggest weights are shown, with magnitude of weights decreasing from left to right. Horizontal lines: positive and negative threshold value assuming a uniform normalized distribution. Blue bar: dominant weight, 'speech' electrode, red bar: dominant weight, 'music' electrode, white bar: non-dominant weight. On the x-axis electrode labels, on the y-axis normalized weight values. (Electrode labels: T: Temporal, C: Central. The number in the label refers to its position on the grid.)

The sign of a weight determined the sign of the activity pattern present in that particular electrode. For example, the time function in Figure 2.1A shows higher activity during music than speech. Therefore, a positive weight indicates that in that particular electrode the power in the 65–95 Hz band was higher during music than speech. A negative weight indicates that there was higher power during speech than music. In Figure 2.1B, higher power during music is depicted with a red bar, higher power during speech with a blue bar.

Results of ECoG and ESM

Figure 2.2 shows the results of ECoG mapping and ESM for each patient. The electrodes with dominant weights (ECoG+ electrodes) were marked with a blue or red dot, blue again indicating higher activity during speech than music, and red representing the opposite activity pattern. Yellow lines connect pairs of electrodes that gave a speech disruption or arrest when electrical currents were delivered. Electrodes are considered ESM+ with the strict rule if there is more than one

yellow line connected to it. With the mild rule, one line suffices for the mark ESM+ electrode.

ECoG results on superior temporal gyrus (STG)
All patients had one or more ECoG+ electrodes on the STG, although the number of ECoG+ electrodes and the exact location differed per patient. Patient 2 and 4 had both 'speech' and 'music' electrodes, patient 1, 3, 5, 7, 8, and 9 had only 'speech', and patient 6 had only 'music' electrodes. There were in total 20 'speech' electrodes on the STG, versus eight 'music' electrodes (blue and red dots in Figure 2.2).

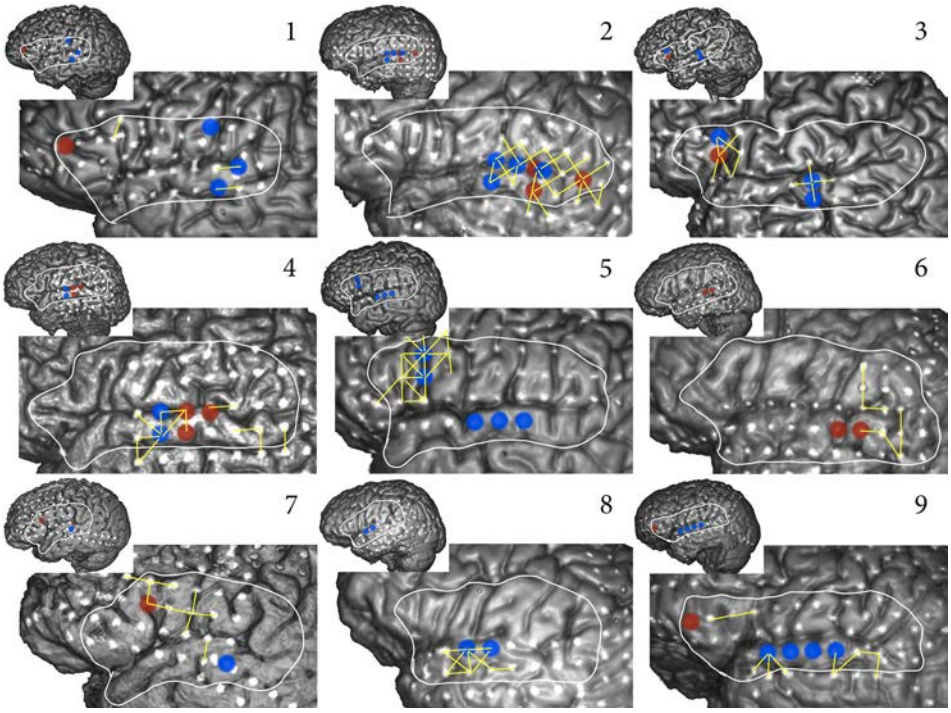

Figure 2.2 Results of ESM and ECoG. Results of each patient are shown; patient number can be found in the upper right corner. In the upper left corner a small picture of the surface of the left side of the brain. Region of interest is delineated with a white line. Below, we show an enlargement of this region of interest. White dots: grid electrodes; when covered with blue dot: 'speech' electrode; when covered with red dot: 'music' electrode. Yellow lines connect electrode pairs that resulted in speech disruption or arrest upon stimulation. Patients 6 and 9 had no significant component remaining after false discovery rate correction, but the activity pattern of the component with the smallest p-value still showed a very strong distinction between speech and music. We therefore decided to show these results as well.

ECoG results on inferior frontal gyrus (IFG)
Even though our test only involved passive listening, we found 'speech' electrodes on the IFG in patients 3 and 5, and 'music' electrodes in patients 1, 3, 7, and 9.

ECoG results outside STG or IFG
There was one ECoG+ electrode outside the STG and IFG, in patient 1. ESM revealed it was located in the motor-tongue area.

ESM results
The localization and extent of language areas as considered critical with ESM differed per patient (yellow lines in Figure 2.2). For example, ESM revealed a large circumscribed language area on the STG in patient 2, whereas patients 6, 7 and 9 had no clearly circumscribed language areas.

Comparison of ECoG and ESM
Table 2.3 shows the results of the comparison of ECoG with ESM. As can be seen in the second and third column, not all electrodes within the region of interest were used for the ESM procedure. Pictures showing which electrodes were used can be found in the Supplementary Figure 2.2. There was, for example, no ESM testing on the STG of patient 5, but there were three 'speech' electrodes. As we cannot know if these 'speech' electrodes are true or false positive results, they are not included in the sensitivity and specificity calculations.

Table 2.3 Results: sensitivity and specificity

Patient	Nr electr ROI	Nr electr ESM	Nr electr ESM+ mild	Nr electr ESM+ strict	Sensitivity mild	Sensitivity strict	Specificity mild	Specificity strict
1	42	28	4	0	0.33	–	0.95	0.89
2	32	27	16	12	0.38	0.50	1.00	1.00
3	31	27	11	5	0.36	0.60	1.00	0.95
4	27	17	11	5	0.45	0.60	1.00	0.83
5	35	14	8	7	0.25	0.29	1.00	1.00
6	36	36	9	5	0.11	0.00	0.96	0.94
7	29	26	10	4	0.10	0.25	0.94	0.95
8	16	16	7	6	0.29	0.33	1.00	1.00
9	32	27	8	4	0.25	0.25	0.84	0.83
Average	31	24	9	5	0.28	0.35	0.97	0.93
Average mild and strict			7		0.32		0.95	

Nr electr ROI = number of electrodes within region of interest.

Sensitivity
With the mild rule for translating pairwise ESM results to ESM results per electrode, sensitivity of the ECoG mapping varied between 0.10 and 0.45, with an average of 0.28. With the strict rule, sensitivity varied between 0.00 (patient 6) and 0.60, with an average of 0.35. The average of the sensitivity of the two rules was 0.32.

Specificity
With the mild rule, specificity varied between 0.84 and 1.00, with an average of 0.97; with the strict rule the specificity was 0.83–1.00, with an average of 0.93. The average specificity of the two rules was 0.95.

Discussion

Our listening task had a low sensitivity, but a high specificity. The high specificity indicates that this test does indeed point to areas that are critical rather than merely involved in language processing.

We are the first to study if discriminating between speech and music can contribute to localizing critical language areas in ECoG. Therefore, we cannot compare our results with studies with the same design. We can, however, compare our results with others studies seeking a way to minimize ESM by using ECoG measures of high-gamma as an alternative method for language mapping. The comparison with such studies, all using language-only tasks, is made in Table 2.4. We list per study the high-gamma frequency band that was studied, sensitivity and specificity, and finally the sensitivity and specificity of this study. It is important to mention again that ECoG results per electrode are in all these studies compared with ESM results of pairs of electrodes. Bauer et al. (2013) and Sinai et al. (2005) use a method that is comparable with our strict rule (method b in Table 2.4).[31,35] Results of Wu et al. (2010) are best comparable with outcome of our mild rule (method a).[29] Arya et al., 2015, Kojima et al., 2012, Miller et al., 2011, and Towle et al. (2008) use a different approach (method c): they determined if ESM+ electrode pairs contained ECoG+ electrodes.[30,33,34,36] For better comparison of our results with these studies, we also calculated sensitivity and specificity using this approach. The average sensitivity and specificity are listed in Table 2.4, results per patient can be found in Supplementary Table 2.1. Note that with this method, our average sensitivity increases substantially (0.58) but specificity decreases (0.79) (Table 2.4).

Table 2.4 shows that studies using the strict method also report poor sensitivity, but high specificity. The four studies using the different approach (method c) report higher sensitivity, but lower specificity. Our sensitivity is equally poor (method a and b), or lower (method c), but our specificity is highest with all three methods.

Table 2.4 Comparison of our results with other ECoG language mapping studies

Study	Frequency band (Hz)	Sensitivity	Specificity	This study (65–95 Hz)	
				Sens. (method)	Spec. (method)
Arya (2015)	70–116	0.89	0.64	0.58 (c)	0.79 (c)
Bauer (2013)	65–95	0.17[a]	0.83[a]	0.35 (b)	0.93 (b)
Kojima (2012)	50–120	0.91/0.83[b]	0.62/0.64[b]	0.58 (c)	0.79 (c)
Miller (2011)	76–200	0.89/0.74[c]	0.66/0.48[c]	0.58 (c)	0.79 (c)
Sinai (2005)	80–100	0.43	0.84	0.35 (b)	0.93 (b)
Towle (2008)	70–100	0.63	0.57	0.58 (c)	0.79 (c)
Wu (2010)	75–100	0.52[d]	0.69[d]	0.28 (a)	0.97 (a)

All studies in the first column compare ECoG measures obtained during language-only tasks with ESM.
Methods: (a) mild rule: ESM+ electrode if part of at least one ESM+ electrode pair; (b) strict rule: ESM+ electrode if part of two or more ESM+ electrode pairs; (c) ECoG+ electrode is part of ESM+ pair. Sens.: sensitivity. Spec.: specificity.
Superscripts:
[a] Results of listening versus rest condition, as this is probably the condition that is best comparable to the results of our listening task (other conditions: speaking versus rest, verb generation versus rest).
[b] Results of temporal and frontal areas, respectively.
[c] Results of noun reading and verb generation, respectively.
[d] Results of high-frequency band only (75–100 Hz) for localizing Broca's and Wernicke's area (with auditory cue).

Our results are in line with studies showing that music is processed in both classical language areas.[41–43] The same and other studies report bilateral activation by language and music, but with a relative specialization of the left STG for language and of the right STG for music processing.[14,38,43] Our finding that there were more 'speech' than 'music' electrodes on the left STG (20 versus 8) might reflect this proposed relative specialization for speech processing. We cannot speculate which particular aspects of speech and music are processed in the cortex underneath our 'speech' and 'music' electrodes, as our task involves listening to language and music as a whole.

Note that in our patients, areas considered critical for language can extend beyond the classical boundaries of Broca and Wernicke. Especially on the STG, the number and extent of ESM+ results varies from patient to patient. A probable explanation is that patients with chronic epilepsy often have altered functional anatomy.[12] Therefore, ESM results cannot be generalized to the healthy population when it comes to localization of language function.

Moreover, it is important to mention that different language tasks can be used for the ESM procedure. Picture naming, which was used in this study, is common, but there are other options, such as auditory naming tasks.[44] Such different approaches would have affected sensitivity and specificity values in our study.

A last point to mention is that ESM has some limitations. The test has never been fully validated, it is not clear exactly how much cortex is affected by stimulation, and results of the tests can be influenced by afterdischarges.[12]

Limitations

It can be seen as a limitation of this study that a non-unique choice has to be made in order to quantitatively compare ECoG results per electrode versus pair-wise ESM results. As discussed above, this is also true for other studies, and this hampers comparison between studies (see Table 2.4). We think that by taking the average value of both mild and strict rules, we come closest to sensitivity and specificity values that are uniquely defined.

Another limitation is the small number of patients and the incomplete coverage of our region of interest with grid electrodes. This is unavoidable, as ECoG is an invasive technique that can cause complications and the risk of complications increases with more extensive brain coverage. In the future, we hope to be able to perform a similar experiment in high-resolution scalp EEG or MEG, which allows a more extensive brain coverage and which would enable us to test both patients and healthy participants.

Conclusion

With our task of listening to alternating language and music phrases, we achieved our goal of localizing critical language areas with ECoG measures of high-gamma activity. Unfortunately, this paradigm suffers from low sensitivity. Our current language and music ECoG task can therefore not replace ESM for localizing critical language areas in the pre-surgical work-up of medically refractory epilepsy patients. Still, this short and simple listening task can be used to quickly get an indication where to expect critical language areas with ESM. Moreover, its undemanding nature makes it applicable in more patients, as it requires attention instead of cooperation.

Supplementary material

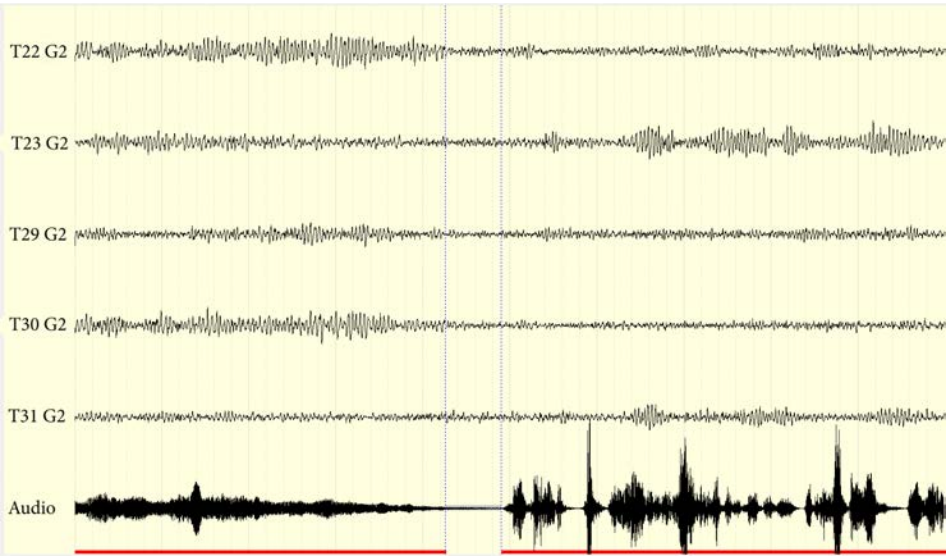

Supplementary Figure 2.1 Simultaneous ECoG traces and sound envelope for patient 4. Shown are, from top to bottom, electrodes T22, T23, T29, T30 and T31, and the synchronized soundtrack. ECoG data were band-pass filtered for the high-gamma band (65–95 Hz). Vertical scale (ECoG) is 50 μV/cm. Horizontal axis represents 10 s. Vertical dashed lines mark end of the first music fragment and start of the second speech fragment. Note gamma band activity during speech or music in the electrodes corresponding to those indicated in Figure 2.1B.

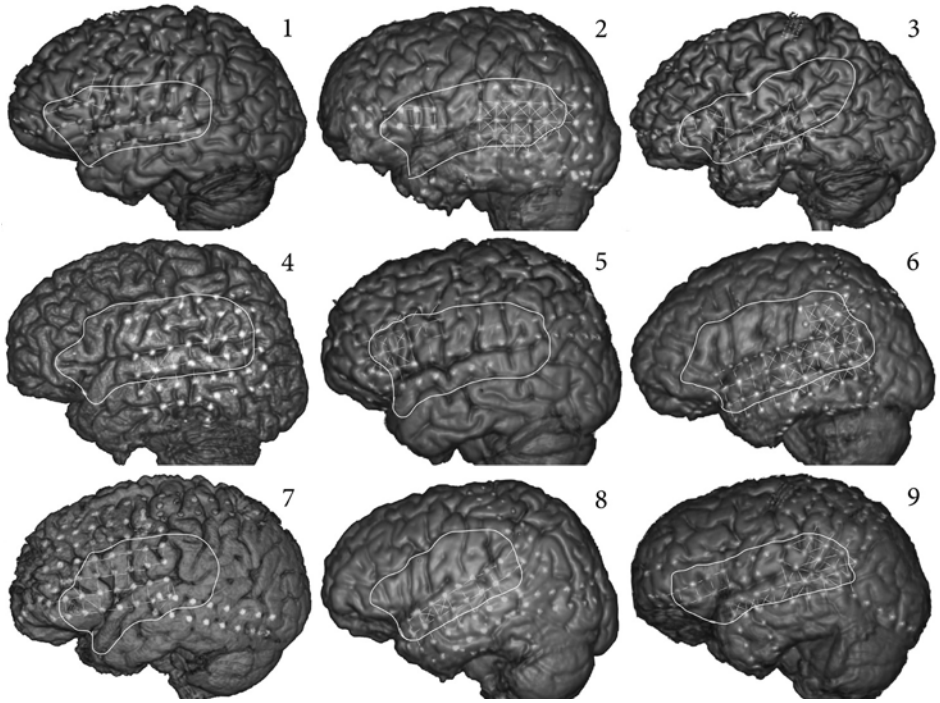

Supplementary Figure 2.2 ESM stimulation sites within region of interest for each patient. Patient number in upper right corner, region of interest delineated with white line. Grid electrodes are depicted as white dots. Electrode pairs that were used for the ESM procedure are connected by thin white lines.

Supplementary Table 2.1 Sensitivity and specificity calculated with method c

Patient	Nr ESM pairs	Nr ESM+ pairs	Sensitivity	Specificity
1	24	3	0.67	0.91
2	47	17	0.88	0.60
3	45	10	0.90	0.80
4	23	8	0.88	0.71
5	23	13	0.62	1.00
6	86	7	0.14	0.82
7	41	8	0.25	0.79
8	25	9	0.67	0.68
9	40	4	0.25	0.81
Average	39	9	0.58	0.79

Nr: number; ESM: electrocortical stimulation mapping

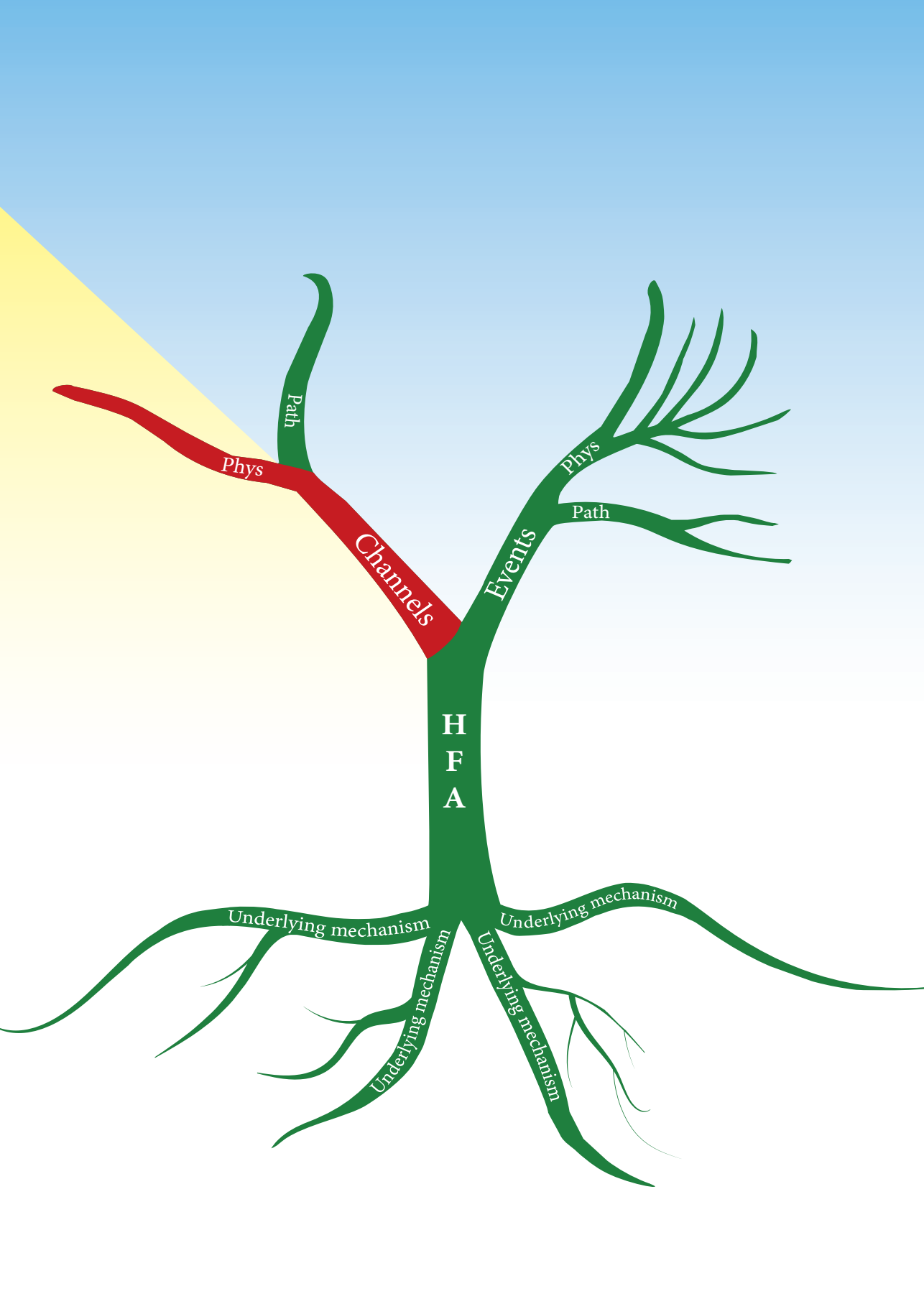
Path
Phys
Channels
Phys
Path
Events
H
F
A
Underlying mechanism
Underlying mechanism
Underlying mechanism
Underlying mechanism

Chapter 3

Electrocorticographic high-gamma language mapping: Mind the pitfalls of comparison with electrocortical stimulation

Anne H. Mooij
Laura C.M. Sterkman
Maeike Zijlmans
Geertjan J.M. Huiskamp

Epilepsy & Behavior 2018; 82:196-199

To the Editor

Several research groups have compared electrocorticographic (ECoG) high-gamma language mapping (HGM) to language mapping using electrocortical stimulation (ESM) as the gold standard. The aim of these studies was to evaluate the clinical utility of ECoG HGM. The conclusion of a recently published review by Arya et al. (2018),[45] which included a meta-analysis, was that ECoG HGM is a specific but not sensitive method for language localization when compared to ESM. The authors state that the value of ECoG HGM remains unclear because of heterogeneity in study designs. For example, studies use different language tasks, different ECoG HGM procedures, and different ESM protocols. The authors conclude that ECoG HGM can only become a potential alternative for ESM if uniform methods are used.

We would like to draw attention to another important issue that influences sensitivity and specificity outcomes when comparing ECoG HGM with ESM. Electrocortical stimulation is usually performed by supplying currents to neighboring electrode pairs. If such currents cause language errors or hesitations, the electrode pair is considered language positive (ESM + pair). However, it is unclear if the language area that is temporarily blocked by the electrical pulses is localized in the cortex between the two electrodes, in the cortex directly underneath one of the electrodes, or in the cortex underneath both electrodes. This uncertainty makes it difficult to compare ESM results with ECoG HGM results because ECoG HGM results are obtained per electrode. Arya et al. mention this issue briefly, but the different ways in which ESM and ECoG HGM results have been compared and the impact of each method on sensitivity and specificity were not addressed.

This letter discusses the papers included in the review by Arya et al.[30,31,33–36,46–53] and some additional papers that fulfilled the inclusion criterion of comparing language localization with ECoG HGM and ESM by calculating sensitivity and specificity.[29,54,55] We excluded studies if ESM was only performed to confirm ECoG HGM results.[56] In addition, we excluded a paper in which three out of four ECoG HGM sessions seem to have been performed while the patients were sedated.[57] Tables with patient characteristics suggested that two studies included the same three patients;[48,58] we excluded the one whose study aim was to answer a cognitive neuroscience question rather (or more) than a clinical research question.[58] Studies in which some, but not all, of the patients seemed to overlap with another study were not excluded.

The included studies contain four approaches for comparing ESM and ECoG HGM results, which are explained below and illustrated in Figure 3.1. Sensitivity is calculated as true positive (TP) divided by TP + false negative (FN). Specificity is calculated as true negative (TN) divided by TN + false positive (FP).

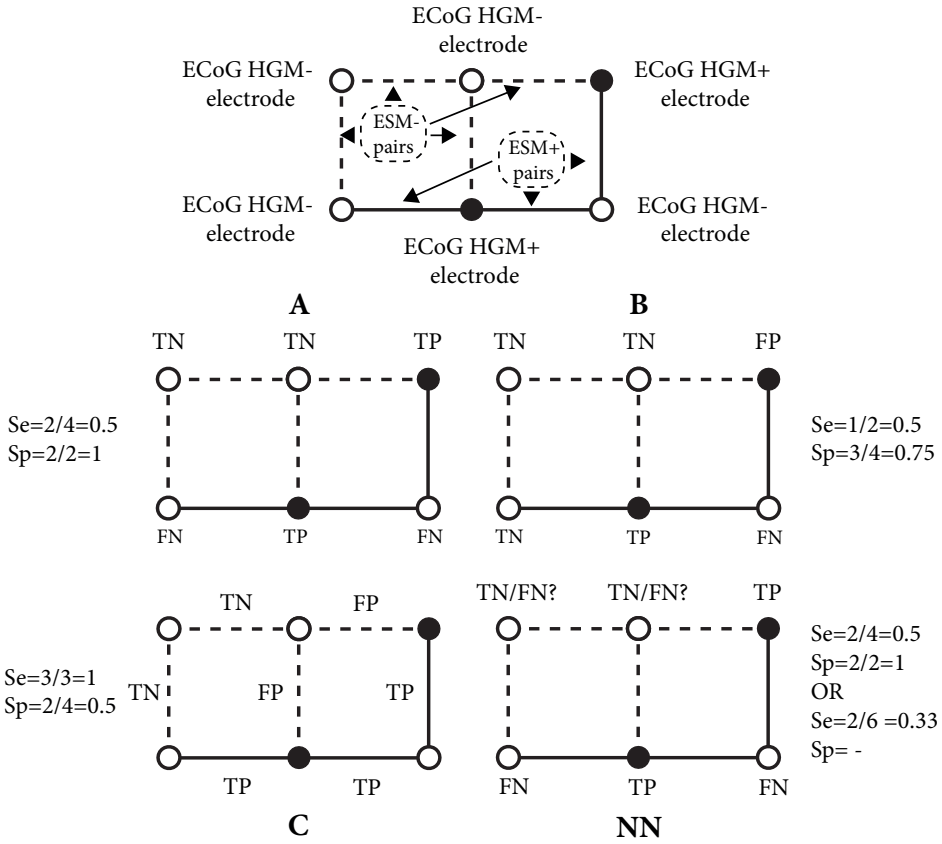

Figure 3.1 Example of a three-by-two grid with two ECoG HGM + electrodes (filled circles) and three ESM + electrode pairs (solid lines). ECoG HGM − electrodes are depicted as open circles, ESM − electrode pairs as dashed lines. Below, the same grid is shown four times to demonstrate the four methods for determining whether electrodes (methods A, B, and NN), or electrode pairs (method C) are considered true positive (TP), false positive (FP), true negative (TN), or false negative (FN). The resulting sensitivity (Se) and specificity (Sp) are also supplied.

- Method A: Every electrode that is involved in at least one ESM + electrode pair is considered ESM +. An ECoG HGM + electrode is considered true positive if that electrode is also an ESM + electrode.[29,46,47,53–55]
- Method B: Every electrode that is involved in two or more ESM + electrode pairs is considered ESM +. This method is similar to method A, but the criteria for ESM + electrodes are stricter.[31,35,46]

Method A yields more ESM + electrodes than method B. As a consequence, an ECoG HGM + electrode is more likely to be true positive, but an ECoG HGM – electrode is more likely to be false negative. Studies with many ECoG HGM + electrodes are therefore more likely to yield a high sensitivity with method A. On the other hand, if the number of ECoG HGM + electrodes is low, sensitivity might be poor because of the large number of false negatives. The chance of finding false positive results is lower in method A than in method B. Thus, specificity is higher for method A.

- Method C: This method determines whether ESM + electrode pairs contain ECoG HGM + electrodes.[30,34,36,46] This method differs from method A and B because it looks at ESM + pairs and then establishes whether those pairs contain ECoG HGM + or ECoG HGM – electrodes. Thus, in method C, the pairwise ESM + results are not converted to results per electrode, and one electrode can contribute to different ESM pairs. As a consequence, an ECoG HGM + electrode that is connected to an ESM + pair will result in a TP ESM pair, whereas that same ECoG HGM + electrode will result in a FP ESM pair when connected to an ESM – pair. The higher number of TP results in relatively high sensitivity, but specificity is lower because of the higher number of FP results.
- Next-neighbor (NN) method: This method applies the same rule for converting ESM pairs to ESM electrodes as method A.[51–53] In addition, an ECoG HGM + electrode is considered true positive if it is a neighbor of an ESM + electrode. It is unclear if the reverse is also true, i.e., if ECoG HGM – electrodes that are neighbors of ESM + are considered false negatives. If this is the case, sensitivity will drop because of the higher number of FN, but if this is not the case, sensitivity will be high because of the high number of TP. The chance of finding a FP result is low with this method, which therefore yields high specificity.

Some papers use a combination of two approaches: for example, method B if an electrode is stimulated in more than one pair and method A when an electrode is stimulated in only one pair (method AB).[48,50] One study used an adapted method C for calculating sensitivity in ESM + pairs but calculated specificity by dividing ESM – pairs in two ESM – electrodes using method A (method AC).[49]

We plotted (1-specificity) against sensitivity for each study to demonstrate the effect of these methods in real data (Figure 3.2). We deduced the method that was used in each paper from text, tables, and/or figures, but this information was not always readily available. If possible, we verified our classification by recalculating results for a patient based on a figure and comparing them to the results reported in a table. If it was clear that ECoG HGM and ESM results were compared per electrode but it was not specified which criteria were used to determine if an electrode was ESM + or ESM –, we assumed that the less strict criteria of method A were used.[47,54,55] One paper did not provide the information needed to determine if they used ESM pairs or ESM electrodes.[33]

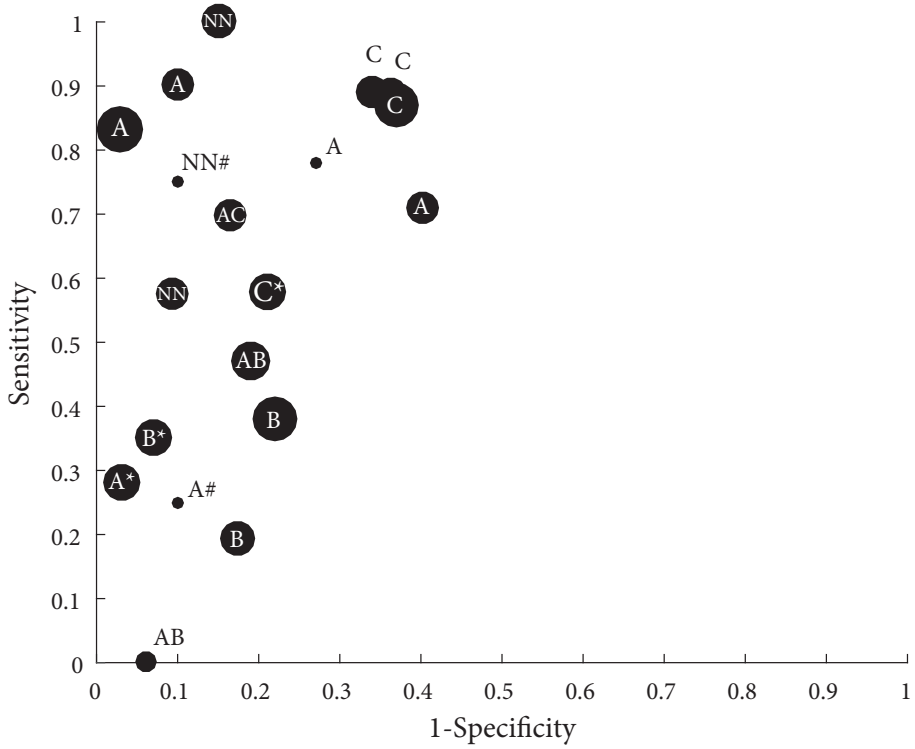

Figure 3.2 Scatter plot of 1-specificity (false positive rate) versus sensitivity. The size of the black circles reflects the sample size per study. Two studies (Korestenkaja et al.[53] and Mooij et al.[46]) calculated sensitivity and specificity in more than one way. The results of Korestenkaja et al. (methods NN and A) are marked with a #, the results of Mooij et al. (methods A, B, and C) are marked with an *.
This figure shows a clustering of most of the studies using method C. All studies using method C report higher sensitivity than specificity. All studies using method B report low sensitivity but high specificity. There is no clear pattern in studies using method A. This is partly due to the fact that high and low sensitivity are both likely results of method A (see above). Another reason is that this category contains studies that were difficult to classify. We therefore cannot exclude the possibility that some studies were inadvertently misclassified.

Conclusion and recommendations

We showed that apart from the heterogeneity in testing methods as reported by Arya et al.,[45] there are also different methods for calculating sensitivity and specificity, and these different methods influence outcome. Comparing sensitivity and specificity between studies is inappropriate as long as these differences in methods of comparison remain. Future research on ESM should clarify which method for converting ESM +/− pairs to ESM +/− electrodes best represents the actual situation in the electrically stimulated cerebral cortex. Until such a clarification is available, research groups should determine sensitivity and specificity using methods A, B, and C, or at least allow reviewers to recalculate values in one uniform method by providing the data required for these calculations. Recalculation requires information about all ECoG HGM positive and negative electrodes and all ESM positive and negative electrode pairs.

If sensitivity and specificity of all studies would be calculated using the same method of comparison, a new, valid attempt could be made to evaluate the effects of the variety in language tasks, ECoG HGM procedures, and ESM protocols.

Part 2

Identifying channels with epileptic activity in intracerebral EEG

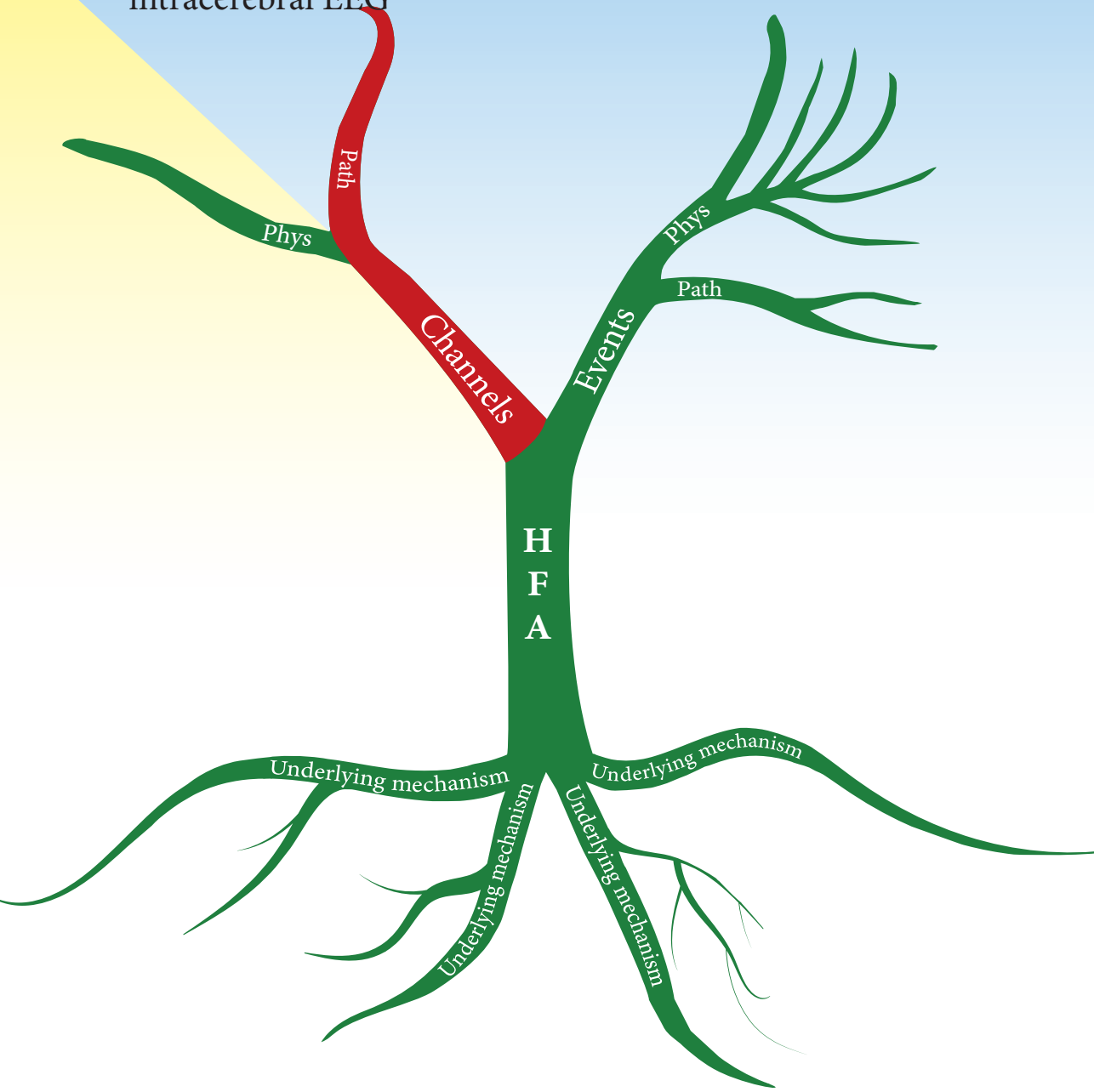

Chapter 4

A skew-based method for identifying iEEG channels with epileptic activity without detecting spikes, ripples, or fast ripples

Anne H. Mooij
Birgit Frauscher
Jean Gotman
Geertjan J.M. Huiskamp

Clinical Neurophysiology 2020; 131:183-192

Abstract

Objective
To develop a method for identifying intracerebral EEG (iEEG) channels with epileptic activity without the need to detect spikes, ripples, or fast ripples.

Methods
We compared the skew of the distribution of power values from five minutes non-rapid eye movement stage N3 sleep for the 5-80 Hz, 80-250 Hz (ripple), and 250-500 Hz (fast ripple) bands of epileptic (located in seizure-onset or irritative zone) and non-epileptic iEEG channels recorded in patients with drug-resistant focal epilepsy. We optimized settings in 120 bipolar channels from 10 patients, compared the results to 120 channels from another 10 patients, and applied the method to channels of 12 individual patients.

Results
The distribution of power values was more skewed in epileptic than in non-epileptic channels in all three frequency bands. The differences in skew were correlated with the presence of spikes, ripples, and fast ripples. When classifying epileptic and non-epileptic channels, the mean accuracy over 12 patients was 0.82 (sensitivity: 0.76, specificity: 0.91).

Conclusions
The 'skew method' can distinguish epileptic from non-epileptic channels with good accuracy and, in particular, high specificity.

Significance
This is an easy-to-apply method that circumvents the need to visually mark or automatically detect interictal epileptic events.

Introduction

Spikes and high-frequency oscillations (HFOs, pathological ripples, 80-250 Hz, and fast ripples, 250-500 Hz) are biomarkers for the epileptogenic zone.[15,17] The identification of spikes and HFOs in the interictal EEG can be challenging. Visually recognizing such events requires training and experience, and even with training and experience marking spikes and HFOs remains time consuming and subjective.[18] Automatically detecting spikes and HFOs is faster and more objective, but such detectors often need visual markings of data on which the detectors can be trained and visual verification to remove false positives.[18]

The goal of this study was to develop a method for identifying channels with epileptic activity in the interictal intracerebral EEG (iEEG) without the need to detect spikes, ripples, or fast ripples. The method we propose is based on the presence of a peak in spectral power in their specific frequency bands during spikes, ripples, and fast ripples. The presence of such a power peak means that if the EEG signal is divided in epochs of a certain duration, there is higher power during epochs containing epileptic events than during epochs without them. The distribution of the power per epoch of an electrographic signal containing such events should therefore show positive skew.

Identifying channels with spikes or HFOs without the need to mark or detect these events in iEEG has been attempted before,[59,60] but these studies focus on events in one frequency band. In contrast, we intend to develop a method that is applicable for low- and high- (ripple and fast ripple) frequency bands. Other methods exist that combine information from the low- and high-frequency band,[61] but these typically result in a single biomarker.

Interictal spikes occur in the irritative zone (IZ).[15] Pathological HFOs and interictal spikes were shown to occur more often inside than outside the seizure onset zone (SOZ).[24,62–64] Thus, channels recording from the IZ and channels recording from the SOZ can contain epileptic activity. However, the clinical relevance of SOZ and IZ differs. The IZ was traditionally used as marker of the epileptogenic zone, but the IZ is usually larger than the area that needs to be resected for seizure freedom.[15] The SOZ is often a subset of the IZ and is considered a better surrogate of the epileptogenic zone.[15]

This study consists of two parts. In the first part, we developed the skew method in a training and testing set that consisted of channels from different patients. We addressed the question whether there was more positive skew in the distribution of power per epoch in channels that were likely to contain epileptic activity, (i.e., SOZ and IZ channels, hereafter called 'epileptic channels'), than in channels that were not likely to contain epileptic activity, (i.e., channels outside SOZ and IZ: non-epileptic channels). We asked this question for the low-frequency band (below 80 Hz), the ripple band (80-250 Hz), and the fast ripple band (250-500 Hz). We then investigated if the potential higher skew of epileptic channels was correlated with the presence of interictal epileptic events: spikes, ripples, and fast ripples. Finally, we calculated sensitivity, specificity, and accuracy for epileptic and non-epileptic

channels in the training and testing set. We obtained these performance measures for each frequency band separately, and after combining the outcome of the three frequency bands.

In the second part, we investigated the potential clinical utility of the skew method by applying it to data of individual patients. We first evaluated the performance of the method in each patient in the same way as in the training and testing set: by calculating sensitivity, specificity, and accuracy for epileptic and non-epileptic channels. We then separated SOZ channels and IZ channels that did not overlap with the SOZ (i.e., exclusively IZ, EIZ) and calculated sensitivity and specificity of the skew method for either of these regions.

Methods

Data

We studied an existing dataset of patients undergoing stereo-EEG at the Montreal Neurological Institute and Hospital between January 2010 and March 2015. The main selection criteria for the dataset were 1) availability of at least one continuous whole night recording obtained at least 72 hours post implantation, 2) no interference with sleep scoring in the scalp EEG because of epileptic activity or non-epileptic anomalies, 3) absence of a secondarily generalized seizure during the 12 hours or a partial seizure during the 6 hours prior to the sleep recording, and 4) recording at a sampling rate of 2000 Hz (see von Ellenrieder et al. 2016).[65] The selection criterion for this particular study was availability of five minutes of non-rapid eye movement (NREM) stage 3 (N3) sleep recorded during the first sleep cycle. We chose NREM sleep because spikes and HFOs were shown to occur most often during NREM sleep.[28,62,64,66–70] Moreover, von Ellenrieder et al. (2017) suggested that the first sleep cycle was the most suitable for studying HFOs in epilepsy, because the rate of pathological ripples and fast ripples was highest, and the contrast between physiological and pathological ripple rate was largest during this sleep cycle.[71] We used five minutes because Zelmann et al. (2009) reported that five minutes of data were likely to offer a representative sample for identifying channels with HFOs.[72] Sleep was scored visually in the scalp EEG according to AASM criteria by a board certified sleep specialist.[26] Thirty-two patients (age: range: 21-57 years, mean: 36.3 years, sd: 9.5 years; 15 female) fulfilled these selection criteria, which were randomly divided in 10 patients for a training set, 10 patients for a testing set, and 12 patients for applying the method in individual patients. Patients gave written informed consent in agreement with the Research Ethics board of the Montreal Neurological Institute and Hospital.

iEEG

Patients were implanted with one of two types of depth electrodes: MNI made in-house or DIXI electrodes (DIXI Medical, France). The MNI electrodes had nine contacts of 0.5-1 mm, distance between contacts was 5 mm. The DIXI electrodes

had 10-15 contacts of 2 mm, distance between contacts 1.5 mm. The differences between these electrodes are not likely to significantly influence the recording of events.[73] The iEEG was recorded with Stellate Harmonie. High-pass filter and low-pass anti-alias filter at acquisition were 0.1 and 500 Hz respectively. Sampling rate was 2000 Hz. We analyzed the iEEG signal in a bipolar montage of neighboring contacts.

Selection of channels in training and testing set
We included only the most medial and most lateral channels of each electrode to avoid analyzing similar signals. We verified that the most medial and most lateral channels were located in different brain regions. For example, an iEEG electrode in the temporal lobe has its medial contacts in the hippocampus while the lateral contacts record from the temporal neocortex. There were 120 such channels in the 10 patients from the training set and also 120 channels in the 10 patients from the testing set.

Settings for calculating skew of the distribution of power per epoch
We tuned the settings for calculating skew on the data from the training set. We first generated time-frequency distributions based on Stockwell transforms defined in each sample of five minute of iEEG data in Matlab (version R2018a, Natick, USA).[74] This was done for each frequency band (from 1 to 80 Hz, 80-250 Hz and 250-500 Hz) separately, each with steps of 1 Hz, and with different settings for the localizing Gaussian width factor w of the Stockwell transform. Width factor w ranged between w = 1 and w = 5 for the low-frequency band, and between w = 1 and w = 15 for the ripple and fast ripple bands. For the calculation of skew we integrated power of the transforms over each frequency band and over epochs of 50, 100, 200, or 500 samples. At a sampling rate of 2000 Hz, this corresponds to 25, 50, 100, and 250 ms epochs.

Optimization of contrast between epileptic and non-epileptic channels: low-frequency band
Interictal epileptic spikes differ from the background activity and other physiological events or rhythms in 1-80 Hz band because there is a short increase in power in many frequencies during a spike. There are several physiological transients and oscillations with power in the lowest (1-2 Hz) frequencies, especially during sleep, such as slow waves and K-complexes. The contrast between spikes and such physiological events is based on the higher frequencies within the 1-80 Hz band. EEG power typically decreases with increasing frequency following a 1/f law,[75] so that the contribution to the total power of such higher frequencies might be small. To maximize this difference, we used two approaches: a) ignoring the lowest frequencies (i.e., starting at 3 Hz, or at 5 Hz), and b) enhancing the contribution of the higher frequencies by applying 1/f correction.

Optimization of contrast between epileptic and non-epileptic channels: ripple and fast ripple bands
HFOs (ripples and fast ripples) show a short increase in power in a narrow frequency band. The center frequency of HFOs can vary, e.g. ripples with a center frequency of 100 Hz or 150 Hz. If a difference in positive skew is caused by the presence of ripples, channels with 150 Hz ripples may, as a consequence of the 1/f law, be more difficult to distinguish from channels without ripples than channels with ripples of lower frequencies. We therefore calculated power both with and without 1/f correction.

Normalization
Power per epoch was normalized by the sum of the power of all epochs of the five minute segment for each of the 120 channels. This normalization was done to reduce the effect of differences in overall power between electrodes and between patients.

Determining which settings show maximum differences between epileptic and non-epileptic channels
We calculated the skew of the distribution of power per epoch using the above mentioned w factors and epoch lengths, with and without 1/f correction, and in the case of the low-frequency band, with or without the lowest frequencies (1-80 Hz, 3-80 Hz, or 5-80 Hz). We tested if the distribution of power per epoch was more positively skewed in epileptic channels than in non-epileptic channels using a one-sided non-parametric Wilcoxon rank sum test (performed in Matlab). We chose the optimal settings as the settings with the smallest p-value, as this reflects the maximal difference between the sum of ranks of epileptic and non-epileptic channels.

Threshold
We considered channels to be epileptic according to this skew method if skew was above a certain threshold. Our first priority was to minimize the number of false positives (i.e., non-epileptic channels wrongly classified as epileptic). We therefore chose to base the threshold on the results of the non-epileptic channels of the training set. We chose the upper fence as threshold, with the formula Threshold T = $q3 \pm 1.5*(q3 - q1)$, in which q1 and q3 are the first and third quartile and q3 – q1 is the interquartile range of the skew values.

Presence of spikes, ripples, and fast ripples
We visually marked for each of the 120 selected bipolar channels of the training set if there was one or more spike, one or more ripple, and one or more fast ripple. Events were marked independently of the skew outcome or classification as epileptic or non-epileptic. The iEEG signal was filtered between 0.3 and 70 Hz for marking spikes, between 80 and 250 Hz for marking ripples, and between 250 and 500 Hz for marking fast ripples. Filters used for viewing the low-frequency

(spike) band were infinite impulse response filters (IIR) of order 3 (0.3 Hz) or order 4 (70 Hz). Filters used for viewing the high-frequency (ripple and fast ripple) bands were finite impulse response (FIR) high-pass filters of order 63. Events were marked on a 15.4 inch screen, time scale was 10 seconds per page for marking spikes and 0.6 seconds per page for marking HFOs. Amplitude scale varied between 10 to 30 μV/mm for the low-frequency signal and between 1 and 3 μV/mm for high-frequency signal, depending on the amplitude of the signal. HFOs were marked if they consisted of four or more oscillations that clearly stood out from the background high-frequency signal. We tested if there was more positive skew in the channels with events than in channels without events using a one-sided Wilcoxon rank sum test.

Comparing training and testing set

We tested per frequency band (low-frequency, ripple, and fast ripple band) if the skew outcomes of the 120 channels from the training set and the 120 channels from the testing set were comparable using a two sample Kolmogorov-Smirnov test (performed in Matlab).

Performance of skew method in training and testing set

We compared the outcome of this skew method to the clinical classification as epileptic (i.e., located in SOZ or IZ) or non-epileptic channel. The clinical classification was done by two clinical neurophysiologists independently of this study. SOZ channels were defined as the channels showing the first unequivocal ictal iEEG change at seizure onset.[76] IZ channels were defined as channels having interictal epileptic spikes. The classification as SOZ or IZ was based on all available iEEG data of a patient (usually 7-21 days of recordings). Non-epileptic channels were defined as being outside SOZ and IZ and not in any lesion visible on CT or MRI.

A channel was labeled true positive (TP) if it was an epileptic channel with skew above the threshold; false positive (FP) if it was a non-epileptic channel with skew above the threshold; true negative (TN) if it was a non-epileptic channel with skew below the threshold; and false negative if it was an epileptic channel with skew below the threshold. We assessed the performance of the skew method by calculating for each frequency band the sensitivity(TP/(TP+FN)), specificity (TN/(TN+FP)), and accuracy ((TP+TN)/(TP+TN+FP+FN)).

Combining low- and high-frequency bands in three steps

We combined the skew outcome of the frequency bands in three steps. A (combination of) frequency band(s) was considered relevant for the identification of epileptic channels if at least twice as many true positives as false positives were found in the training set.

In the first step, we counted channels with skew above the threshold in all three bands. If this combination of bands provided a relevant contribution, we removed the channels that were identified as epileptic from the total set of channels. In the second step, we identified in the remaining set the number of channels with

skew above the threshold in two bands (i.e., fast ripple plus ripple band, fast ripple band plus low-frequency bands, and ripple plus low-frequency band). If any of these combinations of band provided relevant information, we again removed the channels that were identified as epileptic from the set. As third step, we counted the number of channels with skew above the threshold in only one frequency band. We calculated sensitivity, specificity, and accuracy for channels found in the first step, then for those found in the first and second step, and finally for all three steps together.

Performance of skew method in individual patients

We calculated skew in the channels of 12 individual patients. We used the settings that were obtained from tuning on the training set and followed the three steps for combining frequency bands. We included all channels for which a classification as epileptic (SOZ channel or IZ channel) or non-epileptic channel was available. Thus, in contrast to the training and testing set, in which only the most medial and most lateral channels were selected for each electrode, we now included neighboring contacts of an electrode. This resulted in a larger number of channels per patient, allowing calculation of sensitivity, specificity, and accuracy per patient. We also calculated sensitivity and specificity for SOZ channels and EIZ channels (i.e., IZ channels that did not overlap with the SOZ) separately. Finally, we calculated per step the mean of these outcome measures over the 12 patients.

Results

Settings, statistics, and threshold

Epileptic channels had a more positively skewed distribution of power values than non-epileptic channels (Figure 4.1 and Figure 4.2A). For the low-frequency band, optimal settings were w = 1 with an epoch of 25 ms (50 data points), frequency band = 5-80 Hz, and with 1/f correction. For the ripple band, optimal settings were w = 1 with an epoch of 25 ms. For the fast ripple band, it was w = 10 and an epoch of 100 ms. There was no relevant difference between results of ripple and fast ripple bands with or without 1/f correction. To keep the settings similar, we applied the 1/f correction to all three bands.

With these settings, outcome of the one-sided Wilcoxon rank sum test of skew in non-epileptic channels (N = 47) versus epileptic channels (N = 73) were as follows: low-frequency band: $Mdn_{non\text{-}epileptic} = 2.34$, $Mdn_{epileptic} = 18.43$, $Ws = 1459$, $p = 5.00 \times 10^{-14}$, $z = -7.44$, $r = -0.68$; ripple band: $Mdn_{non\text{-}epileptic} = 1.40$, $Mdn_{epileptic} = 15.88$, $Ws = 1728$, $p = 1.02 \times 10^{-9}$, $z = -5.99$, $r = -0.55$; fast ripple band: $Mdn_{non\text{-}epileptic} = 0.42$, $Mdn_{epileptic} = 0.59$, $Ws = 1956$, $p = 9.27 \times 10^{-7}$, $z = -4.77$, $r = -0.44$.

The threshold was 6.6 for the low-frequency band, 5.1 for the ripple band, and 0.6 for the fast ripple band (Figure 4.2).

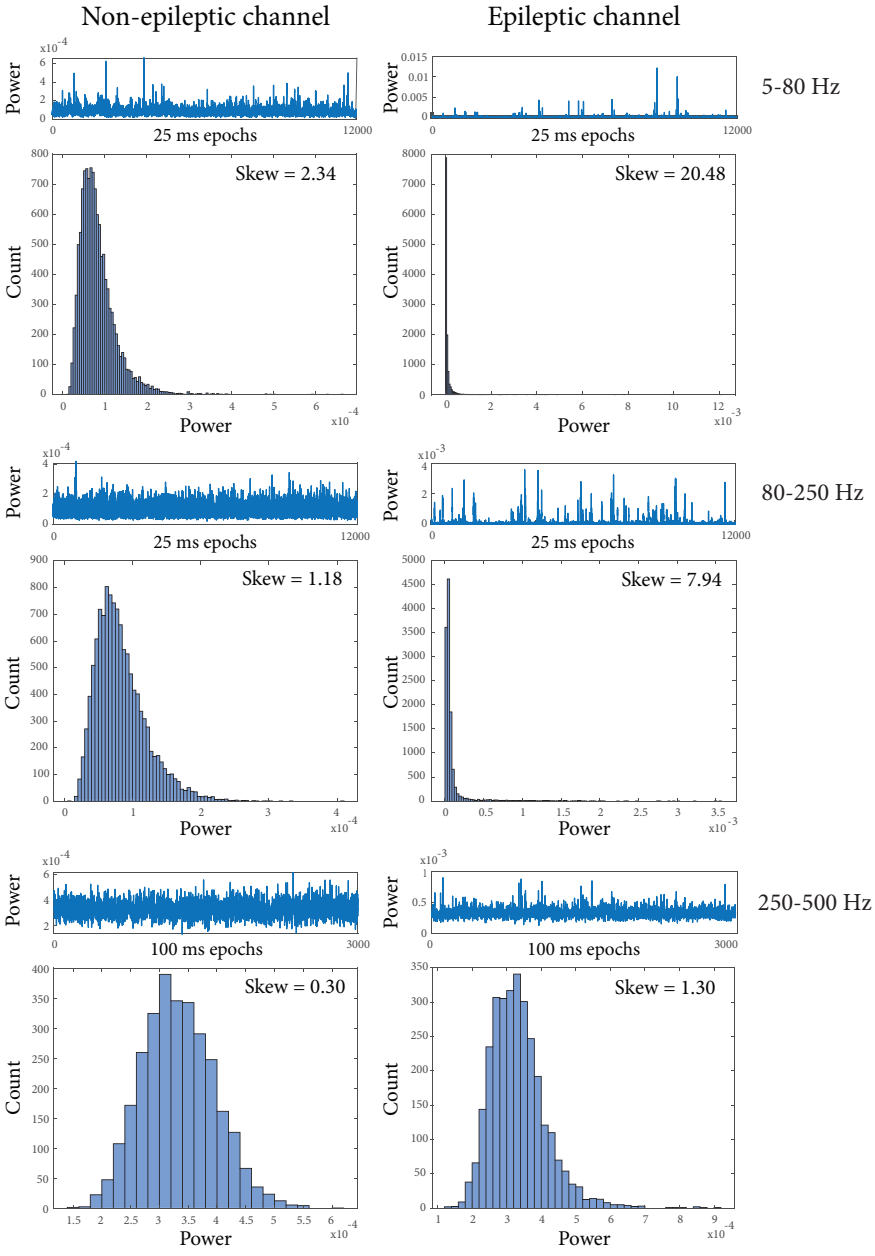

Figure 4.1 Example of a plot of (normalized) power per epoch and a histogram of power per epoch for the low-frequency band, ripple band, and fast ripple band of a non-epileptic and an epileptic channel. Power plots of epileptic channels show more peaks than plots of non-

epileptic channels and the peaks of epileptic channels are one or more order of magnitudes larger. These peaks give rise to a skewed distribution, as shown in the corresponding histograms. All histograms show asymmetrical distributions, but there is more positive skew in the epileptic channel than in the non-epileptic channel in all three bands.

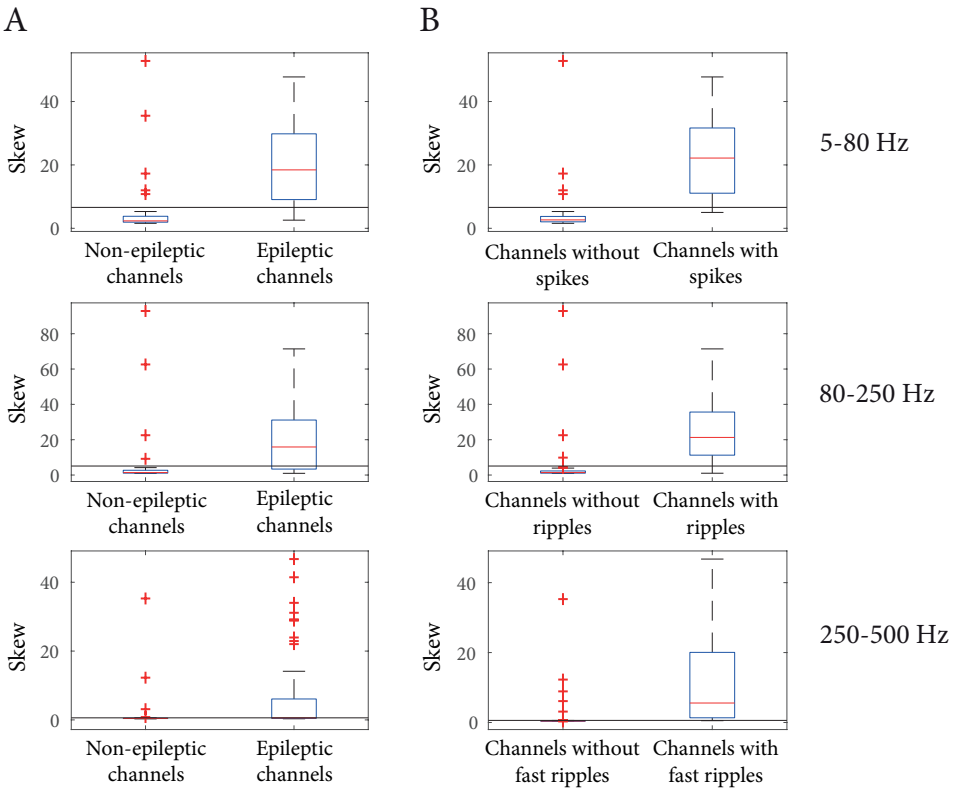

Figure 4.2 Boxplots of skew results of the 120 channels of the training set for the low-frequency band, ripple band, and fast ripple band. The threshold is depicted as a horizontal line. Boxplots in A show the difference in skew between non-epileptic and epileptic channels. Boxplots in B show the differences in skew between the channels without and channels with events. The differences between boxes of channels with and without events are clearer than the differences between boxes of epileptic and non-epileptic channels for all three bands.

Presence of spikes, ripples, and fast ripples

Most events occurred in epileptic channels and most of the channels with one or more events had a skew outcome higher than the threshold (Table 4.1). Non-epileptic channels without events but with skew above the threshold mostly contained artifacts, except for one channel with a changeable signal in the fast

ripple band, but no artifacts. Channels containing artifacts were most often lateral channels from temporal electrodes.

Results of the one-sided Wilcoxon rank sum test of skew in channels without events versus channels with events were as follows: low-frequency band: $Mdn_{no\_spikes} = 2.65$, $Mdn_{spikes} = 22.17$, $Ws = 1714$, $p = 6.65 \times 10^{-19}$, $z = -8.80$, $r = -0.80$; ripple band: $Mdn_{no\_ripples} = 1.40$, $Mdn_{ripples} = 21.29$, $Ws = 2248$, $p = 1.07 \times 10^{-16}$, $z = -8.21$, $r = -0.75$; fast ripple band: $Mdn_{no\_fast\_ripples} = 0.44$, $Mdn_{fast\_ripples} = 5.57$, $Ws = 3774$, $p = 1.41 \times 10^{-15}$, $z = -7.90$, $r = -0.72$. These results indicate that high skew in epileptic channels was correlated with the presence of events.

Table 4.1 Channels with spikes, ripples, and fast ripples and relation to skew outcome

	73 Epileptic channels						47 Non-epileptic channels					
	LF band		R band		FR band		LF band		R band		FR band	
Skew	>T	<T	>T	<T	>T	<T	>T	<T	>T	<T	>T	<T
Event +	60	2	51	4	33	1	1	1	1	1	1	0
Event -	0	11	1	17	3	36	4	41	3	42	3	43

LF: low-frequency band (5-80 Hz); R: ripple band (80-250 Hz); FR: fast ripple band (250-500 Hz). Threshold (T) of low-frequency band = 6.6, threshold of ripple band = 5.1, threshold of fast ripple band = 0.6. Event of LF band: spike; event of ripple band: ripple; event of fast ripple band: fast ripple. Most epileptic channels with skew above the threshold contained events. There were also a few non-epileptic channels with spikes, ripples, or fast ripples. Non-epileptic channels without events but with skew above the threshold contained artifacts.

Performance of training and testing set

The results of the two sample Kolmogorov-Smirnov test were non-significant for all three frequency bands (low-frequency band: $Mdn_{training} = 9.03$, $Mdn_{testing} = 9.04$, $D_{120,120} = 0.14$, $p = 0.17$; ripple band $Mdn_{training} = 3.64$, $Mdn_{testing} = 6.25$, $D_{120,120} = 0.11$, $p = 0.46$; fast ripple band: $Mdn_{training} = 0.47$, $Mdn_{testing} = 0.48$, $D_{120,120} = 0.10$, $p = 0.56$), which means that the training and testing set could be considered as coming from the same population. Specificity was higher in the training set, while sensitivity was equal or higher in the testing set; accuracy was similar in both sets (Table 4.2).

Table 4.2 Performance of skew method per frequency band in training and testing set

	Training: 120 channels			Testing: 120 channels		
EPI	73 channels			74 channels		
NE	47 channels			46 channels		
Freq. band	LF band	R band	FR band	LF band	R band	FR band
TP	60	52	36	62	56	36
FP	5	4	4	11	5	10
TN	42	43	43	35	41	36
FN	13	21	37	12	18	38
Sens.	0.82	0.71	0.49	0.84	0.76	0.49
Spec.	0.89	0.91	0.91	0.76	0.89	0.78
Accuracy	0.85	0.79	0.66	0.81	0.81	0.60

EPI: epileptic channel; NE: non-epileptic channel. LF: low-frequency band (5-80 Hz); R: ripple band (80-250 Hz); FR: fast ripple band (250-500 Hz). TP: true positive; FP: false positive; TN: true negative; FN: false negative. Sens.: sensitivity; Spec.: specificity. Note that accuracy is highest in the low-frequency band, especially for the training set, but that specificity is higher in the ripple and fast ripple bands.

Combining low- and high-frequency bands

All three bands together, ripples plus low-frequency band, and low-frequency band alone provided relevant information for identifying epileptic channels. There were very few channels with skew above the threshold in fast ripple and ripple band, alone or combined, and half or more of these channels were false positives. These (combination of) bands were therefore excluded from the three-step approach. We also excluded the combination of fast ripple plus low-frequency band, because there were no channels with skew above the threshold for this combination of bands.

Specificity of channels containing fast ripples and ripples improved after combining the frequency bands (Table 4.3). For example, the columns with results of all three bands in Table 4.3 contain all channels with skew above the threshold in the fast ripple band; specificity is higher than specificity of the fast ripple band alone (compare with FR columns in Table 4.2).

Table 4.3 Performance of skew method in training and testing set after combining frequency bands

	Training: 120 channels			Testing: 120 channels		
EPI	73 channels			74 channels		
NE	47 channels			46 channels		
Freq. bands	Step 1 FR+R+LF	Step 2 FR+R+LF & R+LF	Step 3 FR+R+LF & R+LF & LF	Step 1 FR+R+LF	Step 2 FR+R+LF & R+LF	Step 3 FR+R+LF & R+LF & LF
TP	34	49	60	31	52	62
FP	2	2	5	2	2	11
TN	45	45	42	44	44	35
FN	39	24	13	43	22	12
Sens.	0.47	0.67	0.82	0.42	0.70	0.84
Spec.	0.96	0.96	0.89	0.96	0.96	0.76
Accuracy	0.66	0.78	0.85	0.63	0.80	0.81

EPI: epileptic channel; NE: non-epileptic channel. LF: low-frequency band (5-80 Hz); R: ripple band (80-250 Hz); FR: fast ripple band (250-500 Hz). TP: true positive; FP: false positive; TN: true negative; FN: false negative. Sens.: sensitivity; Spec.: specificity. Note that specificity of the high-frequency bands improved after combining the bands (compare with results of Table 4.2). All (combinations of) band contained the low-frequency band; the last column of the training and testing part of this table is therefore the same as the LF column of Table 4.2.

Results per patient

Mean specificity over 12 patients was 1 for the first step, 0.99 for the second step, and 0.91 for the third step. Each step identified a larger subset of the epileptic channels, as reflected by the increasing sensitivity (Table 4.4 and Figure 4.3).

Except for one patient, whose SOZ and IZ were completely separate, SOZ and IZ were partially overlapping in all patients listed in Table 4.4. Each of the patients with partially overlapping SOZ and IZ had one or more EIZ channels. The results for SOZ or EIZ vary more than the results for all epileptic channels (Figure 4.3). On average, sensitivity was higher for SOZ channels than for all epileptic channels or EIZ channels for the first two steps (step 1: SOZ: 0.44, versus all epileptic: 0.35 and EIZ: 0.27; step 2: SOZ: 0.61, versus all epileptic: 0.54 and EIZ: 0.44). The third step (i.e., adding channels with skew above the threshold in low-frequency band alone) contributed most to the identification of EIZ channels: the average sensitivity became 0.78 (increase of 0.34), versus 0.76 for all epileptic channels (increase 0.22) and 0.74 for SOZ channels (increase 0.12). Specificity for SOZ or EIZ was lower than for all epileptic channels, indicating that the skew method is not suited to specifically identifying either of these zones.

Table 4.4 Results per patient of the three-steps skew method

#	Diagnosis	Lesion	Main SOZ	EPI	NE	Se 1	Sp 1	Acc 1	Se 2	Sp 2	Acc 2	Se 3	Sp 3	Acc 3
1	L temporoinsular epilepsy	No lesion	Widespread L temporal and insular, maximum temporal pole	43	35	0.28	1	0.60	0.47	1	0.71	0.70	0.94	0.81
2	R frontotemporal epilepsy	Hyperintensity R frontal adjacent to ventricle	R orbitofrontal region	74	3	0.11	1	0.14	0.50	1	0.52	0.80	0.67	0.79
3	L posterior quadrant epilepsy	Encephalomalacia in posterior insula	Posterior insula	10	31	0.20	1	0.80	0.60	1	0.90	0.90	1	0.98
4	L posterior quadrant epilepsy	Bilateral hippocampal atrophy and sclerosis	Posterior quadrant both hemispheres	24	41	0.33	1	0.75	0.42	1	0.78	0.58	0.95	0.82
5	L sided epilepsy	No lesion	No generator identified	2	30	1	1	1	1	1	1	1	0.90	0.91
6	TLE R or bilateral	No lesion, L hippo-campus smaller than R	R mesiotemporal	26	8	0.54	1	0.65	0.73	1	0.79	0.96	1	0.97
7	L temporoinsular epilepsy	Dysplasia or PNET?	L Heschl's gyrus	10	5	0.10	1	0.40	0.20	1	0.47	0.40	1	0.60
8	TLE bilateral	L hippocampal atrophy	Bitemporal neocortex and L amygdala	59	12	0.10	1	0.25	0.27	1	0.39	0.63	0.92	0.68

table continues

#	Diagnosis	Lesion	Main SOZ	EPI	NE	Se 1	Sp 1	Acc 1	Se 2	Sp 2	Acc 2	Se 3	Sp 3	Acc 3
9	TLE bilateral	Periventricular nodular heterotopia	R posterior temporal or widespread bilateral with R posterior temporal maximum	78	0	0.28	NA	NA	0.58	NA	NA	0.82	NA	NA
10	TLE bilateral	No lesion	R mesiotemporal and inferior isthmus	20	34	0.35	1	0.76	0.65	0.94	0.83	0.85	0.68	0.74
11	L OLE	L FCD occipital lateral	L occipital lateral	14	29	0.50	1	0.84	0.64	1	0.88	0.71	1	0.91
12	L TLE	L hippocampal atrophy	L mesiotemporal	23	28	0.43	1	0.75	0.43	1	0.75	0.74	0.93	0.84
				Mean		0.35	1	0.63	0.54	0.99	0.73	0.76	0.91	0.82

SOZ: seizure onset zone; Se: sensitivity; Sp: specificity; Acc: accuracy. L: left; R: right. 1, 2, and 3 refer to the steps of the three-step approach. TLE: temporal lobe epilepsy; OLE: occipital lobe epilepsy; PNET: primitive neuroectodermal tumor; FCD: focal cortical dysplasia. Note that despite the differences in the number of channels, results are fairly similar between patients, especially specificity.

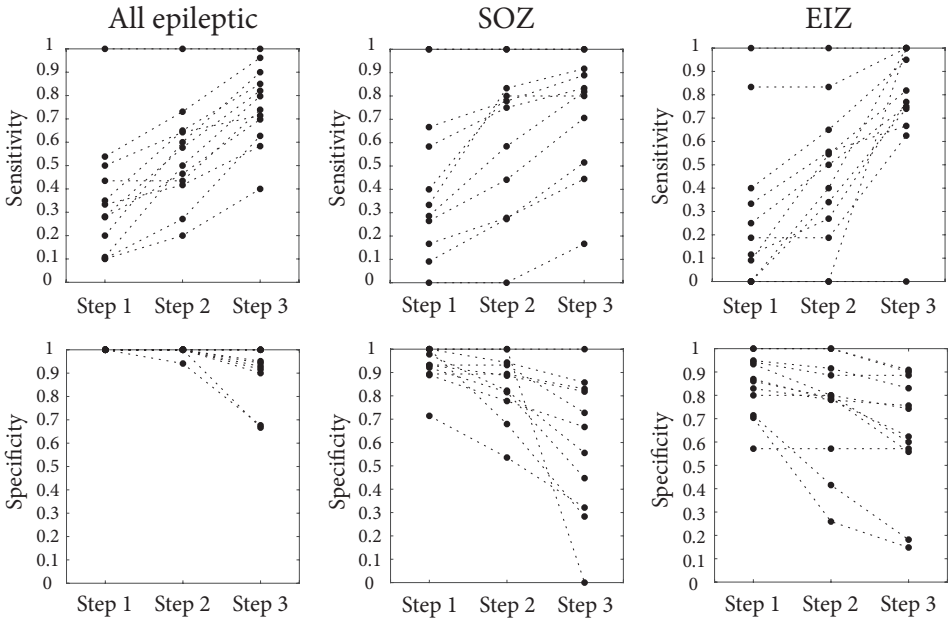

Figure 4.3 Sensitivity and specificity per step of the three-step approach for all epileptic channels, channels in the seizures onset zone (SOZ), and channels in the exclusively irritative zone (EIZ, i.e., IZ channels that do not overlap with the SOZ). Results from the 12 patients listed in Table 4.4. Note that specificity for SOZ or EIZ channels was lower than for all epileptic channels.

Discussion

The main result of this study is that the distribution of power per epoch is significantly more skewed in epileptic channels than in non-epileptic channels. This is true for the low-frequency, ripple, and fast ripple bands and is correlated with the presence of spikes, ripples, and fast ripples. Epileptic channels can be identified with highest accuracy by the low-frequency band; when results of the low-frequency band are combined with the ripple or both high-frequency bands, specificity is almost 100%.

Interictal events

Skew above or below the threshold was strongly correlated with the presence or absence of interictal events. This correlation was confirmed by inspecting the false positive channels (i.e., non-epileptic channels with skew above the threshold), which sometimes contained an interictal spike despite its classification as non-epileptic. False negative channels (i.e., epileptic channels with skew below the threshold) often contained no interictal epileptic events. Thus, the skew method

correctly identified them as channels without interictal epileptic activity in the form of spikes, ripples and fast ripples, even though they were classified as epileptic according to our gold standard (i.e., channel located in SOZ or IZ).

Despite the strong correlation with the presence of events, this skew method is not intended to provide information on the number and timing of events; it only aimed to identify channels with epileptic activity.

Results per band

Accuracy was highest for low-frequency band, but specificity was highest for ripple and fast ripple frequency bands. Physiological ripples did apparently not result in false positives: only one out of four false positives of the training set occurred in a channel with a ripple and no artifacts, the other three false positives in ripple band were also false positive in the fast ripple band, and were caused by artifacts. This might partly be explained by the use of data from the first sleep cycle, with its optimal contrast between pathological and physiological ripples (as explained in the first paragraph of method section, and see von Ellenrieder et al. 2017).[71]

Most physiological ripples seem to occur in the occipital lobe.[17] We included only six patients with channels recording from the occipital lobe, and most of these occipital channels were epileptic channels (i.e., located in SOZ or IZ). Even so, it is unlikely that there were no physiological ripples in these data: these patients (but probably not the exact same minutes of data) have also been included in studies by Frauscher et al. (2015) and von Ellenrieder et al. (2016) in which presumably physiological ripples were found.[65,77] Perhaps physiological ripples gave rise to a less prominent power peak, resulting in less skew. Buzsáki and Lopes da Silva (2012) stated that the generation of physiological events is controlled by many mechanisms, resulting in recruitment of a limited number neurons. As a consequence, the magnitude of physiological events is also limited. In contrast, pathological events are less well regulated. More pyramidal neurons can be involved, and recruitment can occur faster, resulting in a larger and more varying magnitude of pathological events.[78]

Combining frequency bands

All (combinations of) bands containing skew above the threshold in the low-frequency band provided a relevant contribution in training and testing set, except for channels with skew above the threshold in fast ripple plus low-frequency band. It is not likely that combining the low-frequency band with the fast ripple band will increase the number of false positives, because artifacts that affect low-frequency and fast ripple band would also affect the ripple band. We checked this in the results per patients, in which more channels were included. The combination of skew above the threshold in low-frequency plus fast ripple band occurred in four patients, each time only once, and each time as a true positive channel. This finding confirms that this combination of bands can safely be included, even though its yield will be small. We therefore recommend adding it to the three-step approach if this method is applied clinically.

It was not an aim of this study to test if HFOs are better biomarkers for the SOZ or the epileptogenic zone than spikes, as was done in other studies.[79,80] Instead, we combined the results of the three frequency bands, which resulted in the three-step approach. The first step identifies channels with skew above the threshold in all three bands. This small subset of the epileptic channels was identified with 100% specificity in individual patients. These channels may be located in regions with the highest level of epileptogenicity and could therefore be most important to remove during surgery. Epileptic channels identified in the second (skew above the threshold in low-frequency and ripple bands) and third steps (low-frequency band alone) may represent intermediate and low level of epileptogenicity; such channels, especially those identified in the third step, may rather be spared. Testing if this three-step approach indeed has such clinical relevance requires a study that compares results of this skew method with surgery outcome.

The results for SOZ and EIZ separately suggest that the first two steps are most important for identifying channels located in SOZ (whether overlapping with IZ or not), while the third step contributed most to the identification of EIZ channels. It is important to realize, however, that the skew method is not suited to selectively identify the SOZ or the IZ, because neither of these regions exclusively contain interictal events, resulting in poor specificity.

Methodological considerations

An epoch of 25 ms was found optimal for the low-frequency and ripple band. At this epoch length a wavelet transform or short time Fourier transform would not show power values below 40 Hz. The Stockwell transform we used provides time-frequency values for each data point. Values for frequencies with a longer period than the selected epoch length are spread over several such epochs. This spread further increases with increasing w factor, because frequency resolution improves, but time resolution decreases with increasing w factor. The event character of the spike is therefore most served by the optimal time resolution that a low w factor provides (we found w = 1 to be optimal). Still, if there are many spikes, it will be the higher frequency component of these events that is most important. The influence of the higher frequencies was strengthened by using the 5-80 Hz rather than the full 1-80 Hz band, which leaves out the power of slow waves and K-complexes, and by using 1/f correction. The higher w factor for the fast ripple band (w = 10 was optimal) results in a better frequency resolution, at the cost of a poorer time resolution. This was reflected in the longer epoch of 100 ms.

The skew method uses only five minutes of data. Such a short segment has advantages and disadvantages. The most important advantage is that the shorter the segment, the higher the chance that the data are available in all patients. We analyzed data recorded during N3 sleep of the first sleep cycle because of the higher occurrence rate of spikes and pathological ripples and fast ripples during N3 sleep,[28] and the optimal balance of physiological and pathological ripples during the first sleep cycle.[71] Another advantage is that short segments of N3 sleep are more likely to be contiguous. Analyzing different fragments that add up to

the required length is feasible, but it makes the method less easy to apply. On the other hand, the chance that interictal epileptic events occur increases in a longer segment. Considering the strong correlation between events and high skew, a longer segment may thus increase the chance of correct classification of epileptic channels. It is doubtful, however, how much difference a longer segment would make, at least for finding channels with HFOs, because five minutes were reported to be a representative sample length for HFO occurrence in most patients.[72]

The finding that the results of individual patients were similar to those of training and testing set suggests that this a robust method that works in different patients with the same settings and thresholds. Moreover, applying this method in a clinical setting should be feasible because the computation for a five-minute sample could be done in a few minutes.

Comparison with other methods

Our study has similarities to the study by Akiyama et al. (2012), in which kurtosis was used to identify channels with epileptic spikes.[59] Kurtosis was also used by Kirsch et al. (2006) to localize spikes and by Quitadamo et al. (2018) to preselect channels that were likely to contain interictal HFOs.[81,82] Kurtosis and skew are both measures for deviation from a normal distribution. Kurtosis describes how many counts can be found in the tails; many counts in the tails result in a 'peaked' distribution and high kurtosis. Skew is a measure of asymmetry, i.e., if there are more counts on one side of the distribution than on the other. Figure 4.1 not only shows that the power distribution of the epileptic channels is very asymmetrical; the power distributions are also 'peaked'. We tested what the results would be if we had used kurtosis instead of skew. Tuning on the training set resulted in the same optimal settings. With these settings, sensitivity was a little higher but specificity was lower, and this pattern was consistent throughout training, testing, and individual patients data sets (data not shown). As high specificity is most important for a clinical application we preferred the method based on skew.

An advantage of this study compared to other studies that developed methods to classify channels without the need to detect events[59,60] is that we analyze low-frequency, ripple, and fast ripple band, which enables the three-step approach.

Limitations

A limitation of this skew method is that it is sensitive to artifacts, which result in high skew and thus false positives. It can therefore best be used in iEEG, as artifacts due to movements or muscle activity are rare in such recordings.

Conclusion

This skew method can identify epileptic and non-epileptic channels with high accuracy, thereby circumventing the need to mark or detect interictal biomarkers of epilepsy such as spikes, ripples, and fast ripples. Future studies should compare the results of the three steps of this skew method to surgery outcome.

Part 3

Physiological ripples in scalp EEG

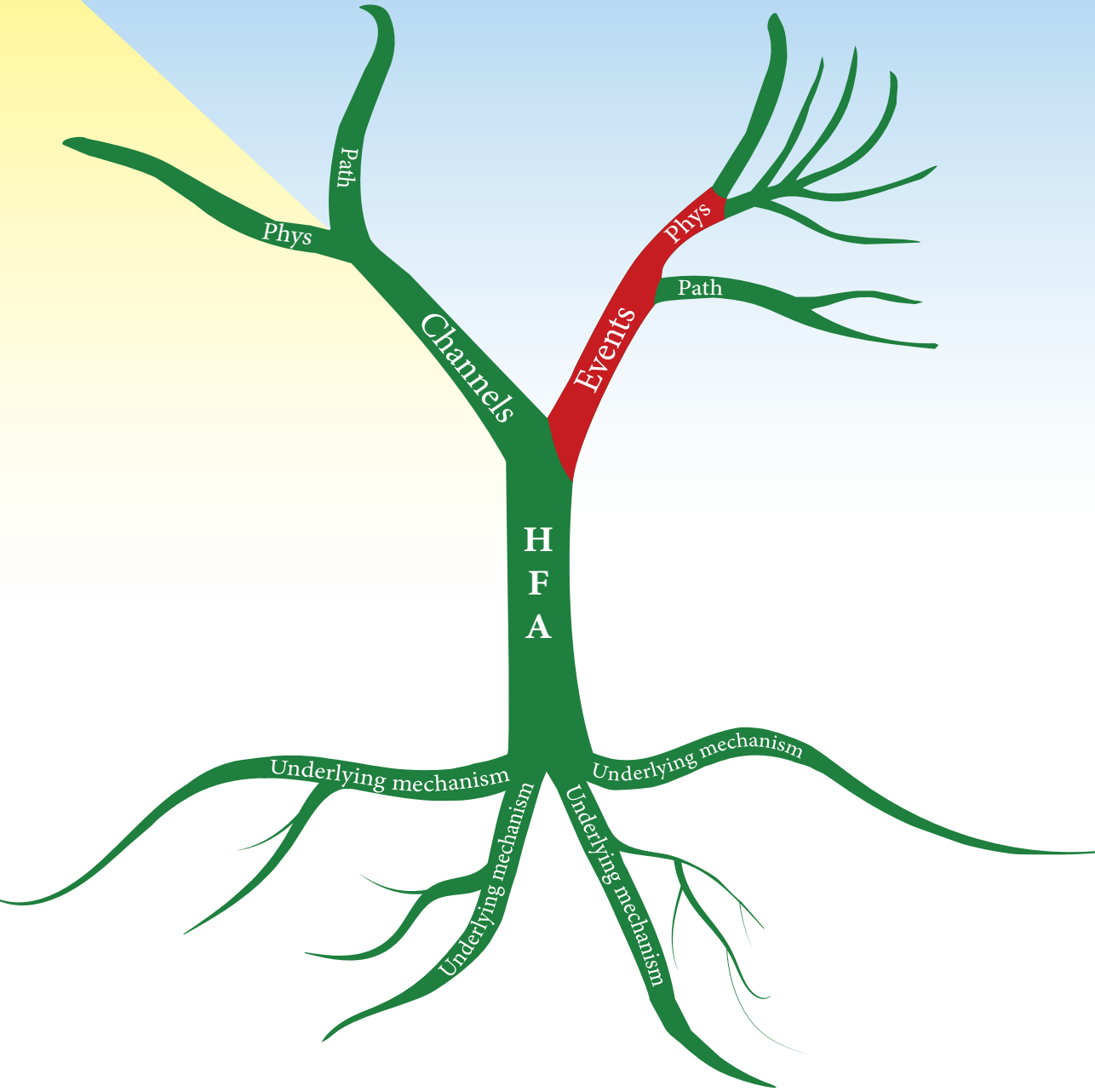

Chapter 5

Physiological ripples (± 100 Hz) in spike-free scalp EEGs of children with and without epilepsy

Anne H. Mooij
Renee C.M.A. Raijmann
Floor E. Jansen
Kees P.J. Braun
Maeike Zijlmans

Brain Topography 2017; 30:739-746

Abstract

Pathological high-frequency oscillations (HFOs, > 80 Hz) are considered new biomarkers for epilepsy. They have mostly been recorded invasively, but pathological ripples (80–250 Hz) can also be found in scalp EEGs with frequent epileptiform spikes. Physiological HFOs also exist. They have been recorded invasively in hippocampus and neocortex. There are no reports of spontaneously occurring physiological HFOs recorded with scalp EEG. We aimed to study ripples in spike-free scalp EEGs. We included 23 children (6 with, 17 without epilepsy) who had an EEG without interictal epileptiform spikes recorded during sleep. We differentiated true ripples from spurious ripples such as filtering effects of sharp artifacts and high-frequency components of muscle artifacts by viewing ripples simultaneously in bipolar and average montage and double-checking the unfiltered signal. We calculated mean frequency, duration and root mean square amplitude of the ripples, and studied their shape and distribution. We found ripples in EEGs of 20 out of 23 children (4 with, 16 without epilepsy). Ripples had a regular shape and occurred mostly on central and midline channels. Mean frequency was 102 Hz, mean duration 70 ms, mean root mean square amplitude 0.95 μV. Ripples occurring in normal EEGs of children without epilepsy were considered physiological; the similarity in appearance suggested that the ripples occurring in normal EEGs of children with epilepsy were also physiological. The finding that it is possible to study physiological neocortical ripples in scalp EEG paves the way for investigating their occurrence during brain development and their relation with cognitive functioning.

Introduction

High-frequency oscillations (HFOs) are oscillations above 80 Hz that are recorded from the brain. They are often defined as four or more oscillations that clearly stand out from the background activity. HFOs are divided in ripples (80–250 Hz) and fast ripples (250–500 Hz). Both physiological and pathological HFOs exist. Pathological HFOs are considered biomarkers for epilepsy.[8,83,84] Physiological ripples that are recorded in the hippocampus play a role in memory consolidation.[6,27,85] Characteristics of physiological and pathological ripples occurring in people with epilepsy overlap,[63,65,86,87] which makes distinguishing between the two types of ripples challenging.

HFOs were first recorded with implanted microelectrodes, but later also with intracranial macroelectrodes.[21,22] The detection of pathological ripples in scalp EEGs with frequent interictal epileptiform discharges or spikes meant that HFO research was no longer restricted to patients undergoing invasive recordings.[23,24]

Recognizing ripples in scalp EEG is challenging because the amplitude of non-invasively recorded ripples is low and because of the occurrence of muscle artifacts. Muscle artifacts hinder ripple marking in two ways. First, artifacts can obscure the signal, resulting in missed ripples (false negatives). Second, the high-frequency component of short muscle artifacts can look like ripples, which, if marked, would be false positives.

The challenges of marking ripples in scalp EEG have been dealt with by selecting recordings with relatively few artifacts and by avoiding most artifacts. Sleep recordings have relatively few artifacts because there is little muscle activity during sleep. Avoiding most artifacts can be done by marking pathological ripples that occur on epileptic spikes, because the search for ripples is then limited to the timeframe of the spike. However, this approach has the disadvantage that all information about ripple activity in traces without spikes is lost.

This study first addressed the question: Which settings promote recognizing ripples in spike-free scalp EEG and prevent confusion with spurious ripples such as high-frequency components of artifacts? The second question was: Do ripples occur in spike free scalp EEG of children with and without epilepsy, and if they do, what are their characteristics? If ripples would occur in normal EEGs of children without epilepsy, we would consider these ripples physiological ripples. If ripples would occur in normal EEGs of children with epilepsy, these ripples could be physiological or pathological ripples.

Materials and Methods

Inclusion criteria

We retrospectively studied EEGs of children (17 years or younger) who had visited our outpatient first seizure clinic because they were suspected of having had one or more (first) seizure(s). We selected all children who fulfilled the following

inclusion criteria: 1) EEG recorded at high sampling rate (2048 Hz) and containing at least 10 min of sleep recording, 2) no seizures and no interictal epileptiform discharges or other abnormalities during wake or sleep EEG, according to the clinical reports of specialized epileptologists, 3) no use of anti-epileptic drugs during EEG recording, 4) no structural lesion on MRI (if available), and 5) at least 1 year of follow-up.

Inclusion started in May 2013 because data were routinely sampled at high-frequency from that date, and ended in February 2016 to allow a follow-up period of at least 1 year.

We asked informed consent for studying the EEGs and clinical files from parents and from children who were, at the time of the study, 16 years or older. The study was approved by the Medical Research Ethics Committee of the University Medical Center Utrecht who judged that the Dutch Medical Research Involving Human Subjects Act did not apply, provided that data were coded and handled anonymously and informed consent was obtained.

Follow-up and diagnosis

Not all children who visited our outpatient clinic had or developed epilepsy. When we started the study, most children were no longer consulting a pediatric neurologist in our hospital. RR telephoned all parents and children who were over 16 years to collect follow-up data. The minimum follow-up was 1 year. A specialized pediatric neurologist (KB), who was blinded for the results of the ripple marking, determined the diagnosis based on the clinical file and the outcome of the telephone conversation. Children were categorized in two groups: 1) no diagnosis of epilepsy, and 2) diagnosis of epilepsy. Both groups had two subgroups: 1a) no epilepsy and no other brain disorder, 1b) no epilepsy, but another brain disorder (for example migraine or autism), 2a) benign-course epilepsy (for example benign occipital epilepsy syndrome), and 2b) other types of epilepsy (for example frontal lobe epilepsy).

Data acquisition

Scalp EEGs were recorded with Micromed Smart Acquisition Module (SAM) and with SD PLUS FLEXI acquisition system (Micromed, Treviso, Italy). Data were sampled at 2048 Hz, low-pass anti-alias filter at acquisition was 900 Hz for SAM and 553 Hz for FLEXI. We used conventional 10 mm Ag–AgCl electrodes that were placed according to the international 10–20 system.

Recognizing ripples and avoiding confusion with artifacts

We visually marked ripples in Stellate Harmonie (Montreal, Canada). The signal was filtered between 80 Hz (finite impulse response high-pass filter of order 63, as implemented in Harmonie) and 250 Hz (finite impulse response low-pass filter, order 63), amplitude scale was set to 1 μV per mm. We selected sleep recordings and started marking when most artifacts had subsided, even if this was after sleep onset. If short artifacts, for example caused by an arousal or by sudden movements

of the head or limps, obscured the signal, we excluded the time-frame of the EEG in which these artifacts occurred for all channels. In this way, all obvious artifacts were discarded.

We discovered that it was easiest to recognize ripples and to prevent confusion with spurious ripples such as high-frequency components of artifacts when we split the window vertically and viewed the high-frequency signal simultaneously in bipolar (double banana) and average montage. Time scale of both windows was 0.4 s per page. The advantage of viewing the signal in average montage was that ripples often stood out more clearly from the background activity compared to the same event viewed in bipolar montage. However, a disadvantage of the average montage was that an artifact recorded by one electrode, for example T7, could in an average montage give rise to spurious ripples on several channels, even those located far from the electrode with the artifact. This problem did not occur in a bipolar montage: an artifact in T7 was visible in channels F7-T7 and T7-P7 only. The bipolar montage was therefore important to determine if the ripple that was spotted in the average montage was false or real. We also checked the signal below 80 Hz in both montage to make sure the event was no muscle artifact or filtering effect. If we would remain doubtful if a ripple was real despite these precautions, we did not mark the ripple.

We marked ripples in both montages and in all channels. Events were marked as ripples if they consisted of four or more oscillations that clearly stood out from the background activity. If background low-amplitude ripple band activity built up to visually recognizable ripple oscillations, we started marking when the oscillations stood out clearly from the overall background activity of the channel. When the time-window of a ripple partly overlapped with that of a ripple on another channel, we marked both ripples. Ripple marking was done by AM and checked by MZ.

Cumulative ripple rate

We used ripple rate per minute, calculated over a period of 10 minutes, as a measure of frequency of ripple occurrence. We first summed the number of ripples occurring in all channels per minute. If the sleep recording was longer than 10 minutes, we selected the ten consecutive minutes in which the maximum number of ripples occurred. The actual time available for marking ripple during those 10 minutes might be shorter because of the occurrence of artifacts. Thus, cumulative ripple rate per minute was calculated by taking the total number of ripples occurring in the 10 minutes with the maximum number of ripples for that child and dividing it by 10 minutes minus the duration of artifacts during those 10 minutes.

Ripple characteristics and distribution

Ripples are marked in bipolar montage in almost all HFO studies. We calculated frequency, duration, and root mean square amplitude of ripples marked in bipolar montage to enable comparison with these characteristics reported in other studies. Frequency was calculated from the number of zero crossings, root mean

square amplitude was computed as the square root of the average power. All ripple characteristics were calculated in filtered (80–250 Hz) data using Matlab (version R2015b, The MathWorks Inc., USA.).

We counted the number of ripples per channel and summed the number of ripples per channel of all children for a general overview of the distribution of these events.

Results

Characteristics of included children and occurrence of ripples across diagnostic groups

Twenty-six children met the inclusion criteria. We obtained informed consent for using the EEGs and clinical data for 23 children (14 boys), aged 11 months to 14 years at the time of the recording. Ten children had no epilepsy, and no other brain disorder (category 1a). Seven had no epilepsy, but another brain disorder (category 1b): there were two children with migraine, two children with autism spectrum disorder, one child with a chromosomal microduplication and autism, one child with GLUT1 (Glucose Transport type 1) deficiency syndrome, and one child with a history of acute symptomatic seizures during bacterial meningitis. Three children had benign-course epilepsy (category 2a), and three children had other types of epilepsy (category 2b). We found ripples in the EEGs of 20 out of 23 children: in 9 out of 10 EEGs of children in category 1a, in all EEGs of children in category 1b and 2a, and in 1 out of 3 EEGs of children in category 2b. Characteristics of included children are provided in Supplementary Table 5.1.

Ripple rate

The longest sleep recording was 47 min, the shortest 10 min. Most events occurred in the first 10 min of the sleep recording in most children (16 out of 20 children). In two children, most ripples occurred in 10 min that partly overlapped with the first 10 min; in the other two children, most ripples occurred in completely different 10 min epochs.

Cumulative bipolar ripple rate ranged from 0.0 to 25.0 ripples per minute, ripple rate in most children was below 5 ripples per minute (Figure 5.1; Supplementary Table 5.1).

Ripple characteristics

Ripples had a regular shape (Figure 5.2B), more so than ripples on epileptic spikes (Figure 5.2D). The EEG with spikes, illustrated in this figure, was not included in this study; the examples of ripples on spikes are provided for comparison with the examples of ripples marked in this study. Examples of the corresponding low-frequency signal are provided in Figure 5.2A and C, examples of EEG traces containing both low- and high-frequencies are provided in Supplementary Figure 5.1.

Median frequency ranged from 91 to 116 Hz. The mean of the 20 medians was 102 Hz. Median duration ranged from 55 to 85 ms, the mean of medians was

69 ms. Root mean square amplitude ranged from 0.76 to 1.39 μV, mean of medians was 0.95 μV. An impression of the amplitude of the ripples can be obtained from Figure 5.2B.

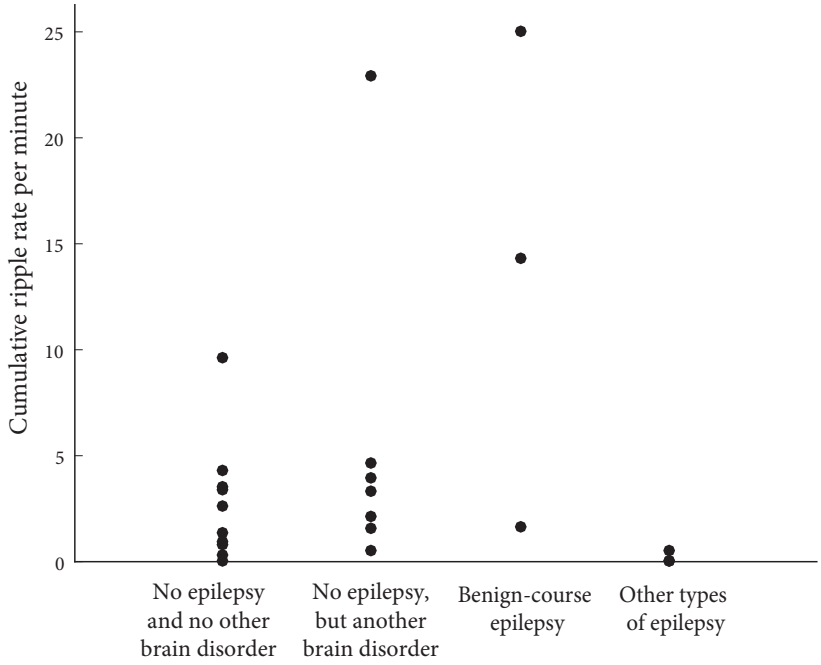

Figure 5.1 Plot of the ripple rate per child in each diagnostic category. Cumulative ripple rate per minute was calculated by taking the total number of ripples (in the 10 minutes with the maximum number of ripples for that child) and dividing it by 10 minutes (minus the duration of artifacts during those 10 minutes). Ripples occurred across all diagnostic categories.

Ripple distribution

Total number of ripples per child ranged from 4 to 364 for channels in bipolar montage, and from 4 to 238 for channels in average montage. We summed the number of events per channel of all children and found that most events occurred on Cz-Pz (374 ripples, 26% of total number of ripples marked in bipolar montage), Fz-Cz (224 ripples, 16%), and Pz-O2 (139 ripples, 10%). For the average montage, the three channels with most ripples were Cz (364 ripples, 34% of total number of ripples marked in average montage), Pz (129 ripples, 12%), and C4 (101 ripples, 9%). The average montage seemed the more precise montage for studying the localization of ripples. For example, Figure 5.2B shows that ripples occurring on bipolar channels Fp1-Fz, Fz-Cz, and Cz-Pz are only visible on Fz and Cz in the average montage. Distribution of all ripples marked in average montage is shown in Figure 5.3.

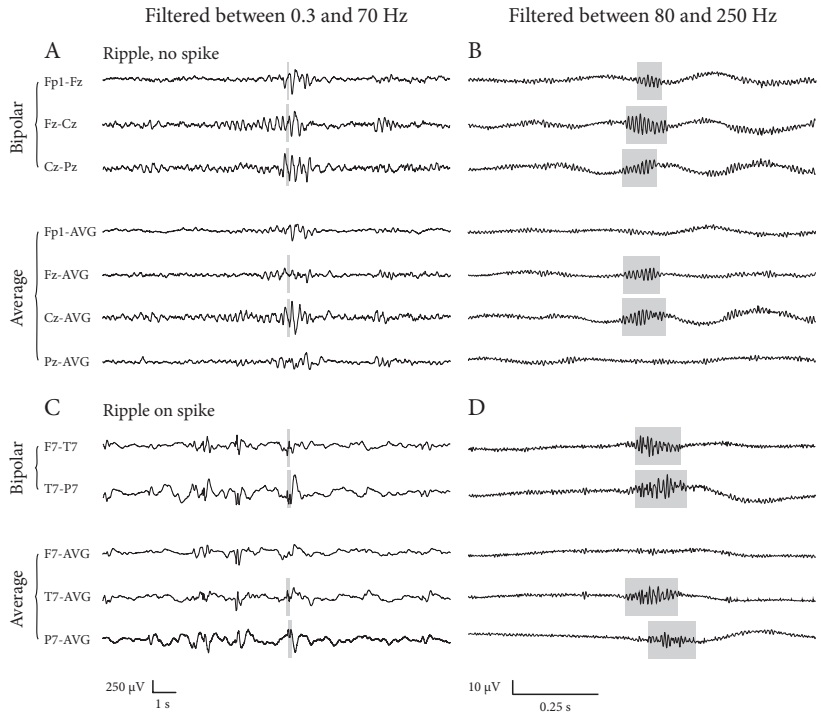

Figure 5.2 Examples of ripples marked in this study (B), which do not occur on spikes (see corresponding grey area in (A)) and of ripples (D) that occur on epileptic spikes (see corresponding grey area in (C)). The EEG with epileptic spikes was not included in this study, the examples are shown for comparison with the ripples shown in (D). The EEG traces in A and C are filtered between 0.3 and 70 Hz, time scale is 15 s per page, amplitude scale is 30 µV per mm. The EEG traces in B and D are filtered between 80 and 250 Hz, time scale is 1 s per page, amplitude scale is 1 µV per mm. Channels are shown in bipolar and average montage. Note the difference in appearance of the regular ripples in B and the more irregular ripples in D.

Ripple rate and age

The choice to study children was a practical one: recording at high sampling rate started in our hospital in this cohort of children. We had no specific hypothesis about a relation between ripple rate and age, but noticed that high ripple rates seemed to occur particularly in young children. We plotted the data to get an impression if this might be a topic that would merit future research in a bigger cohort. A scatter plot with age on the x-axis and cumulative ripple rate on the y-axis showed that high ripple rates occurred in children under five, and the oldest two children, who were 13 and 14 years old when the EEG was recorded, had no

ripples (Figure 5.4). This suggested there might be an age-related pattern. On the other hand, most children between 1 and 9 years old had ripples rates between 0 and 5 ripples per minute, without any clear age-related trend.

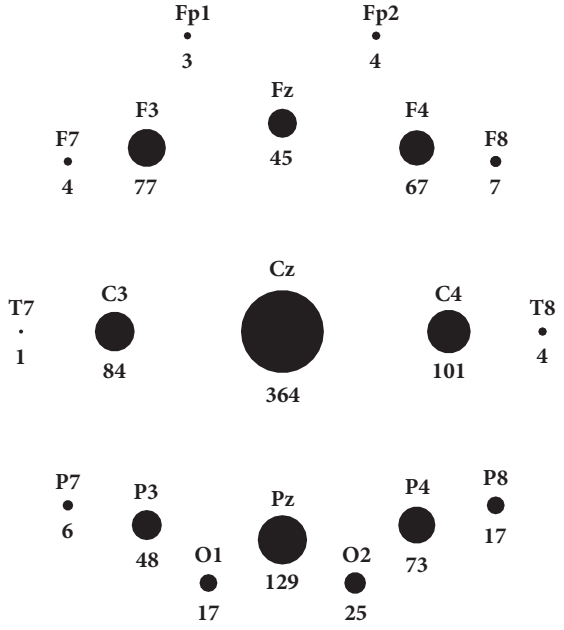

Figure 5.3 Schematic overview of the number of ripples per channel, marked in average montage. Number of ripples is written underneath the black circle that represents the channel, and reflected in the size of the black circle. Ripples occurred most frequently in central and midline channels, particularly Cz.

Discussion

This HFO study showed that it is feasible to mark ripples in spike-free scalp EEGs. Comparing the occurrence, distribution, and shape of ripples in bipolar and average montage, as well as double-checking the unfiltered signal in both montages, promotes recognizing ripples and prevents confusion with spurious ripples such as high-frequency components of artifacts.

Ripples occurred in 16 out of 17 normal EEGs of children without epilepsy. These ripples were considered physiological ripples. They had a regular shape; their appearance differed from the shape of pathological ripples that occur on spikes.

Ripples also occurred in four out of six normal scalp EEG of children with epilepsy. These ripples had the same regular shape as ripples marked in the EEGs of healthy children. We therefore think that the ripples marked in EEGs of children with epilepsy were also physiological. Another reason to think these ripples were

physiological is that pathological ripples are probably rare in spike-free scalp EEG. A study that looked at the occurrence of pathological ripples in EEGs with different spike rate found that there were fewer pathological ripples when spike rate was lower.[88] Melani et al. (2013) also included five EEGs without spikes; they found a few pathological ripples in only one of them.[88] Two of the three children with benign-course epilepsy (category 2a) included in this study had high ripple rate (Figure 5.1); it seems unlikely that so many pathological ripples should occur in spike-free EEGs. As for category 2b: two of the three children in this category had no ripples, the third, with epilepsy of unclear classification, had a ripple rate of 0.5 (i.e., 5 ripples in 10 min). Because of their regular shape and their occurrence in normal background, we think it unlikely that these ripples were pathological, but we cannot rule out this option completely.

Frequency and duration of ripples presented in this study were similar to those reported in previous studies on characteristics of physiological ripples.[63,65,87] Amplitude was not comparable, which is inherent to the fact that those studies used invasive recording techniques. Ripple rate was comparable to the rate reported by von Ellenrieder et al. (2016).[65]

Comparing distribution is complicated because electrode localization differs per patient when using invasive recording techniques. However, the centrally located ripples reported in this study might be the same type of oscillations that Wang et al. (2013) found in the primary motor cortex.[63] Our results differ from those of Alkawadri et al. (2014), who reported that highest rates of non-epileptic ripples occurred in occipital contacts.[87] We can think of two reasons why the number of occipital ripples might have been underestimated in the present study. First, most ripples occurred on central and midline channels. It is therefore plausible that the number of ripples would have been higher in an Oz channel (or Pz-Oz, in a bipolar montage) than in (Pz-)O2 or (Pz-)O1. The second reason is that if people sleep lying on their back, most artifacts in scalp EEG occur in occipital channels. The chance of finding spurious ripples was therefore higher in these channels. This had no effect on the procedure for marking ripples, which was the same as in other channels, but we were especially cautious when marking ripples in occipital channels, and as a result we might inadvertently have discarded some true ripples.

We could not find any studies on spontaneously occurring physiological HFOs recorded with scalp EEG. In the field of cognitive neuroscience most reports focus on high-frequency spectral power that is evoked or induced by a stimulus or task. This approach has the advantage that one knows when to expect the high-frequency activity, and challenges of artifacts can sometimes be dealt with by averaging the evoked response. Spontaneously occurring high-frequency activity that was visible on time-frequency plots has also been reported. Menicucci et al. (2013) recorded activity up to 125 Hz in healthy sleeping adults and Chu et al. (2014) found activity up to 95 Hz in healthy sleeping children of 0–18 years.[89,90] However, neither of these studies provided detailed information about oscillations, and, as Buszáki and Lopes da Silva (2012) wrote: "…increased power in a given band does not warranty the presence of an oscillation".[78]

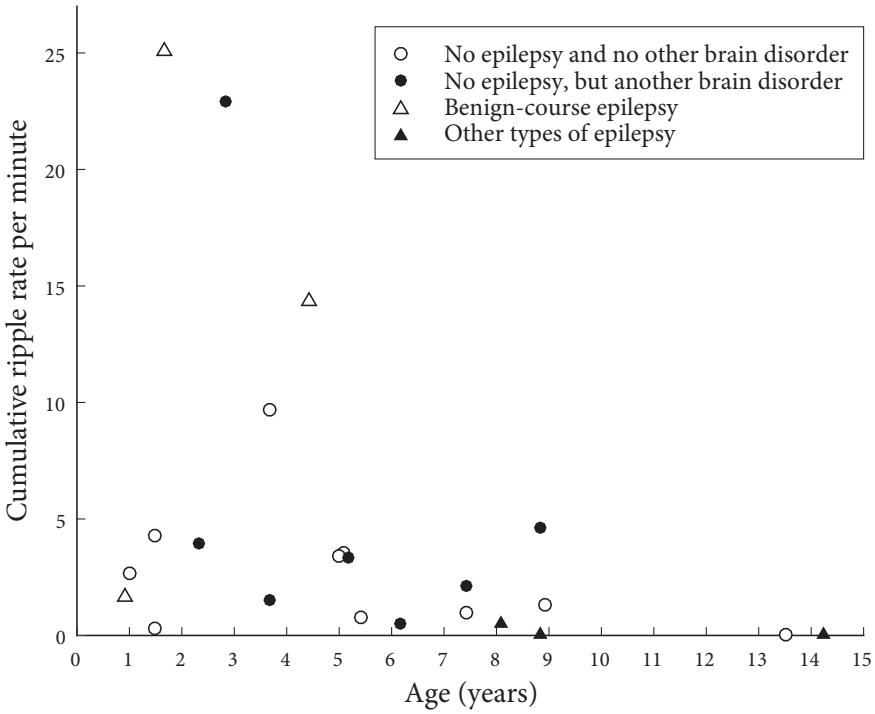

Figure 5.4 Scatterplot of age versus cumulative ripple rate. Ripple rates of children without a neurological diagnosis are plotted as open circles, ripple rates of children without epilepsy, but with another brain disorder as closed circles. Ripple rate of children with benign-course epilepsy are plotted as open triangles, ripple rate of children with other types of epilepsy as closed triangles.

The figure of ripple rate and age showed no clear age-related pattern, but there might be a trend of a decreasing ripple rate in older children. The previously mentioned study of children of 0–18 years reported that high-frequency power increased steadily after 5 years, most prominently in the central regions.[90] Although this central distribution matches the distribution found in our study, Chu et al. (2014) might have reported about different high-frequency activity. They studied a wider and lower frequency band (50–100 Hz) than our observed frequencies (91–116 Hz) and we cannot retrieve any details of the oscillations, because the authors provided only time-frequency plots. However, these potentially conflicting findings suggest that the development of physiological HFOs in children is a relevant topic for future research. Future studies are also needed to test if these ripples occur in adults.

Can these physiological ripples be related to the hippocampal physiological ripples that play a role in memory consolidation? We know of no studies that show a direct link between physiological ripples in the hippocampus and neocortex,

but the HFO literature suggests that hippocampal and neocortical ripples might be connected through sleep oscillations such as spindles and slow waves. Several papers report that the physiological ripples occurring in the hippocampus are linked to such sleep phenomena (for example,[27,85]) and coupling between neocortical ripples and sleep phenomena was shown in healthy animals[91,92] and in people with chronic epilepsy and implanted electrodes.[65,77,93] While checking the unfiltered signal, we noticed that the ripples reported here also seem to co-occur with sleep phenomena. Our first impression was that ripples were not limited to spindles and slow waves, but also occurred during sharper physiological transients such as vertex waves and hypnagogic hypersynchrony. Our next step will be to do a quantitative analysis of the co-occurrence of ripples and sleep oscillations. The fact that we study spike-free EEGs might be advantageous for investigating the relation between physiological ripples and sleep phenomena, as interictal spikes were shown to affect sleep patterns.[94]

Limitations

A limitation of this study is the small number of subjects. Unfortunately, such a small sample size is hard to avoid. The required high sampling rate limited the period in which children could be included, because routine recording at high sampling rate started in 2013. Moreover, normal sleep EEGs were rare, particularly in children with epilepsy. Of the 315 children with an EEG recorded at high sampling rate, only 26 fulfilled all the inclusion criteria.

A second limitation is that the normal EEGs were obtained in a clinical setting. None of the children in this study suffered from chronic epilepsy when the EEG that was analyzed in this study was made, and ten children had no neurological diagnosis after a follow-up period of at least 1 year. The similarity in appearance of ripples occurring in normal EEGs of children across diagnostic groups, including healthy children, suggests that the ripples described in this study are physiological. We can, however, not rule out the option that the ripples found in the children with a brain disorder other than epilepsy reflect some kind of pathological, albeit not epileptic, events. We hope that the finding that it is possible to study ripples in normal scalp EEG will inspire research on spontaneously occurring HFOs in healthy participants who have never been suspected of having any neurological or psychiatric disorder. Such studies are also needed to investigate the relation of these ripples to physiological brain functions.

Conclusion and future directions

This is the first study to report spontaneously occurring physiological ripples recorded with scalp EEG. The next step is to investigate their occurrence across sleep stages and their co-occurrence with sleep oscillations. Future studies should clarify if these ripples occur only in children, with a potential relation to brain development, or can also be found in adults.

Supplementary material

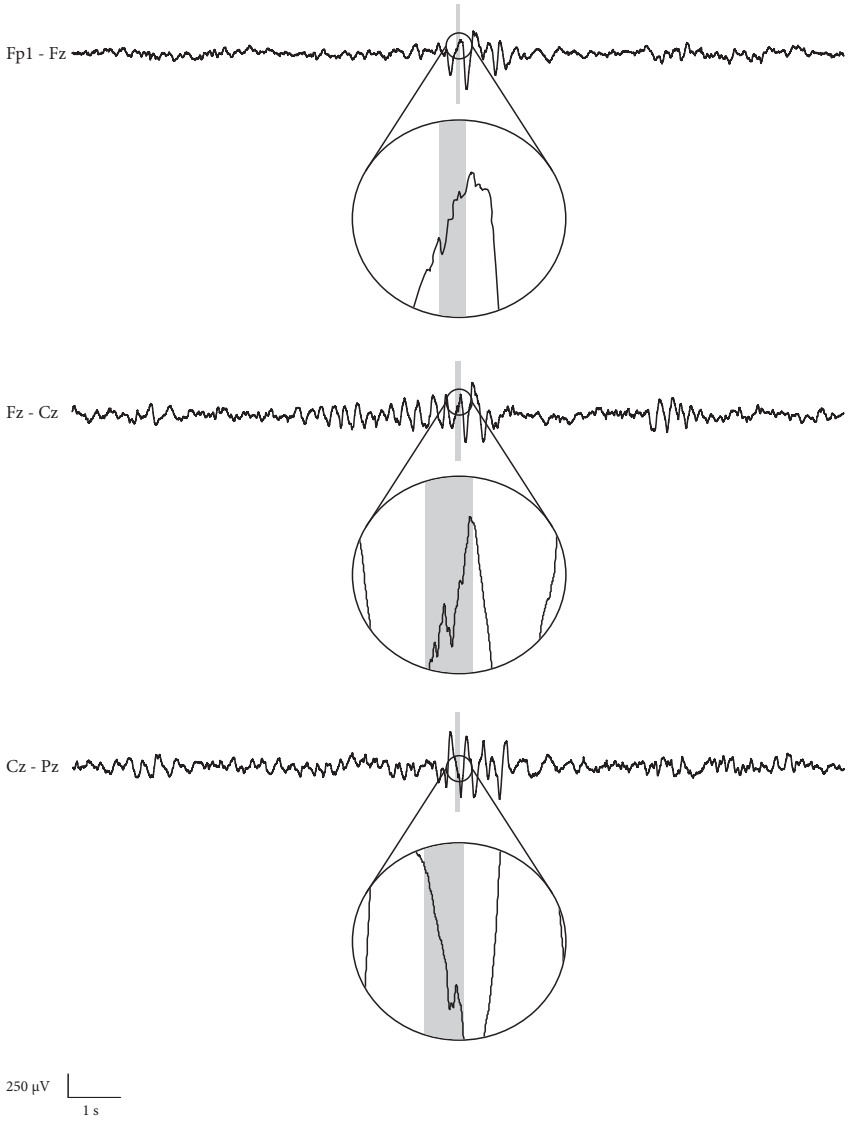

Supplementary Figure 5.1 Examples of EEG traces containing low- and high-frequencies. This figure shows the same traces as in Figure 5.2A (bipolar channels), but the low-pass filter is 250 Hz instead of 70 Hz. Time scale is 15 seconds per page, amplitude scale is 30 µV per mm. An enlargement of the grey area containing the ripple marking (see also Figure 5.2B) is shown below each trace.

Supplementary Table 5.1 Characteristics of included children

Subject number	Gender	Age at time of sleep EEG	Ripple rate per minute[1]	Duration follow-up	Diagnosis	Diagnostic category[2]
1	M	1y8m	25.0	3y7m	Probably benign childhood epilepsy variant, exact classification unclear	2a
2	M	3y8m	1.6	3y4m	Glut 1 deficiency syndrome, no epilepsy	1b
3	M	14y3m	0.0	3y4m	Idiopathic generalized epilepsy with nocturnal GTCS	2b
4	F	13y6m	0.0	3y3m	No epilepsy, no diagnosis	1a
5	M	2y4m	3.9	3y5m	Autism	1b
6	M	1y6m	4.3	3y3m	No epilepsy, no diagnosis	1a
7	M	5y1m	3.5	3y3m	No epilepsy, possibly sleep disorder	1a
8	M	2y10m	22.9	3y1m	No epilepsy at time of follow-up, in the past acute symptomatic seizures during bacterial meningitis	1b
9	M	3y8m	9.7	3y0m	Diagnosis unclear, epilepsy highly unlikely	1a
10	F	5y0m	3.4	2y9m	No epilepsy, no other diagnosis	1a
11	F	7y5m	1.0	2y9m	No epilepsy, tics	1a
12	M	8y11m	1.3	1y9m	No epilepsy, no other diagnosis	1a
13	M	8y10m	4.7	2y7m	No epilepsy, tic syndrome, and autism spectrum disorder	1b
14	F	7y5m	2.1	2y6m	CACNA1A deficiency, migraine, no proof of diagnosis epilepsy	1b
15	F	8y10m	0.0	2y0m	Frontal lobe epilepsy of unknown cause	2b
16	M	5y2m	3.3	2y0m	No proof of epilepsy, chromosomal microduplication syndrome and autism	1b

table continues

Sub-ject num-ber	Gen-der	Age at time of sleep EEG	Ripple rate per minute[1]	Duration follow-up	Diagnosis	Diagnostic category[2]
17	F	0y11m	1.7	2y1m	Benign infantile epilepsy syndrome	2a
18	M	1y6m	0.3	2y0m	No epilepsy, no diagnosis	1a
19	F	4y5m	14.3	1y9m	Benign occipital epilepsy syndrome	2a
20	M	1y0m	2.7	1y7m	No epilepsy, no diagnosis	1a
21	F	6y2m	0.5	1y3m	Migraine, epilepsy not definitely excluded	1b
22	F	8y1m	0.5	1y0m	Epilepsy, unclear classification	2b
23	M	5y5m	0.8	1y0m	No clear epilepsy, no other diagnosis	1a

[1] Calculated by taking the total number of ripples (of all channels in the 10 minutes with the maximum number of ripples for that child) and dividing it by 10 minutes (minus the duration of artifacts during those 10 minutes).
[2]1a) No epilepsy and no other brain disorder; 1b) No epilepsy, but another brain disorder; 2a) Benign-course epilepsy; 2b) Other types of epilepsy
GTCS: Generalized tonic-clonic seizures

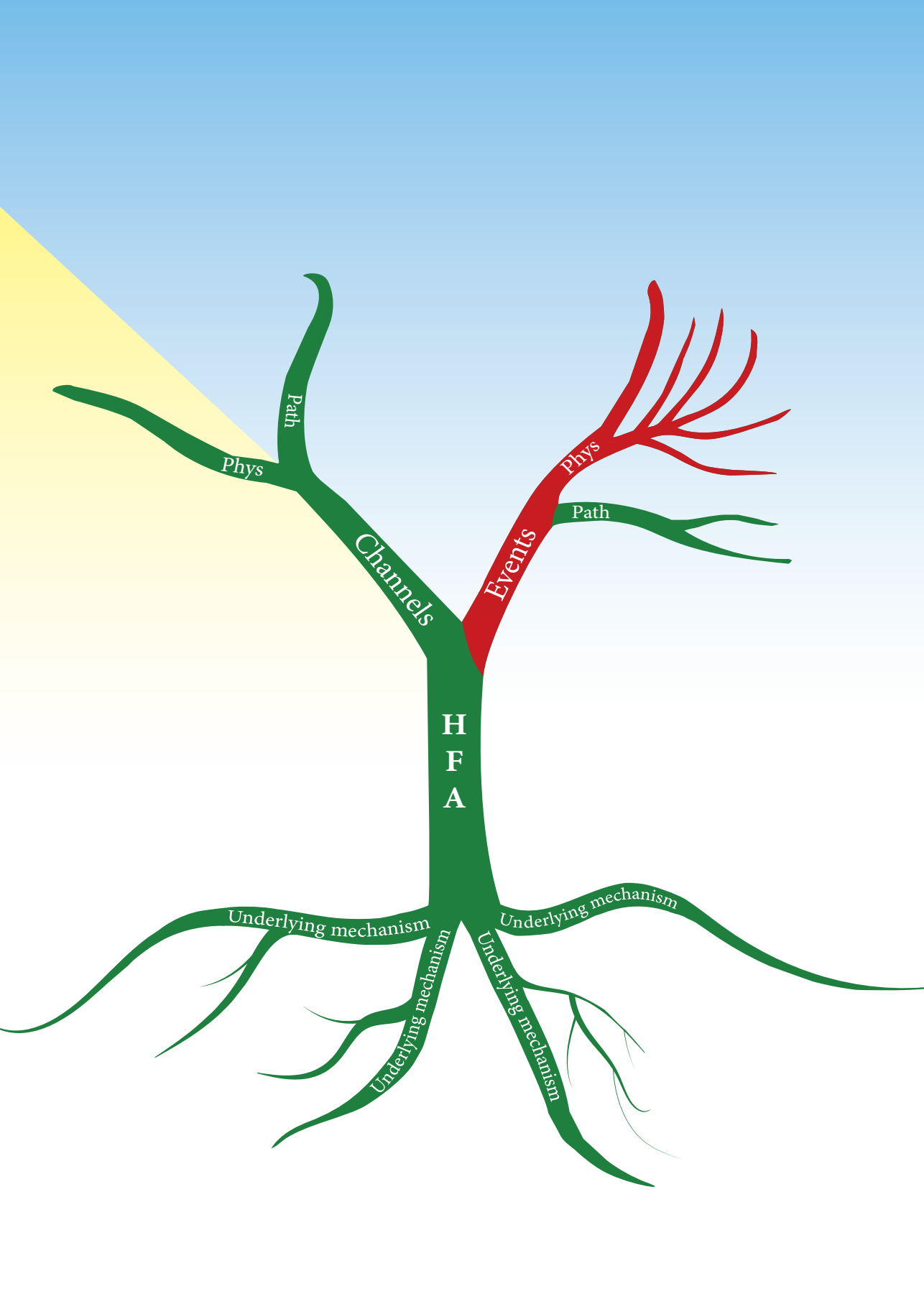
Phys
Path
Channels
Events
Phys
Path
H
F
A
Underlying mechanism
Underlying mechanism
Underlying mechanism
Underlying mechanism

Chapter 6

Ripples in scalp EEGs of children: co-occurrence with sleep-specific transients and occurrence across sleep stages

Anne H. Mooij
Birgit Frauscher
Sophie A.M. Goemans
Geertjan J.M. Huiskamp
Kees P.J. Braun
Maeike Zijlmans

SLEEP 2018; 41:1-9

Abstract

Objectives
A dialogue between hippocampal ripples (80-250 Hz) and neocortical sleep-specific transients is important for memory consolidation. Physiological neocortical ripples can be recognized in scalp EEGs of children. We investigated how often scalp-EEG recorded ripples co-occur with different types of sleep-specific transients, the distribution and spatial extent of ripples with and without co-occurring sleep-specific transients, and the occurrence of ripples across sleep stages.

Methods
We marked ripples in daytime sleep-EEGs of 19 children and determined for each ripple if it co-occurred with a sleep-specific transient. We compared the distribution of ripples without co-occurring sleep-specific transients to the distribution of all ripples. We estimated the spatial extent of simultaneously occurring ripples by counting how many EEG regions they comprised. We compared ripple rate per sleep stage using Friedman's analysis of variance and Wilcoxon signed-rank test.

Results
74.4% of ripples co-occurred with sleep-specific transients: 27.8% with vertex waves, 14.7% with hypnagogic hypersynchrony, 13.7% with slow waves, 12.2% with spindles, and 6.0% with K-complexes. Ripples without co-occurring sleep-specific transients showed the same central dominance but a significantly less pronounced midline dominance than the overall distribution pattern. Spatial extent was larger when ripples co-occurred with sleep-specific transients. Ripple rates during nonrapid eye movement (N) sleep stages N1 and N2 were higher than during N3 ($T = 22.00$, $p = 0.02$ and $T = 23.00$, $p = 0.01$).

Conclusions
Scalp-EEG recorded physiological ripples co-occur with various sleep-specific EEG-transients, especially with vertex waves. These ripples occur most frequently during light sleep.

Introduction

Ripples are brain oscillations of frequencies between 80 and 250 Hz. Ripples have been recorded in the hippocampus and neocortex of animals and humans.[19,20,63,65,70,71,77,86,87,91–93,95–104] There are physiological ripples and pathological ripples. Pathological ripples are considered biomarkers for epilepsy.[8,83,84] Physiological ripples that occur in the hippocampus interact with neocortical sleep oscillations.[85,105,106] The resulting hippocampal-cortical dialogue is important for memory consolidation.[6,27,85,107] Physiological neocortical ripples also co-occur with sleep-specific transients.[65,77,91–93,96]

Differentiating physiological from pathological ripples is difficult, because characteristics such as frequency, duration, and amplitude overlap.[63,65,86,87] Ripples that are recorded invasively in people with chronic epilepsy are considered physiological if they occur in channels without interictal epileptiform discharges and outside the seizure-onset zone.[65,77,86,87,103] A problem of this definition is that epileptic spikes occurring in the seizure onset zone can affect activity recorded in spike-free channels outside the seizure onset zone. For example, Gelinas et al. showed that epileptic spikes from the hippocampus can induce seemingly physiological spindles recorded in the neocortex.[94]

The risk of studying spike-induced spindles or confusing physiological ripples with pathological ripples can be minimized by studying scalp EEGs of healthy participants. We have recently reported that ripples can be recognized in spike-free scalp EEGs recorded during sleep.[108] In this study, we analyzed the same spike-free scalp EEGs to address the following research questions: 1) Do scalp-EEG recorded ripples co-occur with sleep-specific transients? 2) Is the previously described[108] central and midline dominant distribution pattern of ripples due to the preferred location of co-occurring sleep-specific transients? 3) Is there a difference in spatial extent between ripples with and ripples without co-occurring sleep-specific transients? 4) What is the ripple rate per sleep stage?

Methods

Participants

We previously reported that we found ripples in scalp EEGs of 20 children.[108] All EEGs were judged by a specialized clinical neurophysiologist to be free of epileptic discharges or other abnormalities. None of the children used antiepileptic drugs when undergoing the EEG. All MRIs (if available) were normal. One child underwent an MRI after the completion of our previous study. The MRI showed a structural lesion (mesial temporal sclerosis). This child was therefore excluded from the present study.

We included the remaining 19 children, aged 11 months to 8 years. The children visited our outpatient clinic after a first seizure-like event, the EEGs were recorded to investigate if they had epilepsy. The diagnosis was established after a follow-

up period of at least 1 year. Nine children had no epilepsy and no other brain disorder. Seven children had no epilepsy, but another brain disorder, such autism or migraine. Three children probably had benign-course epilepsy: these children had only a few seizure-like events and the last of these events occurred in 2015 (two children) or 2016 (one child).

Parents of the included children gave informed consent. The study was approved by the Medical Research Ethics Committee of the University Medical Center Utrecht, who judged that the Dutch Medical Research Involving Human Subjects Act did not apply, provided that data were coded and handled anonymously and informed consent was obtained.

Sleep recordings

We studied daytime sleep-EEGs; the duration of the recorded sleep varied from 10 to 46 min. The EEGs of 16 children were recorded after partial sleep deprivation. Duration of sleep deprivation varied with age. Three children slept spontaneously during the EEG without prior sleep deprivation.

Ripple marking

Scalp EEGs were recorded with Micromed Smart Acquisition Module (SAM) and with SD PLUS FLEXI acquisition system (Micromed, Treviso, Italy). Data were sampled at 2048 Hz, and low-pass anti-alias filter at acquisition was 900 Hz for SAM and 553 Hz for FLEXI. We used conventional 10 mm Ag-AgCl electrodes that were placed according to the international 10-20 system.

Ripples were marked in Stellate Harmonie (Montreal, Canada) as described previously.[108] Briefly, the signal was filtered between 80 Hz (finite impulse response high-pass filter of order 63) and 250 Hz (finite impulse response low-pass filter of order 63), amplitude scale was set to 1 μV per mm. Events were marked as ripples if they consisted of four or more oscillations that clearly stood out from the background activity. We minimized the chance of marking spurious ripples such as high-frequency components of artifacts by simultaneously viewing ripples in bipolar and average montage and double-checking the unfiltered signal. The time scale of both windows was 0.4 s per page. Ripple marking was done independently of the marking of sleep-specific transients or sleep stages. We used ripples marked in bipolar (double banana) montage for further analyses.

Marking of sleep-specific transients

Sleep-specific transients were marked in bipolar (double banana) montage by a board-certified sleep specialist who did not mark the ripples. A ripple was considered to co-occur with a sleep-specific transient if it occurred at any point within the longer duration of the sleep-specific transient. Thus, the sleep specialist marked for each ripple if there was an ongoing vertex wave, sleep spindle, slow wave, K-complex, hypnagogic hypersynchrony, or positive occipital sharp transient of sleep on the same channel. All sleep-specific transients were defined according to AASM criteria.[26]

Marking of sleep stages
Sleep was scored visually in 30 s epochs according to AASM criteria.[26] Electrodes F3, C3, and O1 as well as F4, C4, and O2 were referenced against the contralateral ear. The starting point for ripple marking was the moment after sleep onset that most artifacts had subsided, regardless of the sleep stage. This starting point might therefore lie after onset of nonrapid eye movement sleep stage 1 (N1), or, if artifacts persisted throughout N1, in N2. If short artifacts, for example, caused by an arousal or by sudden movements of the head or limps, obscured the signal, we excluded the time frame of the EEG in which these artifacts occurred for all channels. The duration of each sleep stage minus the duration of artifact epochs was calculated using Matlab (version R2015b, The MathWorks Inc., United States).

Spatial distribution
Ripples showed a central and midline dominant distribution pattern, as reported previously for ripples marked in average montage[108] and as shown in Figure 6.1 for ripples marked in bipolar montage. Sleep-specific transients are known to occur at certain 'preferred' locations. In children, vertex waves are found mostly on central or frontocentral channels,[109,110] spindles and K-complexes on central channels,[109,110] and slow waves on occipital channels.[111] Hypnagogic hypersynchrony is a generalized sleep-specific transient.[26,109] We expected that if ripples co-occurred in time and place with sleep-specific transients, their central and midline dominance would at least partly be due to the preferred location of sleep-specific transients. To evaluate if this was the case, we compared the distribution of ripples without co-occurring sleep-specific transients to the distribution of all ripples, from anterior to posterior and from left to right, using the χ^2 goodness of fit test. Statistical tests were performed in SPSS (IBM SPSS Statistics 23, IBM Corporation, United States).

Spatial extent
Ripples could occur alone or in clusters (Supplementary Figure 6.1). Ripples would be considered to belong to the same cluster if they started while there was an ongoing ripple on another channel. For brevity, all moments at which ripples occurred, alone or in clusters, will hereafter be called 'ripple moments.'

We estimated the spatial extent of ripple moments by counting how many scalp EEG areas were involved in the anterior-posterior direction (maximal 4 areas), in the left-right direction (maximal 5 areas), and in total (maximal 20 areas). The boundaries of the areas were determined in the anterior-posterior direction by the positions of the electrodes in 10-20 system placement. The left-right boundaries were less straightforward because we had no ripple markings in a transverse montage. The left-right boundaries were therefore chosen in between two adjacent 'bananas' of the double banana montage. Thus, the virtual boundaries of the bipolar channel Fz-Cz would lie halfway in between Fz-Cz and F3-C3 on the left and halfway in between Fz-Cz and F4-C4 on the right. The anterior boundary was Fz and the posterior boundary was Cz. Electrodes Fp1 and Fp2 were treated

as midline electrodes (Fpz) when connected to Fz, and O1 and O2 were treated as Oz when connected to Pz.

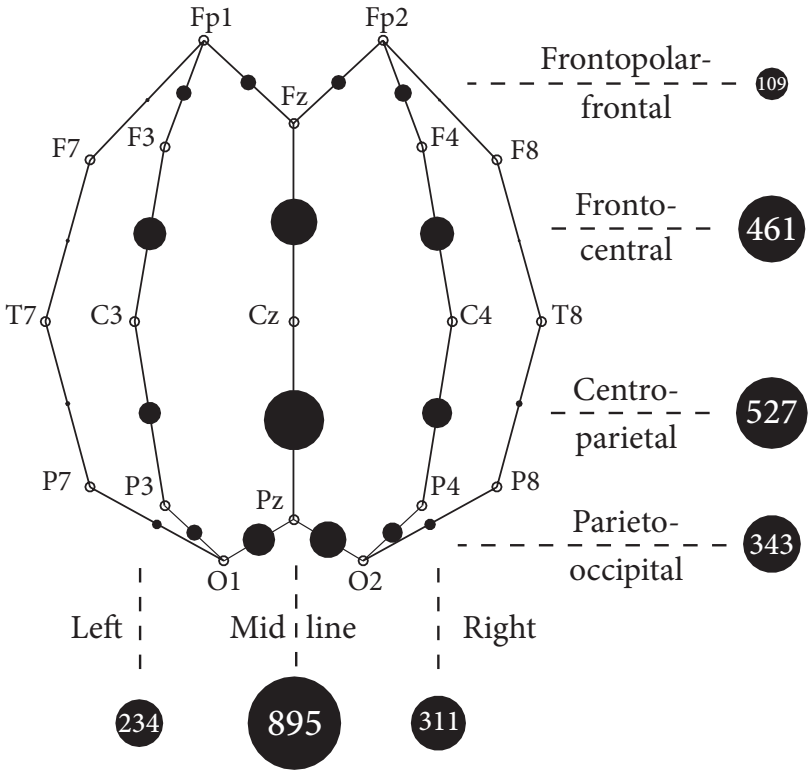

Figure 6.1 Distribution of ripples marked in bipolar montage, the total number of ripples occurring in all frontopolar-frontal, frontocentral, centroparietal, and parieto-occipital channels, and the total number of ripples occurring in all channels on the left, midline, and right.

Ripple rate per sleep stage

We tested if there was a significant difference between ripple rates during N1, N2, and N3 (these daytime sleep recordings did not contain rapid eye movement (REM) sleep) using Friedman's two-way analysis of variance by ranks (Friedman's ANOVA). We set α at 0.05. We used Wilcoxon's signed-rank test for post hoc testing. The same tests were performed for the rate per sleep stage of ripple moments. Statistical tests were performed in SPSS (IBM SPSS Statistics 23, IBM Corporation, United States).

Sleep-specific transients occur more often during certain sleep stages. For example, vertex waves occur mostly during N1 and slow waves occur most often

during N3.[26] Thus, if most ripples would co-occur with vertex waves, one would expect a higher ripple rate during N1, but if ripples co-occur most often with slow waves, ripple rate would be higher during N3. To assess ripple rate per sleep stage independently of co-occurring sleep-specific transients, we tested if there was a significant difference between ripple rates during N1, N2, and N3 for ripples and ripple moments without co-occurring sleep-specific transient.

Results

Co-occurrence with sleep-specific transients

We marked 1440 ripples in total, 25.6% of which had no co-occurring sleep-specific transient. The division per co-occurring sleep-specific transient of the remaining 74.4% was as follows: vertex waves: 27.8%; hypnagogic hypersynchrony: 14.7%; slow waves: 13.7%; spindles: 12.2%; and K-complexes: 6.0% (examples in Figure 6.2 and Supplementary Figure 6.2). There was one ripple that co-occurred with a positive occipital sharp transient of sleep.

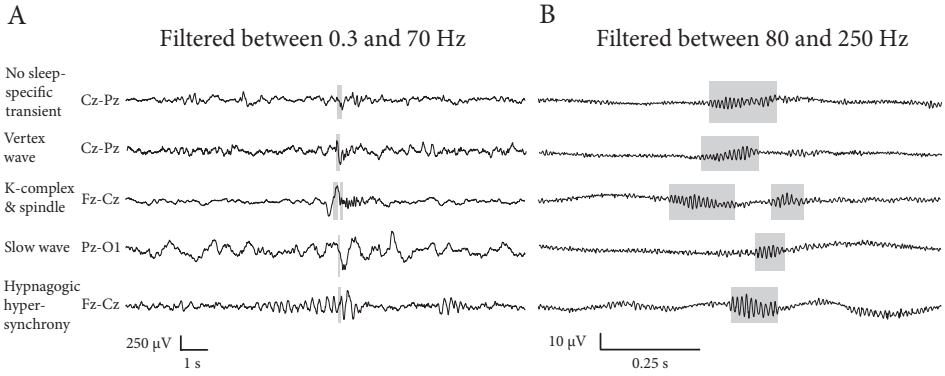

Figure 6.2 Examples of ripples with and without co-occurring sleep-specific transients. Examples were taken from EEGs of five different children. A) Traces were filtered between 0.3 and 70 Hz. Time scale is 15 s per page, amplitude scale is 30 µV/mm for all traces accept the trace with vertex wave and the trace with K-complex and spindle. The amplitude scale of these traces is 20 µV/mm to make the vertex wave and spindle more visible. B) Traces were filtered between 80 and 250 Hz. Time scale is 1 s per page and amplitude scale is 1 µV/mm. Gray areas in B correspond to gray areas in A.

Ripples co-occurred with two or more sleep-specific transients in all children (Supplementary Table 6.1). There were ripples without co-occurring sleep-specific transient in the EEGs of 17 out of 19 children. Ripples co-occurring with vertex waves were most prevalent: they were found in EEGs of 18 out of 19 children. Prevalence of ripples co-occurring with other sleep-specific transients

was as follows: ripple and slow wave: 15/19; ripple and spindle: 14/19; ripple and K-complex: 12/19; and ripple and hypnagogic hypersynchrony: 5/19.

Distribution per sleep-specific transient

As expected, ripples that co-occurred with vertex waves and spindles were recorded mostly on (fronto)central channels and ripples co-occurring with slow waves mostly on occipital channels (Figure 6.3). The distribution of ripples co-occurring with K-complexes resembled the distribution of ripples co-occurring with slow waves. Ripples co-occurring with vertex waves, spindles, slow waves, and K-complexes all showed a clear midline dominance. Ripples co-occurring with hypnagogic hypersynchrony were more evenly distributed, both in the anterior-posterior direction and from left to right.

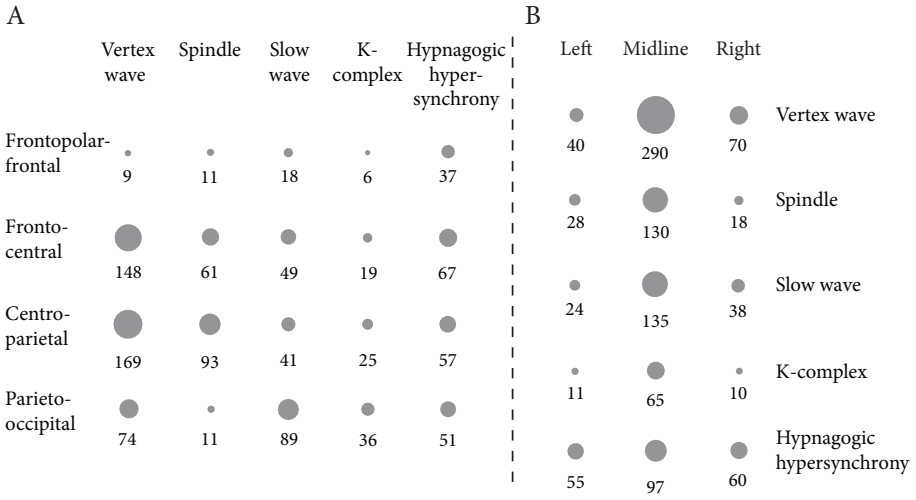

Figure 6.3 A and B: Number of ripples per location and per type of co-occurring sleep-specific transient. Note the central and midline dominance of ripples co-occurring with vertex waves and spindles, the occipital and midline dominance of ripples co-occurring with slow waves and K-complexes, and the more even distribution of ripples co-occurring with hypnagogic hypersynchrony.

The anterior-posterior distribution pattern of ripples without co-occurring sleep-specific transient resembled the overall distribution pattern ($\chi^2(3) = 0.91$, $p = 0.82$, Figure 6.4A). Ripples without co-occurring sleep-specific transients also showed a midline dominance, but significantly less pronounced than the general distribution pattern ($\chi^2(2) = 31.96$, $p = 1.15 \times 10^{-7}$; Figure 6.4B).

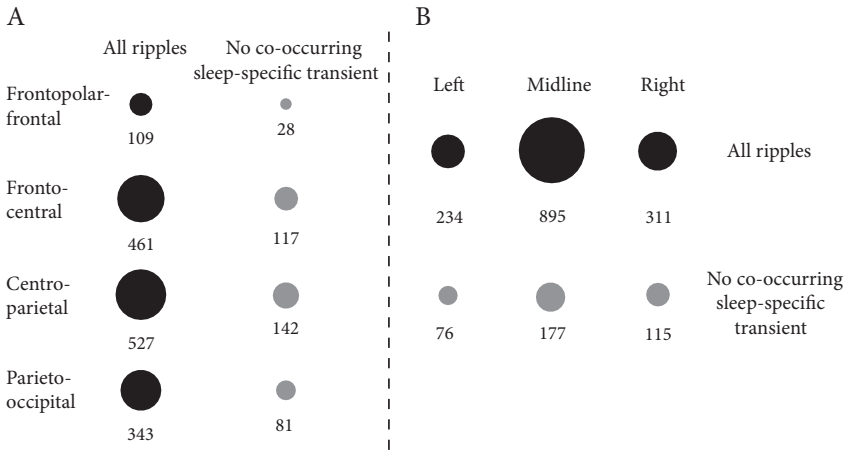

Figure 6.4 A and B: Comparison of the distribution of ripples without co-occurring sleep-specific transient to the distribution of all ripples. Note that the distribution pattern is the same in the anterior-posterior direction. The distribution from left to right differs, with a less pronounced midline dominance for ripples without co-occurring sleep-specific transient.

Spatial extent

There were 727 ripple moments. One hundred eighty-eight ripple moments contained no co-occurring sleep-specific transient on any of the channels with ripples, 514 ripple moments contained one type of co-occurring sleep-specific transient, and 25 ripple moments contained more than one type of co-occurring sleep-specific transient.

Spatial extent was larger in the anterior-posterior direction than in the left-right direction in all categories (Figure 6.5). Ripple moments without co-occurring sleep-specific transients were often solitary ripples, hence the small extent in both directions. The extent of ripple moments that contained ripples co-occurring with hypnagogic hypersynchrony clearly stood out from the extent of ripple moments with other types of co-occurring sleep-specific transients.

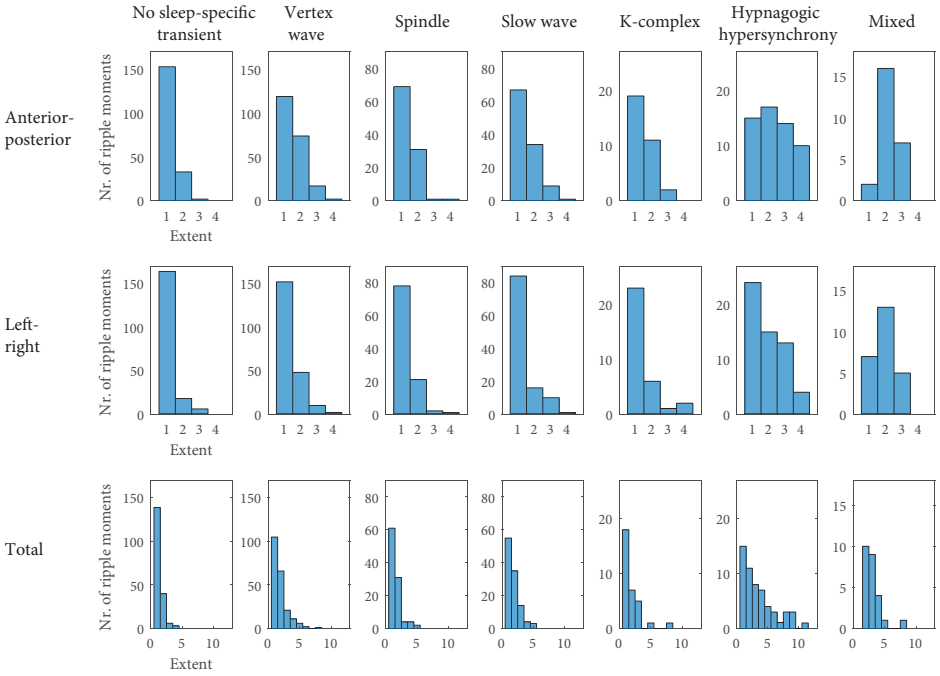

Figure 6.5 Histograms of spatial extent of ripple moments. On the x-axis the extent in anterior-posterior direction (top row), in left-right direction (middle row), and total extent (bottom row). On the y-axis the number of ripple moments. 'No sleep-specific transient ripple moments' contained only ripples without a co-occurring sleep-specific transient. 'Mixed ripple moments' contained simultaneously occurring ripples that co-occurred with different types of sleep-specific transients. Ripple moments named after one type of sleep-specific transient contained at least one ripple that co-occurred with that sleep-specific transient. If there were simultaneous ripples on other channels, they either co-occurred with that sleep-specific transient or they occurred without a co-occurring sleep-specific transient. Solitary ripples had an extent of one in all three graphs; this was the case for many ripple moments without a co-occurring sleep-specific transient. The number of bars with extent values above one was highest in histograms of 'hypnagogic hypersynchrony ripples moments,' indicating that these ripple moments had the largest spatial extent.

Occurrence of ripples across sleep stages

Thirty-one percent of all ripples occurred during N1, 29% during N2, and 40% during N3. Median ripple rate was 2.5 ripples/minute during N1 (range: 0.0-92.6), 3.2 ripples/minute during N2 (range: 0.0-26.8), and 1.5 ripples/minute during N3 (range: 0.0-3.8; Figure 6.6 and Supplementary Table 6.2).

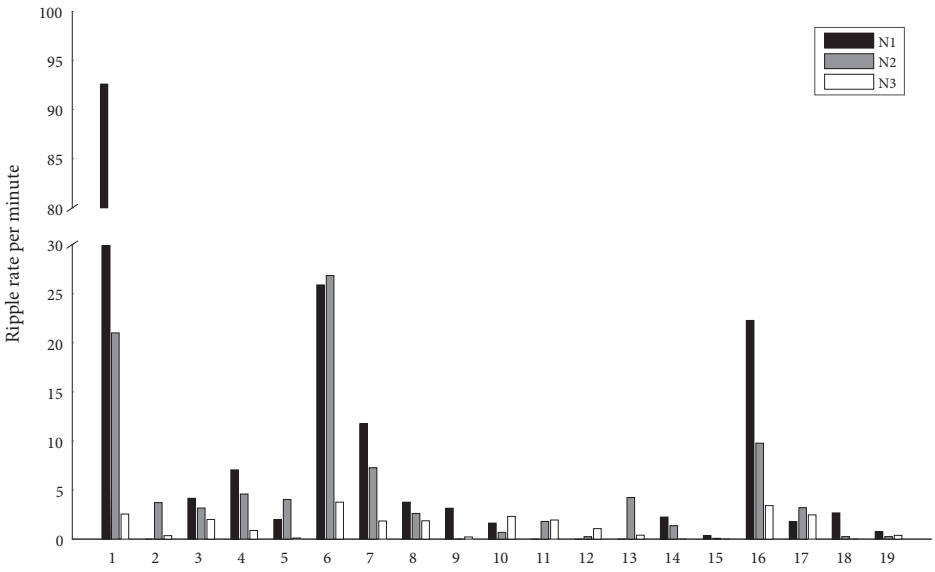

Figure 6.6 Bar graphs of ripple rate per sleep stage for each child. Not all N stages occurred in all children, and sometimes there were no ripples during a sleep stage. Ripple rate differed considerably between children, but in most cases, ripple rate was higher during N1 and N2 than during N3.

Ripple rate differed considerably between children (Figure 6.6 and Supplementary Table 6.2). The variability is less pronounced for rate per sleep stage of ripple moments, in which simultaneously occurring ripples are counted as one ripple moment.

Ripple rates during N1 and N2 were significantly higher than ripple rates during N3 (Friedman's ANOVA: $\chi^2(2) = 6.48$, $p = 0.04$, post hoc testing: N1 vs. N3: $T = 22.00$, $z = -2.38$, $p = 0.02$; N2 vs. N3: $T = 23.00$, $z = -2.72$, $p = 0.01$). Ripple rates during N1 and N2 were not significantly different ($T = 63.00$, $z = -0.98$, $p = 0.33$). The results for the rate per sleep stage of ripple moments were similar (Friedman's ANOVA: $\chi^2(2) = 8.69$, $p = 0.01$; N1 vs. N2: $T = 89.00$, $z = 0.15$, $p = 0.88$; N1 vs. N3: $T = 26.00$, $z = -2.17$, $p = 0.03$; and N2 vs. N3: $T = 18.00$, $z = -2.94$, $p = 0.003$), but the rates per sleep stage of ripples and ripple moments without co-occurring sleep-specific transient did not differ significantly between N1, N2, and N3 (ripples: $\chi^2(2) = 1.33$, $p = 0.51$; ripple moments: $\chi^2(2) = 2.37$, $p = 0.31$).

Discussion

Almost 75% of ripples co-occurred with various sleep-specific transients. Ripples without co-occurring sleep-specific transient showed the same central dominance as the overall distribution pattern, but the midline dominance was significantly less pronounced. Ripples moments containing co-occurring sleep-specific transients had a larger spatial extent than ripples moments without co-occurring sleep-specific transients. Ripple rate per minute was highest during N1 and N2 sleep.

The finding that almost 75% of ripples co-occurred with a sleep-specific transient suggests that the presence of a sleep-specific transients makes the occurrence of a ripple more likely, for example by facilitating ripple generation. Sleep-specific transients are, however, not indispensable for ripple generation, because 25% of ripples occurred without a sleep-specific transient.

This study showed that the previously reported midline dominant distribution pattern was partly due to the preferred location of co-occurring sleep-specific transients, but that the central dominance is a characteristic of the ripples themselves.

The co-occurrence of ripples with slow waves and spindles is in line with studies on invasively recorded ripples.[65,77,91–93,96] K-complexes can be considered a special type of slow wave,[112] so the finding that ripples co-occur with K-complexes is not surprising. We could not find literature reporting that ripples co-occur with vertex waves, even though this was the sleep-specific transient that co-occurred with ripples most often and in most children. The combination of a physiological sharp wave and a co-occurring ripple has so far only been described in the hippocampus. The frequency of the neocortical ripples reported here, which ranged from 91 to 116 Hz, matches the frequency of putative physiological ripples that were recorded in the hippocampus of people with epilepsy.[20,70,97–99] Thus, both hippocampus and neocortex can generate sharp-wave ripple 'complexes' with ripples of similar frequencies. The underlying mechanism generating sharp waves and ripples in hippocampus and neocortex is likely to differ, but the finding that a large proportion of ripples co-occurred with vertex waves indicates that vertex wave-ripple combinations are a relevant topic for future research.

Ripples often occurred in clusters, i.e. ripples were often recorded simultaneously at several electrodes. This suggests that physiological ripples are generated in a large brain area or that physiological ripples are simultaneously generated in different brain areas. Sleep-specific transients might facilitate more widespread physiological ripple generation, as ripple moments with co-occurring sleep-specific transients had a larger spatial extent than ripple moments without co-occurring sleep-specific transients.

There was considerable variability in ripple rates in EEGs of different children. Part of this variability is likely to be physiological, but methodological and technical factors may also play a role. An exceptionally high ripple rate was seen in the EEG of the first child. The majority (55%) of the ripples observed in the

EEG of this child co-occurred with hypnagogic hypersynchrony. Spatial extent of ripples co-occurring with hypnagogic hypersynchrony was largest (Figure 6.5). Thus, if all ripples co-occurring with hypnagogic hypersynchrony are counted separately, ripple rate rapidly increases. Spatial clusters have no influence on the rate per minute if simultaneously occurring ripples are counted as one ripple moment; the rate per minute of ripple moments in the EEG of this child therefore stands out less (Supplementary Table 6.2).

Exceptionally low or even zero rates may partly be due to the fact that in some EEGs the signal was more noisy than in others. Ripples were defined as four or more oscillations that clearly stood out from the background. Thus, if the background is noisy, it is likely that fewer ripples stand out from this background. Another factor that might contribute to low ripple rates is the number of (muscle) artifacts. Artifacts can obscure the signal, which might result in missed ripples. Moreover, the high-frequency component of short artifacts can look like ripples. We thought that it was important to minimize the number of such false ripples, even if this might inadvertently result in an underestimation of the number of true ripples in EEGs with quite a few artifacts.[108]

Despite the variability, ripple rates were in general higher during light sleep (N1 and N2) than during N3 stage. Co-occurring sleep-specific transients affect ripple rate per sleep stage, because rate per sleep stage did not differ for ripples without co-occurring sleep-specific transients. It is therefore possible that sleep-specific transients that occur during light sleep, such as vertex waves and hypnagogic hypersynchrony, facilitate the generation of ripples more than sleep-specific transients that occur during deep sleep, such as slow waves. This idea fits with the finding that only 13.7% of ripples co-occurred with a slow wave, even though this is the most common sleep-specific transient. The finding that ripple rate was higher during N1 than N3 cannot be attributed to ripples co-occurring with hypnagogic hypersynchrony in large clusters, because the rate per minute of ripples moments was also higher during N1 and N2 compared with N3. Thus, there are relatively more ripple moments during N1 and N2 compared with N3 and this seems related to the type of co-occurring sleep-specific transient during light sleep independently of the number of ripples per ripple moment.

All in all, the results of this study suggest that 1) sleep-specific transients might facilitate the generation of ripples, perhaps to promote coordination of ripples across different brain regions, but 2) (visible) sleep-specific transients are not indispensable for ripple generation, and 3) sleep-specific transients of light sleep probably facilitate the generation of ripples more than sleep-specific transients of deep sleep.

The finding that these neocortical ripples co-occurred with slow waves and spindles suggests that they could be involved in the hippocampal-cortical dialogue that is important for memory consolidation. Support for this hypothesis comes from a recent study in animals that showed that neocortical ripples co-occur with ripples in the hippocampus during sleep. Moreover, the coupling between hippocampal and neocortical ripples was strengthened after performance of a

hippocampus-dependent memory task.[96] If the neocortical ripples reported here are indeed part of the hippocampal-cortical dialogue, this would mean that they are not a child-specific EEG phenomenon. Future research should investigate if these ripples can be found in scalp EEGs recorded in healthy adults.

Limitations

A limitation of this study is that we analyzed EEGs that were recorded for clinical reasons. All of the included EEGs were free of epileptic spikes or other abnormalities, but some of the children had a neurological or psychiatric diagnosis. There are several reasons to think that the ripples reported here are physiological. First, ripples in children with a neurological or psychiatric disease resembled ripples that were recorded in healthy children and their appearance differed from the appearance of pathological ripples.[108] Second, pathological ripples are probably rare in spike-free scalp EEG.[88] The finding that ripples co-occurred with various sleep-specific transients is a third argument in favor of these ripples being physiological. Moreover, we minimized the chance of studying sleep-specific transients that were induced by epileptic spikes occurring in areas that are not recorded with scalp EEG (such as the hippocampus) by excluding the child with symptomatic epilepsy. Even so, it would have been preferable to study completely healthy participants.

A second limitation is the short duration of the sleep recordings and the absence of REM sleep. Whole night sleep recordings without preceding sleep deprivation would be preferable for future studies.

A third limitation is that we used a rather crude measure of spatial extent. We already mentioned the absence of data from a transverse bipolar montage, but any bipolar montage might lead to overestimating the true extent. For example, ripples that simultaneously occur on bipolar channels Fz-Cz and Cz-Pz could be the same event recorded by Cz. In that case, we would overestimate the extent. However, ripples on Fz-Cz and Cz-Pz could also reflect ripples occurring in a greater area between Fz and Pz electrodes, in which case our extent estimation would be more accurate. Using an average montage would do more justice to local events but might miss ripples that occur between electrode positions. A more accurate estimation of the extent would therefore require higher density EEG.

Conclusion and future directions

Our results suggest that research on sleep-specific transients that co-occur with hippocampal and neocortical ripples should be extended, particularly to include vertex waves. Research in humans should explore if these ripples can also be found in scalp EEGs of adults, as this would enable more research on the role of physiological neocortical ripples in cognitive functioning.

Supplementary material

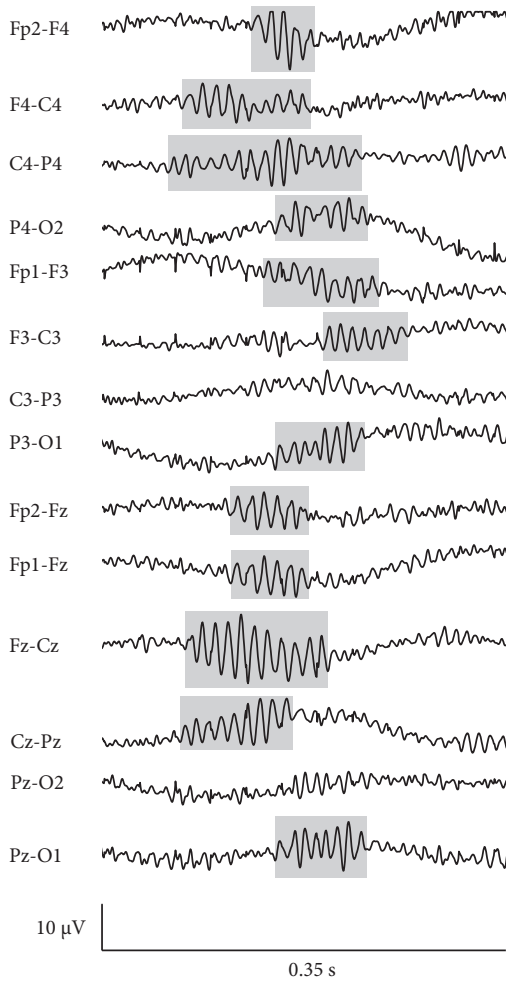

Supplementary Figure 6.1 Example of a ripple cluster. All traces were recorded at the same moment in the same child. Traces were filtered between 80 and 250 Hz. Time scale is 1 second per page, amplitude scale is 1 µV/mm. Gray areas indicate ripple markings.

Clusters could potentially involve four anterior-posterior regions: frontopolar-frontal (regions around Fp2-F4, Fp2-Fz and Fp1-Fz taken together as *Fpz*-Fz, and Fp1-F3); frontocentral (regions around F8-T8, F4-C4, Fz-Cz, F3-C3, F7-T7), centroparietal (regions around T8-P8, C4-P4, Cz-Pz, C3-P3, T7-P7), and parieto-occipital (regions around P4-O2, Pz-O2 and Pz-O1 (together Pz-*Oz*), P3-O1), and five left-right regions: the midline (*Fpz*-Fz, Fz-Cz, Cz-Pz, Pz-*Oz*) region, the inner right (Fp2-F4, F4-C4, C4-P4, P4-O2) and inner left (Fp1-F3, F3-C3, C3-P3, P3-O1) regions, and the outer right (Fp2-F8, F8-T8, T8-P8, P8-O2) and outer left (FP1-F7, F7-T7, T7-P7, P7-O1) regions. This ripple cluster covered all four anterior-posterior regions: frontopolar-frontal (Fp2-F4, *Fpz*-Fz, and Fp1-F3), frontocentral (F4-C4, Fz-Cz, F3-C3), centroparietal (C4-P4, Cz-Pz), and parietal-occipital (P4-O2, Pz-*Oz*, P3-O1) (anterior-posterior extent = 4). It covered three out of five left-right regions: the midline (*Fpz*-Fz, Fz-Cz, Cz-Pz, Pz-*Oz*) region and the inner right (Fp2-F4, F4-C4, C4-P4, P4-O2) and inner left (Fp1-F3, F3-C3, P3-O1) regions (left-right extent = 3). There were no ripples in the outer left and outer right regions. In total, 11 areas were involved (Fp2-F4, *Fpz*-Fz, Fp1-F3, F4-C4, Fz-Cz, F3-C3, C4-P4, Cz-Pz, P4-O2, Pz-*Oz*, P3-O1, total extent = 11).

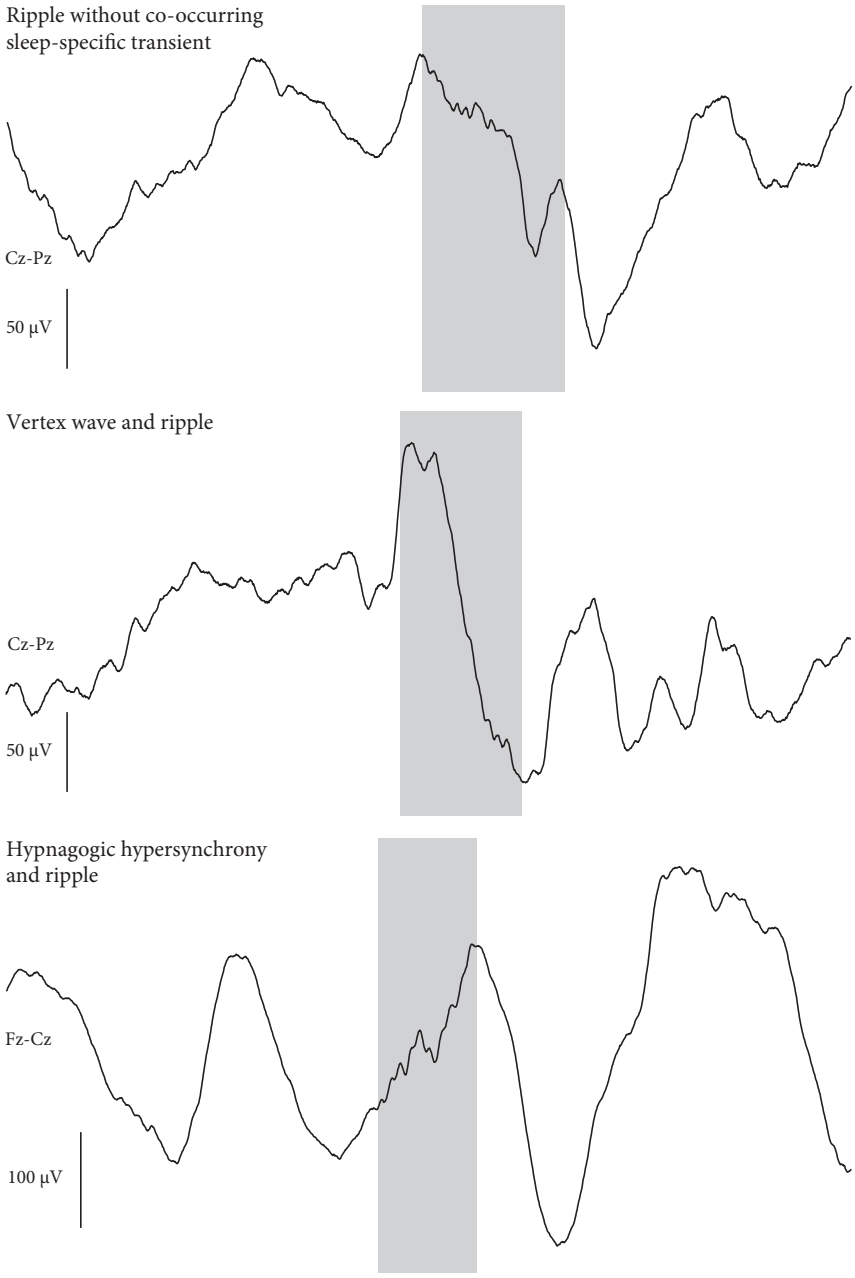

figure continues

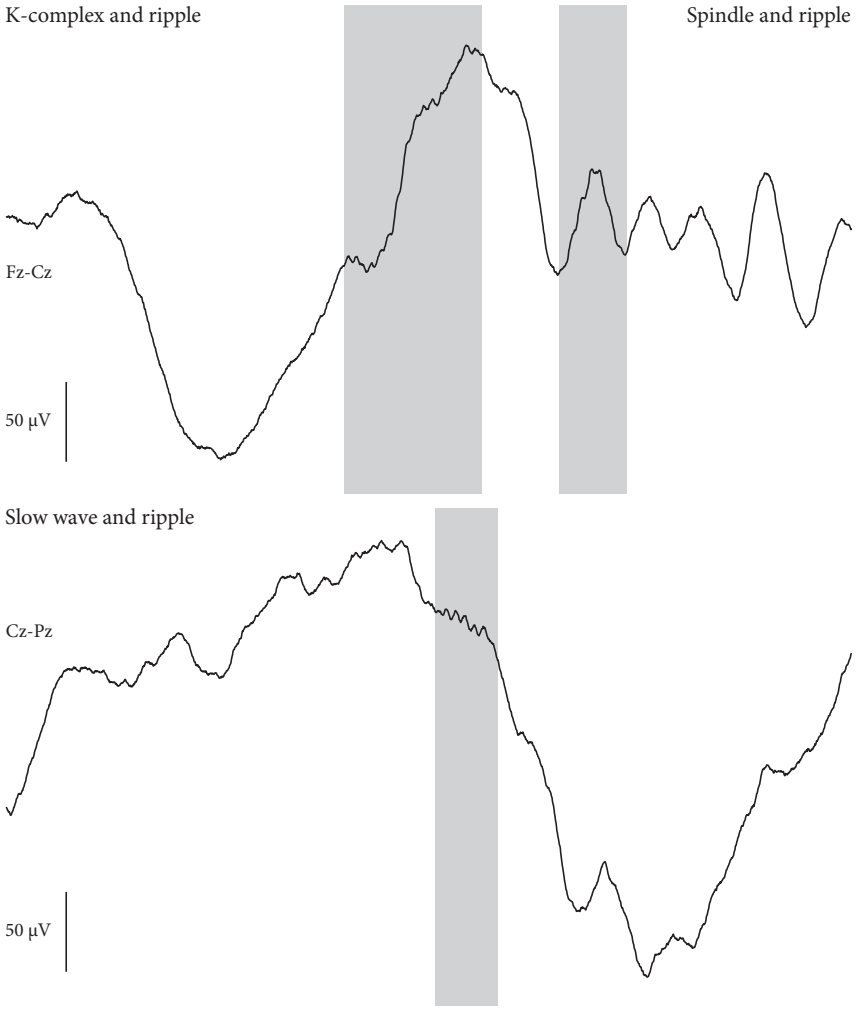

Supplementary Figure 6.2 Traces of Figure 6.2 showing both the low-frequency activity, as shown in Figure 6.2A, and the high-frequency activity, as shown in Figure 6.2B. The signal was not filtered. Time scale is 1 second per page, amplitude scale is 3 μV/mm, except for the trace with hypnagogic hypersynchrony, which has an amplitude scale of 5 μV/mm. Gray areas indicate where ripples were marked. Ripples are visible as small bumps on the sleep-specific transient.

Supplementary Table 6.1 Number of ripples per type of co-occurring sleep-specific transient for each child

	No sleep-specific transient	Vertex wave	Spindle	Slow wave	K-complex	Hypnagogic hypersynchrony	POST	Total
1	66	53	23	23	0	199	0	364
2	4	3	3	8	3	0	0	21
3	7	18	10	2	0	3	0	40
4	16	17	5	10	4	0	0	52
5	15	28	4	2	3	0	0	52
6	84	64	53	47	23	0	0	271
7	32	29	9	39	4	0	0	113
8	32	20	15	7	9	0	0	83
9	2	0	0	1	6	0	0	9
10	1	10	0	0	0	0	0	11
11	32	11	17	25	0	0	0	85
12	17	6	0	4	5	0	0	32
13	12	6	1	8	6	0	0	33
14	2	8	0	0	0	5	0	15
15	0	2	1	0	0	1	0	4
16	40	116	14	17	20	0	1	208
17	5	1	17	2	0	4	0	29
18	0	4	0	0	1	0	0	5
19	1	4	4	2	2	0	0	13
Total	368	400	176	197	86	212	1	1440

POST: Positive occipital sharp transient (of sleep)

Supplementary Table 6.2 Duration of each sleep stage, ripple rate per sleep stage, and ripple moment rate per sleep stage for each child

	N1			N2			N3		
	Duration	Ripple rate	Ripple moment rate	Duration	Ripple rate	Ripple moment rate	Duration	Ripple rate	Ripple moment rate
1	2.48	92.60	29.79	2.48	21.01	11.72	32.12	2.55	1.49
2	0.22	0	0	3.50	3.71	2.86	22.68	0.35	0.31
3	3.13	4.16	2.24	7.26	3.17	2.34	2.00	2.00	1.00
4	1.70	7.05	1.76	3.26	4.60	3.06	28.43	0.88	0.56
5	3.00	2.00	2.00	10.89	4.04	2.85	17.92	0.11	0.11
6	0.70	25.90	5.75	5.29	26.85	10.40	29.46	3.77	1.93
7	2.98	11.75	5.04	3.44	7.27	2.62	28.69	1.85	0.98
8	7.71	3.76	3.76	1.53	2.62	2.62	26.79	1.87	1.87
9	1.91	3.15	0.52	2.49	0	0	13.63	0.22	0.07
10	1.23	1.63	1.63	4.37	0.69	0.69	2.60	2.31	2.31
11	2.12	0	0	3.34	1.80	1.50	40.56	1.95	1.38
12	0.00	-	-	4.15	0.24	0.24	29.03	1.07	0.65
13	0.07	0	0	4.95	4.24	2.02	29.90	0.40	0.23
14	3.12	2.24	1.28	5.87	1.36	1.02	0	-	-
15	8.55	0.35	0.23	12.27	0.08	0.08	23.92	0	0
16	3.59	22.28	10.86	3.99	9.78	3.51	26.07	3.41	1.69
17	2.81	1.78	1.43	3.13	3.19	2.56	5.67	2.47	1.76
18	1.50	2.67	0.67	3.99	0.25	0.25	30.98	0	0
19	3.99	0.75	0.25	8.00	0.25	0.13	20.92	0.38	0.33

N = Non-rapid eye movement sleep. Duration in minutes, rate per minute.

Part 4

Physiological and pathological ripples in scalp EEG

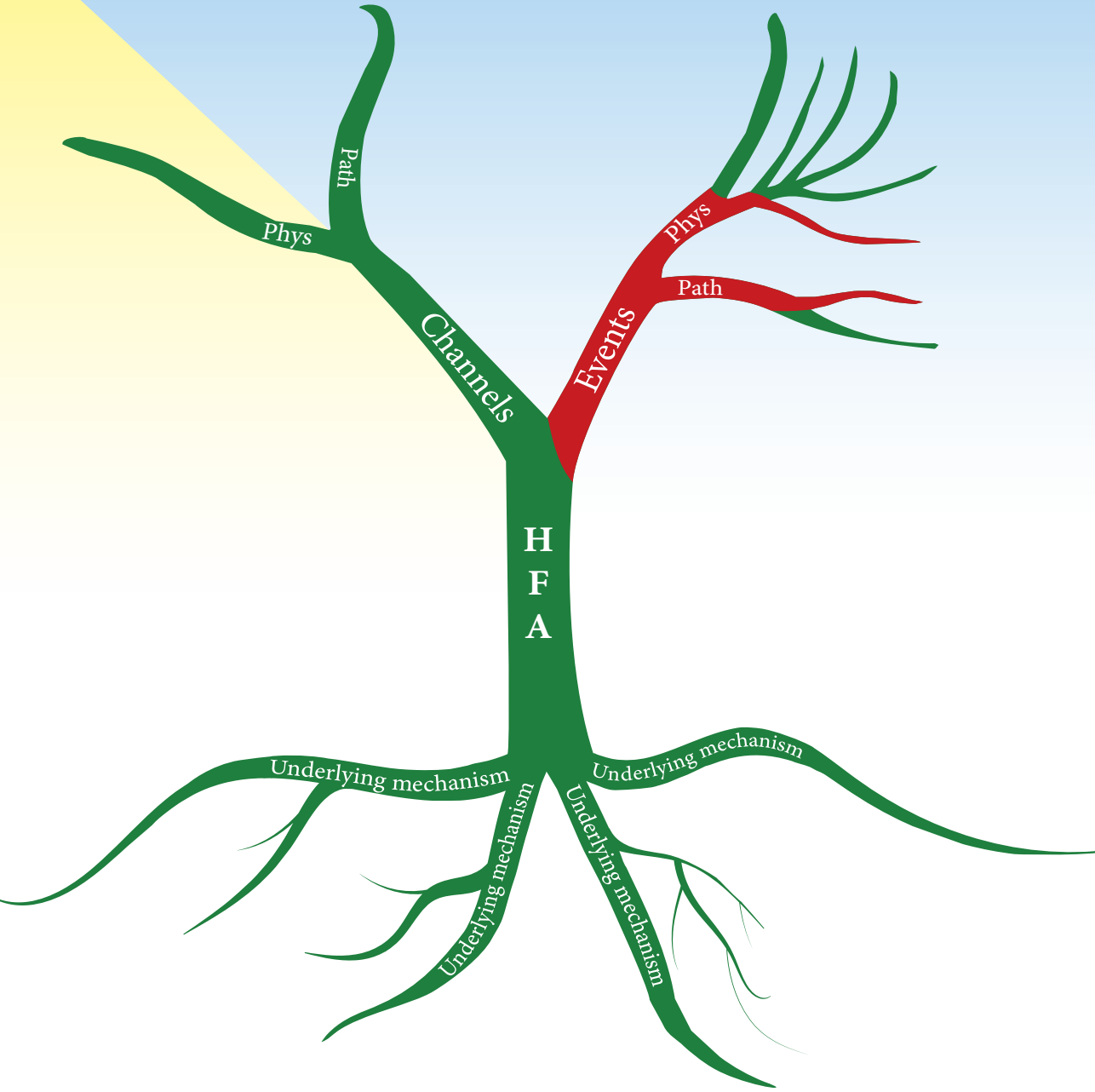

Chapter 7

Scalp-EEG recorded physiological and pathological ripples

Anne H. Mooij
Geertjan J.M. Huiskamp
Emmeke Aarts
Cyrille H. Ferrier
Kees P.J. Braun
Maeike Zijlmans

In preparation

Abstract

Objective
To compare characteristics of scalp-EEG recorded ripples co-occurring with vertex waves or interictal epileptiform discharges (IEDs: spikes or sharp waves).

Methods
We visually marked ripples in sleep EEGs of 28 children. We used multilevel statistics to compare the start of ripples relative to the start of the co-occurring event (vertex wave or IED), and duration, frequency, and root mean square (RMS) amplitude of vertex wave- and IED-associated ripples.

Results
We found ripples co-occurring with vertex waves in EEGs of children with and without epilepsy. All children with EEGs containing ripples co-occurring with IEDs had epilepsy. Ripples started significantly (χ^2 (1) = 30.03, $p < 0.001$) later if they co-occurred with vertex waves (+105.4 ms, i.e., after the start of vertex waves) than if they co-occurred with IEDs (-5.3 ms, i.e., before IED start). Ripples co-occurring with vertex waves had a significantly longer duration (77.4 ms vs. 46.1 ms), lower frequency (103.2 Hz vs. 132.3 Hz), and lower RMS amplitude (1.1 μV vs. 2.1 μV, all $p < 0.001$) than ripples co-occurring with IEDs, regardless of the diagnosis. The frequency of ripples co-occurring with IEDs recorded in children with Rolandic epilepsy and one child with possibly Panayiotopoulos-associated seizures was higher than the frequency of other pathological ripples.

Significance
The similarity of their characteristics suggests that all ripples co-occurring with vertex waves were physiological, and consistently different from pathological ripples that co-occurred with IEDs. This is the first study on characteristics of physiological and pathological ripples recorded with scalp EEG. The difference in the timing of the ripple relative to the start of the co-occurring event suggests that beneath the superficial similarities between these two types of sharp EEG transients and their co-occurring ripples lie differences in generating mechanisms. Ripples recorded in children with Rolandic epilepsy seem to form a pathological ripple subgroup.

Introduction

Ripples are physiological or pathological brain oscillations with frequencies between 80-250 Hz.[113] Physiological ripples are related to cognitive functions. They were, for example, shown to be involved in memory retrieval and consolidation.[7,107] Pathological ripples are considered biomarkers for epilepsy.[8,9] Considering this difference in neurophysiological significance, it is important to be able to recognize physiological and pathological ripples. To this end, several studies have compared duration, frequency, and amplitude of presumable physiological and pathological ripples.[63,65,86,87,100,101,103,114,115] The results are contradictory (see Supplementary Table 7.1 for an overview of the results per study), especially for duration and frequency. Differences between amplitudes of presumably physiological and pathological ripples seem to be more consistent and suggest that physiological ripples may have lower amplitudes than pathological ripples.

All of these studies have been performed on intracranial EEG recordings. A disadvantage of studying physiological activity in intracranial EEG of people with chronic epilepsy is that epileptic activity may influence physiological activity even outside epileptic regions. For example, Gelinas et al. (2016) showed that epileptic spikes from the hippocampus can induce seemingly physiological spindles recorded in the neocortex.[94] Doubt about the physiological nature of ripples need not exist in scalp EEGs recorded in healthy participants.

Previous studies have shown that physiological ripples often co-occur with sleep-specific transients,[77,116] whereas pathological ripples can co-occur with spikes.[22,24,88] We previously reported that ripples recorded in normal scalp EEG occurred most often with vertex waves.[116] Vertex waves are physiological sleep-specific transients, but they resemble pathological interictal epileptiform discharges (IEDs: spikes [20-70 ms], or sharp waves [70-200 ms]) in several ways: they are multiphasic, short, sharp transients that clearly stand out from the background EEG.[26,113] This makes vertex waves and IEDs interesting EEG events for studying co-occurring ripples. Relevant questions are if the ripples are similar, like the appearance of the co-occurring sharp EEG transients, or if are they different, reflecting the difference in neurophysiological meaning of vertex wave and spikes. Moreover, if there is a difference between physiological ripples co-occurring with vertex waves in normal EEGs of people without epilepsy and pathological ripples co-occurring with IEDs in people with epilepsy, we want to know if this difference is preserved for ripples co-occurring with vertex waves in EEGs of people with epilepsy, especially if their EEGs also contain IEDs.

To answer these questions, we compared several characteristics of ripples co-occurring with vertex waves recorded in scalp EEGs with or without IEDs of children with or without epilepsy, and ripples co-occurring with IEDs. The first characteristic of interest is the start of ripples relative to the start of co-occurring vertex waves or IEDs. Pathological ripples co-occurring with spikes were found to start before the start or during the first phase of the spike,[117] suggesting that the ripples are not generated by spikes. We previously reported that 74% of

physiological ripples co-occurred with sleep-specific transients and speculated that sleep-specific transients may facilitate physiological ripple generation; however, the start of physiological ripples relative to the start of co-occurring sleep specific transients was not investigated in that study.[116] We also compared ripple duration, frequency, and amplitude, as was done in the above mentioned studies on presumable physiological ripples and pathological ripples recorded with intracranial EEG.

We addressed the questions: 1) Do scalp-EEG recorded ripples start before, at the same time, or after co-occurring vertex waves or IEDs? 2) Do ripples co-occurring with vertex waves or IEDs have the same or different duration, frequency, and amplitude?

Methods

Participants

We retrospectively studied EEGs of children (17 years or younger) who had visited our outpatient first seizure clinic between May 2013 and May 2016 because they were suspected of having had one or more (first) possible seizure(s). We selected children who fulfilled the inclusion criterion of having a sleep EEG recorded at high sampling rate (2048 Hz) in which ripples co-occurring with vertex waves or IEDs could be found. All EEGs were day-time recordings with a minimum of 10 minutes of sleep. A specialized pediatric neurologist determined the diagnosis based on all information available in the clinical files until the end of follow-up (May 2019). The Medical Research Ethics Committee of the University Medical Center Utrecht judged that the Dutch Medical Research Involving Human Subjects Act did not apply and written consent was not required, provided that data were coded and handled anonymously.

EEG recordings

Scalp EEGs were recorded with Micromed Smart Acquisition Module (SAM) and with SD PLUS FLEXI acquisition system (Micromed, Treviso, Italy). Data were sampled at 2048 Hz, low-pass anti-alias filter at acquisition was 900 Hz for SAM and 553 Hz for FLEXI. We used conventional 10 mm Ag-AgCl electrodes that were placed according to the international 10-20 system.

Marking ripples

We first marked ripples in Stellate Harmony (Montreal, Canada) in the whole sleep EEG recordings, whenever the signal-to-noise ratio allowed proper judgement. The signal was filtered between 80 Hz (finite impulse response high-pass filter of order 63) and 250 Hz (finite impulse response low-pass filter of order 63), amplitude scale was set to 1 μV per mm, time scale was 0.9 seconds per page. This was the setting that showed each recorded data sample for the size of the screen. We marked as ripples four or more oscillations that clearly stood out from

the background EEG signal. If background low-amplitude ripple band activity gradually built up to visually recognizable ripple oscillations, we started marking when the oscillations stood out clearly from the overall background activity of the channel and stopped marking when this was no longer the case.

Marking start of vertex waves and IEDs

We viewed the low-frequency EEG at the time of each ripple to see if there was a co-occurring vertex wave or IED. These events were identified following standard definitions.[26,113] The EEG signal was filtered between 0.3 and 70 Hz, using infinite impulse response filters (IIR) of order 3 (0.3 Hz) or order 4 (70 Hz). Time scale was 10 seconds per page (on a 15.4 inch screen), amplitude scale varied between 10 to 30 μV per mm depending on the amplitude of the signal.

We marked the start of vertex waves and IEDs for each child in the channel that contained most ripples co-occurring with vertex waves or IEDs (Figure 7.1). We would know that there was a co-occurring ripple, but we made the ripple itself invisible when marking the vertex wave or IED, so that we could not be biased by the timing of the ripple. The start marker of the vertex wave or IED was placed at the start of the first downward or upward deflection.

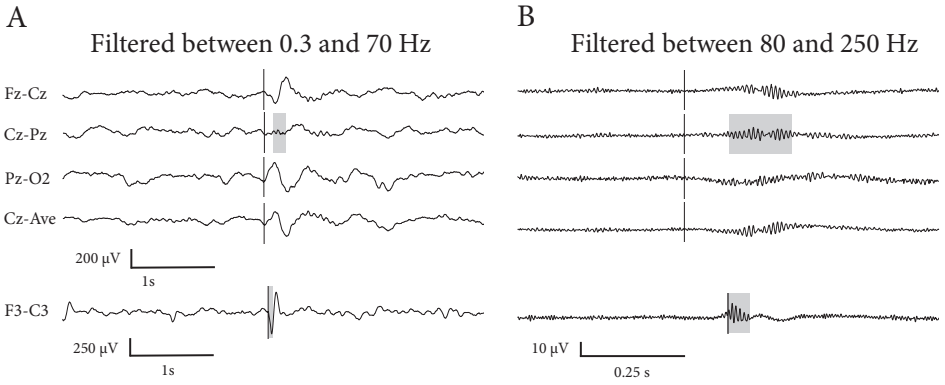

Figure 7.1 Example of ripples (in B) co-occurring with vertex waves (first four traces in A) and an IED (spike, last trace in A). A vertical line has been placed at the start of the vertex wave or spike. Time scale was 5 seconds for all traces in A, amplitude scale was 15 μV/mm for the first four traces, and 20 μV/mm for the last trace. Time scale was 1 second and amplitude scale was 1 μV/mm for all traces in B. Gray markings and vertical lines in A correspond to the same markings in B. The vertex wave in Cz-Pz (second trace) is not visible, the start marker has been placed based on the signal of the neighboring contacts (Fz-Cz and Pz-O2, first and third trace) and of the Cz channel in average montage (fourth trace). Note that the ripple is also visible in Fz-Cz and Cz-Average in B. The physiological ripple occurs about 100 ms after the start of the vertex wave, while the pathological ripple starts at the same time as the spike.

Most ripples co-occurring with vertex waves occurred in channel Cz-Pz,[116] but the vertex wave was often not clearly visible in this channel (example in Figure 7.1), presumably because Cz-Pz was located directly above the source of the vertex wave. If it was unclear from the Cz-Pz signal where the marker to depict the start of the vertex wave should be placed, we placed the marker based on the signal in neighboring bipolar contacts (Fz-Cz and Pz-O2 or Pz-O1) and the corresponding channels in average montage (Fz-, Cz-, or Pz-Average). If it was still not clear where the marker should be placed, the ripple and co-occurring event were not included in the analyses.

Calculating ripple characteristics

We calculated for each ripple: 1) The duration (in ms) from start to stop of the ripple markings. 2) The frequency (in Hz), calculated as 1/duration of one oscillation. Duration of one oscillation was calculated by dividing the duration of the ripple by the total number of oscillations. The total number of oscillations was calculated as the number of zero crossings of the filtered ripple band within the duration of the marked ripple divided by two. 3) The root mean square (RMS) amplitude (in μV).

Multilevel analyses

Since multiple observations from each patient were included, the data were nested. We used a multilevel analysis to accommodate for this dependency in the data. At least three observations per patient are needed for a multilevel analysis. Thus, only ripples from EEGs with at least three ripples co-occurring with vertex waves or IEDs in the channel with most events were included in the analysis.

We first fitted a model with random intercepts to quantify the amount of dependency in the data. We compared this model to a model with a fixed intercept to determine the statistical significance of the dependency. We then added the type of co-occurring event (vertex wave or IED) as fixed effect to the model to determine if there was a difference in characteristics of ripples co-occurring with these events while controlling for dependency in the data. Finally, we tested if there was any unexplained intercept variance left in the last model. Differences between models were tested using a difference in deviance (-2 x Log Likelihood) test, which is chi-square distributed. The used α was set at 0.05.

We performed the same analysis for the ripple start relative to vertex wave or IED start and for ripple duration, frequency, and RMS amplitude. We also performed this analysis for the number of oscillations, because the interpretation of the results of ripple duration and frequency depends on the number of oscillations of the ripples. For example, if one type of ripple has a shorter duration than the other, this may be because of a difference in the number of oscillations, because of a difference in frequency (with the same number of oscillations, ripples with higher frequency have a shorter duration), or both.

Results

Children, EEGs, and diagnoses

We included 28 children (Table 7.1). Seventeen children had a normal EEG with ripples co-occurring with vertex waves (1-17). Three of these children were diagnosed with benign course epilepsy (15-17). Eleven children (18-28) had an EEG with IEDs. Nine of these children were diagnosed with epilepsy. In two children the diagnosis remained unclear during follow-up (18 and 22). There were ripples co-occurring with IEDs in seven of the 11 EEGs with IEDs (22-28), while four of these EEGs only contained ripples co-occurring with vertex waves, but not with the IEDs (18-21). Two children used anti-epileptic drugs when the EEG was recorded: levetiracetam (20) and valproic acid (21).

EEGs excluded from multilevel analysis.

Nine EEGs were excluded because they contained less than three ripples with co-occurring vertex waves or IEDs (4, 6, 7, 13, 14, 18, 19, 21, 22 in Table 7.1) in the channel that contained most events. One EEG (28 in Table 7.1) contained polyspikes and waves and co-occurring ripples. We report the results of this patient separately.

Multilevel analysis of ripple characteristics

Ripples started on average 110.7 ms later if the co-occurring event was a vertex wave than if the co-occurring event was an IED (Table 7.2 and Figure 7.2). Ripples co-occurring with vertex waves had a longer duration, lower frequency, and lower amplitude than ripples co-occurring with IEDs (Table 7.2 and Figure 7.3). For all characteristics, the remaining (unexplained) intercept variance was significant at $p < 0.001$, indicating that there was significant variation between the results per patient left after taking the type of co-occurring event into account. The frequency of ripples co-occurring with IEDs was higher, but the number of oscillations was also smaller. Thus, the duration of ripples co-occurring with IEDs would have been shorter even if the frequency had been the same.

Relation to EEG type (i.e., normal or containing IEDs) and to diagnosis

Despite the variability between and within children, the start of the ripples relative to the start of co-occurring vertex waves (downward pointing triangles in Figure 7.2) was consistent throughout normal EEGs and EEGs with IEDs (above and below the horizontal line) and EEGs of children with and without epilepsy (white and black downward pointing triangles). Moreover, ripple duration, number of oscillations, frequency, and RMS amplitude were similar for all ripples co-occurring with vertex waves (open circles in Figure 7.3). These findings indicate that the ripples co-occurring with vertex waves in EEGs with IEDs (18-21) or in children with a (probable) diagnosis of epilepsy (15-17 and 19-21) closely resemble those occurring in patients without epilepsy (1-13) and thus reflect a physiological phenomenon.

Table 7.1 Characteristics of included children and EEGs

		Gender	Age at EEG	Follow up	Diagnosis	R+V wave	R+ IED
NORMAL, NO IED PRESENT IN EEG	1	M	1y6m	5y7m	No epilepsy, no other brain disorder	6	0
	2	F	5y0m	5y1m	No epilepsy, no other brain disorder	7	0
	3	M	8y11m	4y1m	No epilepsy, no other brain disorder	7	0
	4	M	1y0m	3y11m	No epilepsy, no other brain disorder	1	0
	5	M	5y1m	5y7m	Possibly sleep disorder	9	0
	6	M	3y8m	5y8m	Glut 1 deficiency syndrome, no epilepsy	2	0
	7	M	5y5m	3y4m	No diagnosis, epilepsy highly unlikely	2	0
	8	M	3y8m	5y4m	No diagnosis, epilepsy highly unlikely	5	0
	9	M	2y10m	5y5m	No epilepsy, history of bacterial meningitis with acute symptomatic seizures two years before the analyzed EEG was recorded	10	0
	10	M	8y10m	4y11m	Tic syndrome and autism spectrum disorder	3	0
	11	M	2y4m	5y9m	Autism	4	0
	12	M	5y2m	4y4m	Autism, chromosomal microduplication syndrome	3	0
	13	F	7y5m	4y10m	Migraine, CACNA1A deficiency	2	0
	14	F	6y2m	3y7m	Migraine, epilepsy not definitely excluded	1	0
	15	M	1y8m	5y11m	Probably benign childhood epilepsy variant, exact classification unclear	10	0
	16	F	0y11m	4y5m	Benign infantile epilepsy syndrome	3	0
	17	F	4y5m	4y1m	Benign occipital epilepsy syndrome	35	0

table continues

		Gender	Age at EEG	Follow up	Diagnosis	R+V wave	R+ IED
IED PRESENT IN EEG	18	F	8y8m	3y10m	Clinical aspects of events not suspect for epilepsy, could be tics	1	0
	19	F	8y7m	5y4m	Epilepsy due to bilateral subcortical band heterotopia caused by DCX mutation	1	0
	20	F	3y10m	5y0m	Epilepsy with generalized febrile and afebrile seizures, no etiology identified	5	0
	21	M	2y11m	3y4m	Epilepsy with mild developmental delay due to TANC2 mutation	2	0
	22	M	4y1m	4y10m	Panayiotopoulos-associated seizures or vasovagal collapse	0	2
	23	F	0y6m	5y7m	Rolandic epilepsy (BECTS), rare seizures	0	3
	24	F	9y3m	3y1m	Rolandic epilepsy (BECTS), frequent seizures and 66% IED augmentation in sleep	0	163
	25	M	9y11m	3y3m	Rolandic epilepsy (BECTS), frequent seizures and ESES	0	70
	26	F	2y3m	3y6m	Epilepsy due to bilateral polymicrogyria caused by intrauterine CMV infection	0	314
	27	F	0y8m	3y10m	Epilepsy, no etiology identified, prematurity and developmental delay	0	16
	28	M	0y4m	5y5m	Epilepsy, generalized seizures and episode of epileptic encephalopathy, caused by chromosomal translocation syndrome	0	97[1]

[1]The EEG of this patient showed polyspikes and co-occurring ripples.

R + V wave: ripple co-occurring with vertex wave; R + IED: ripple co-occurring with interictal epileptic discharge (IED: spike or sharp wave). M: male, F: female. Age at time of the sleep EEG and duration of follow-up in years (y) and months (m). BECTS: Benign epilepsy with centro-temporal spikes. ESES: electrical status epilepticus of sleep. CMV: cytomegalovirus.

The table is sorted based on the EEG, starting with normal EEGs without IEDs and then EEGs with IEDs (first column). It is also sorted based on diagnosis, starting with no brain disorder, then brain disorders other than epilepsy (e.g. autism and migraine), followed by (benign) epilepsies. Note that there were three children with (probably) benign childhood epilepsy but normal EEG (15-17), and four EEGs that contained only ripples co-occurring with vertex waves despite the presence of IEDs in the EEG (18-21). The last two columns show the number of events in the channel with most ripples co-occurring with vertex waves or IEDs.

Table 7.2 Ripple characteristics

	Ripples co-occurring with vertex waves	Ripples co-occurring with IEDs	Difference and statistical significance
Ripple start relative to vertex wave or IED start (ms)	105.4 ms 95% PI: [61.4, 149.4]	-5.3 ms 95% PI: [-49.3, 38.7]	110.7 ms 95% CI: [86.6, 134.8] $\chi^2(1) = 30.03$, $p < 0.001$
Duration (ms)	77.4 ms 95% PI: [47.7, 107.0]	46.1 ms 95% PI: [24.5, 83.8]	31.4 ms 95% CI: [17.6, 45.1] $\chi^2(1) = 13.01$, $p < 0.001$
Number of oscillations	8.0 oscillations 95% PI: [5.5, 10.6]	6.0 oscillations 95% PI: [4.2, 9.3]	2.1 oscillations 95% CI: [1.0, 3.2] $\chi^2(1) = 9.34$, $p < 0.01$
Frequency (Hz)	103.2 Hz 95% PI: [83.4, 123.0]	132.3 Hz 95% PI: [109.4, 149.0]	29.2 Hz 95% CI: [18.7, 39.6] $\chi^2(1) = 17.96$, $p < 0.001$
RMS amplitude (μV)	1.1 μV 95% PI: [0.6, 1.6]	2.1 μV 95% PI: [1.6, 2.6]	1.0 μV 95% CI: [0.7, 1.4] $\chi^2(1) = 20.32$, $p < 0.001$

IED: interictal epileptiform discharge (spike or sharp wave). PI: predictive interval. CI: confidence interval. RMS: root mean square. The PI is the interval in which 95% of the means per patient are expected. The CI is the interval in which the true value of the parameter can be expected to occur with 95% confidence. In the above table, the PIs are based on all children in each category (i.e., EEG containing ripples co-occurring with vertex waves or with IEDs), while the CIs are reported for the differences between the ripples co-occurring with vertex waves or IEDs. Note that all characteristics differ significantly between ripples co-occurring with vertex waves and ripples co-occurring with IEDs.

Ripple subtypes

There seemed to be a bimodal frequency distribution of the IED-ripples (Figure 3C). The groups were too small to separate within a multilevel analysis, but when plotting amplitude against frequency (Figure 7.4), three subgroups of ripples could be distinguished. Vertex wave-associated ripples (open circles) had low frequencies and RMS amplitudes (1-21 Table 7.1, pooled N: 119, frequency: mean: 102.9 Hz, mdn: 102.4 Hz, sd: 9.8 Hz; amplitude: mean: 1.1 μV, mdn: 1.0 μV, sd: 0.3 μV). Ripples co-occurring with IEDs were divided in two subgroups: ripples in the EEGs of four children with the 'idiopathic' epilepsy syndromes Rolandic epilepsy (23, 24, 25) and possible Panayiotopoulos syndrome (22) had high frequencies (pooled N: 238, mean: 147.1 Hz, mdn: 147.0 Hz, sd: 10.6 Hz) and intermediate RMS amplitudes (mean: 1.9 μV, mdn: 1.9 μV, sd: 0.5 μV), while ripples occurring in EEGs of two patients with symptomatic epilepsy syndromes (26-27) had high RMS amplitudes (pooled N: 330, mean: 2.7 μV, mdn: 2.7 μV, sd: 0.8 μV) and intermediate frequencies (mean: 114.5 Hz, mdn: 113.8 Hz, sd: 9.7 Hz).

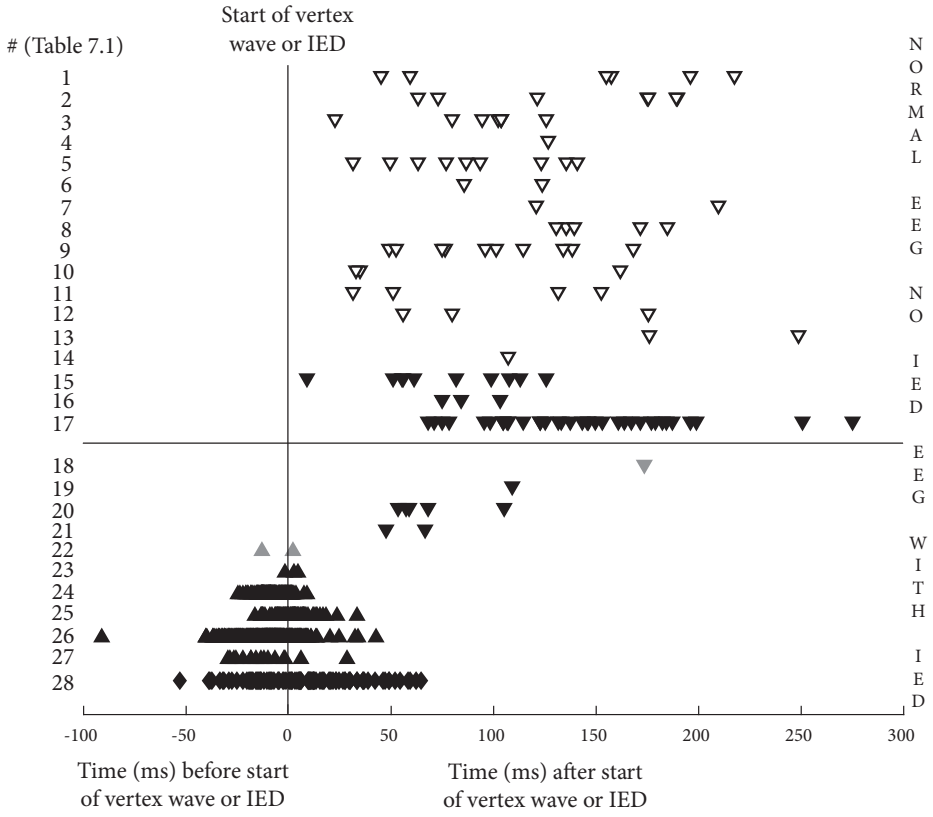

Figure 7.2 Timing of ripple start relative to the start of co-occurring vertex waves or interictal epileptic discharges (IEDs: spike or sharp wave). Results of all ripples of all children are plotted following the order of Table 7.1. Ripples co-occurring with vertex waves are plotted as downward pointing triangles, ripples co-occurring with IEDs as upward pointing triangles, ripple co-occurring with polyspikes as diamonds. Open triangles: no diagnosis of epilepsy (only ripples co-occurring with vertex waves); gray triangles: diagnosis of epilepsy uncertain; black triangles or diamonds: diagnosis of epilepsy. Ripples occurring in normal EEG are plotted above the horizontal line, ripples in EEGs containing IEDs are plotted below the horizontal line. Start of the vertex wave or IED is depicted as the vertical line at zero. Note that all ripples co-occurring with vertex wave occur after the start of the vertex wave, regardless of the diagnoses (open, gray, or black downward pointing triangles) or type of EEG (above or below horizontal line). Ripples co-occurring with an IED start around the start of the IED.

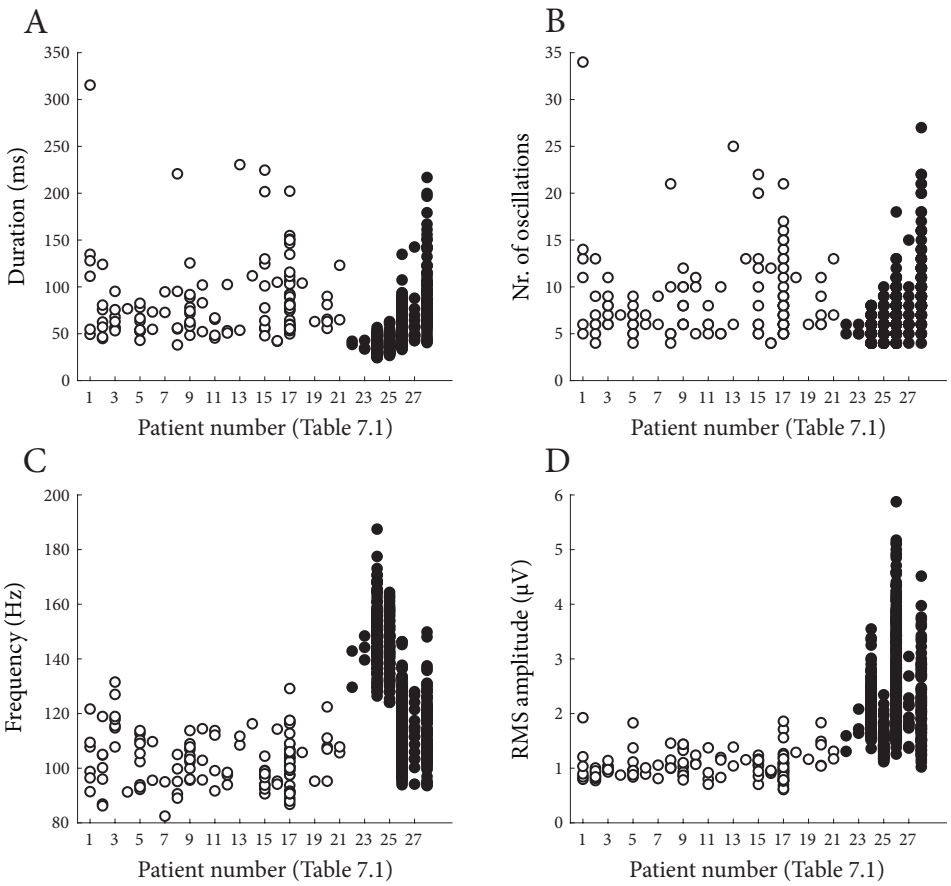

Figure 7.3 Ripple characteristics plotted per child. Number on the x-axis corresponds to number in Table 7.1. Duration in ms (A), number of oscillations (B), frequency in Hz (C), and root mean square (RMS) amplitude in μV (D). Note that frequency was higher for ripples co-occurring with IEDs in patient 22-25.

Ripples co-occurring with polyspikes

The EEG of one child contained ripples co-occurring with polyspikes (28 in Table 7.1). These ripples started on average 7.6 ms after the start of polyspikes (mdn: 6.3 ms, sd: 25.5 ms), which falls within the 95% predictive interval (PI) of ripples co-occurring with IEDs (Table 7.2). The mean duration was 92.6 ms (mdn: 85.4 ms, sd: 35.8 ms), which is outside the 95% PI for ripples co-occurring with IEDs. The mean of the number of oscillations was 10.6 (mdn: 9.5, sd: 4.4), which is also outside the 95% PI for IED-ripples. The mean frequency was 114.6 Hz (mdn: 113.4 Hz, sd: 11.5 Hz), which is just inside the 95% PI for all pathological ripples, and comparable to the frequency of the pathological ripple subtype with lower

frequency (gray + in cloud of gray circles in Figure 7.4). Mean amplitude was 2.1 μV (mdn: 2.0 μV, sd: 0.7 μV), which is inside the 95% PI for ripples co-occurring with IEDs.

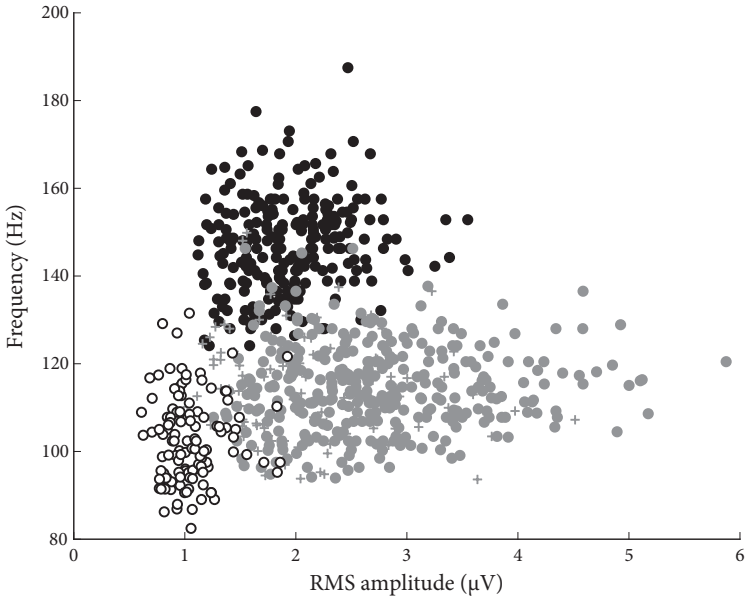

Figure 7.4 Scatter plot of root mean square (RMS) amplitude in μV and frequency in Hz, showing differences between physiological ripples (open circles) and two pathological ripple subtypes. Note that amplitude of ripples co-occurring with vertex waves and ripples co-occurring with IEDs barely overlap, while frequency divides the group of IED-ripples into two subgroups. Ripples co-occurring with polyspikes are plotted as +; these ripples fall within the range of the pathological subtype with high amplitude and intermediate frequency.

Discussion

Physiological ripples start on average about 100 ms after the start of the vertex wave, while pathological ripples and IEDs start approximately at the same time. Vertex-wave associated ripples seem to have had a longer duration, lower frequency, and lower amplitude than ripples co-occurring with IEDs. Ripples on Rolandic spikes may represent a pathological ripple subtype with higher frequency than ripples that co-occur with IEDs in EEGs of children with symptomatic epilepsy types.

IEDs and pathological ripples

The observed start of ripples in relation to the start of the IED is in line with results of Clemens et al. (2007) and van Klink et al. (2015).[117,118] This finding suggests that IEDs have no role in the generation of pathological ripples. It is more likely that the same underlying pathological processes can generate both IEDs and ripples: sometimes only one of the two will occur, and when they both occur, this happens approximately at the same time. This interpretation seems compatible with previously reported hypotheses regarding the underlying mechanisms of IEDs and HFOs. IEDs are supposedly generated by the synchronous discharges of a group of pyramidal cells that are hyperexcitable, perhaps because of altered or failing inhibition.[84,119–122] Pathological ripples are also proposed to be generated by synchronization of action potential firing within groups of interconnected pyramidal neurons.[120,121,123]

Vertex waves and physiological ripples

Physiological ripples seem to represent a summation of synchronous, inhibitory, postsynaptic potentials (IPSPs) on the membranes of pyramidal cells.[121,123] The role of co-occurring vertex waves is not clear, but the finding that vertex waves start before the start of the ripple suggests that they may have a facilitating role in the generation of ripples. Perhaps their role is comparable to the role of sharp waves in the sharp wave-ripple complexes that occur in the hippocampus. Hippocampal sharp waves represent a burst of activity from neurons in the CA3 region that discharges interneurons in the CA1 region. The interaction between CA1 pyramidal cells and interneurons gives rise to the ripple.[78,95,120]

We do not know of studies that draw such a parallel between sharp waves in the hippocampus and vertex waves in the neocortex. However, Buszáki (2015) stated that there are similarities between the hippocampal sharp wave and the neocortical K-complex.[95] K-complexes and vertex waves have the same distribution (frontal-central or central maximum near the vertex) and both can occur in response to external stimuli.[112,113,124] The appearance of vertex waves is more similar to hippocampal sharp waves than the appearance of K-complexes; the latter usually have longer duration and a more complex shape.[26,113,124]

Characteristics of physiological and pathological ripples

As reported in the introduction, results of invasive studies that compare frequency, duration and amplitude are contradictory or overlapping,[63,65,86,87,100,101,103,114,115] especially for duration and frequency. A lower amplitude for presumably physiological ripples compared to the amplitude of pathological ripples seemed to be the most consistent result (Supplementary Table 7.1). The scalp-EEG recorded ripples in this study also showed lower amplitudes for physiological than for pathological ripples, but with less overlap than between invasively recorded ripple types. Buzsáki and Lopes da Silva (2012) offered an explanation for a lower amplitude of physiological ripples.[78] They stated that, in general, the generation of physiological events is controlled by many mechanisms. As a result, the number

of recruited neurons is limited, and this is reflected in the limited magnitude of physiological events. In contrast, pathological events are less well regulated. More pyramidal neurons can be involved, and recruitment can occur faster. This results in events with larger and more varying magnitude.[78]

Physiological and pathological ripples in the same EEG

We showed that characteristics of ripples co-occurring with vertex waves were consistent, regardless of the type of EEG (normal or containing IEDs) or diagnosis (no diagnosis of epilepsy or epilepsy). Our study does not describe the characteristics of presumably physiological ripples occurring in EEGs that also contained IED-associated ripples. We found both types of ripples in only one EEG (22 in Table 7.1), but the presumably physiological ripples co-occurred with other sleep-specific transients than vertex waves (namely, spindles and K-complexes), and were therefore not analyzed in this study. That same EEG even contained a ripple that co-occurred with what may have been a vertex wave, but the possibility that the co-occurring event was a spike could not be excluded. We could therefore not include it as either of these events in the analysis. We noted, however, that the duration, frequency, and amplitude of the ripple co-occurring with this dubious vertex wave were like those of physiological ripples, but that the ripple started 6 ms after the start of the co-occurring event, which would be expected of pathological ripples. This may therefore have been an example of some kind of 'intermediate physiological-pathological ripple' type, but one example is not sufficient to draw such a conclusion. Likewise, we cannot conclude that a change in characteristics of physiological ripples in people with chronic epilepsy is the explanation for the overlap of their characteristics with pathological ripples in intracranial EEG.

Since frequency, duration, and amplitude were not sufficiently different for discrimination, researchers have sought other ways to discriminate physiological and pathological ripples recorded with intracranial EEG. For example, physiological and pathological ripples have been found to be coupled to different phases of slow waves, although results again overlapped.[65,77,102] In this study, the start of the ripple relative to the start of the vertex wave varied within and between patients, but was consistently different than the start of pathological ripples compared to IED start. Again, a future study is needed to investigate if this would change, as seemed to be the case for the one potential 'intermediate ripple', in EEGs containing both ripples co-occurring vertex waves or other physiological sleep-specific transients and ripples co-occurring with IEDs.

Pathological ripple subtypes: ripples co-occurring with polyspikes and ripples on Rolandic spikes

The long duration of ripples co-occurring with polyspikes was mostly explained by the larger number of oscillations. Perhaps these ripples are 'poly-ripples', which, like polyspikes, consist of repetitive ripples but look like one long ripple.

A few other studies reported frequencies of scalp-EEG recorded ripples on Rolandic spikes. Similar frequencies to the ones found in this study (mean

147.1 Hz) were reported by Ikemoto et al. (2018) and Ohuchi et al. (2019), while Kobayashi et al. (2011) and Shibata et al. (2016) reported lower mean frequencies.[125–128] More studies are needed to confirm that ripples co-occurring with Rolandic spikes form a ripple subtype with higher frequencies than other ripples co-occurring with IEDs.

Limitations

The number of ripples per patient varied and was sometimes small, especially for ripples co-occurring with vertex waves. The small number of children with Rolandic epilepsy prevented an analysis of the ripple subtype that ripples on Rolandic spikes seemed to represent.

Since our cohort did not include children who had both ripples on true vertex waves and ripples associated with unequivocal IEDs on the vertex, we could not compare the characteristics of presumed physiological and pathological ripples occurring within the same patient and at the same location.

Conclusion and future directions

We studied ripples co-occurring with two types of sharp EEG transients and found that they are different types of high-frequency oscillations, as reflected by the observed difference in timing of the start of the ripples relative to the start of vertex waves or IEDs, and by the differences in duration, frequency and amplitude. Future studies are needed to investigate if vertex waves are neocortical equivalents of hippocampal sharp waves. Future research is also needed to determine whether ripples co-occurring with Rolandic spikes form a pathological ripple subtype with relatively high frequency, and if characteristics of physiological ripples are different in EEGs that also contain pathological ripples.

Supplementary material

Supplementary Table 7.1 Overview of studies comparing duration, frequency, and amplitude of presumably physiological and pathological ripples

	Duration/frequency/amplitude of physiological ripples compared to pathological ripples		
Intracranial recordings	**Duration**	**Frequency**	**Amplitude**
Nagasawa et al., 2012[101] (a)	Longer, mdn 298 vs. 180 ms	Higher, mdn 105 vs. 85 Hz (n.s.)	Lower, +409% vs. +636 % (n.s.)
Wang et al., 2013[63] (b)	Longer, mdn 71 vs. 51 ms	Reported lower, but mdn the same: 111 Hz	Lower, mdn 10 vs. 15.9 μV
Matsumoto et al., 2013[86] (c)	Shorter, mean 12.1 vs. 23.1 ms	Higher, mean 264.2 vs. 188.4 Hz	Lower, mean ? vs. 9.07 z-scores compared to background
Alkwadri et al., 2014[87] (d)	Longer, mdn 173 vs. 126 ms	Lower, but mdn almost equal: 100 vs. 102 Hz	Higher, mdn. 56 vs. 50 μV
Malinowska et al., 2015[114] (e)	Almost equal, mean 59 vs. 60 ms	Almost equal, mean 99.44 vs. 98.44 Hz	Almost equal, 20.28 vs. 21.12 μV
Von Ellenrieder et al, 2016[65] (f)	Shorter, mdn 70 vs. 84 ms	Almost equal, mdn 111 vs. 109 Hz	Lower, mdn 2.17 vs. 4.85 μV
Bruder et al., 2017[100] (g)	Slightly shorter, mdn 47.5 vs. 50.5 ms	Slightly higher, mdn 134.8 vs. 130.8 Hz	Lower, mdn 3.24 vs. 3.96 μV
Pail et al., 2017[103] (h)	Slightly longer, mean 56.12 vs 54.40 ms	NA	Lower, mean 56.30 vs. 77.47 (i)
Cimbalnik et al., 2018[115] (j)	Shorter, 12 (or 18?) vs. 27 ms (k)	Higher, 133.60 vs. 125.14 Hz	Almost equal, 31.94 vs 31.75 μV

n.s.: not significant. Mdn: median.

(a) Pathological ripples: recorded in "epileptogenic site of interest"; physiological ripples: spontaneously occurring in occipital lobe outside seizure focus. Amplitude specified as augmentation (in %) compared to event-free reference period.

(b) Type 1, pathological ripples: superimposed on interictal epileptic discharge (IED), type 2, presumable physiological ripples: occurring independent of IED.

(c) Pathological ripples: spontaneously occurring in SOZ; physiological ripples: induced by a visual or motor task. Note: mean frequency of physiological ripples lies in the fast ripple range (250-500 Hz).

(d) Pathological (epileptic) HFOs: occurring in channels with IEDs or in SOZ; physiological ripples: occurring in remaining channels.

(e) Pathological ripples: occurring in SOZ; physiological ripples: occurring outside SOZ (results from Table 2, interictal ripples)

(f) Pathological ripples: occurring in SOZ; physiological ripples: occurring outside SOZ and outside exclusively irritative zone (EIZ). Results of EIZ are also given; they are in between results of ripples recorded in SOZ and non-epileptic channels.
(g) Pathological ripples: co-occurring with spikes or occurring in SOZ; physiological ripples: co-occurring with sleep spindles outside SOZ (Table 2).
(h) Pathological ripples: occurring in SOZ; physiological ripples: outside SOZ and irritative zone (IZ). Results of IZ are also reported; they are in between results of SOZ and non-epileptic channels.
(i) We were not sure in which units ripple amplitude was expressed.
(j) Pathological ripples: occurring in SOZ; physiological ripples: occurring in patients with facial pain without a history of seizures. Task induced physiological ripples in patients with epilepsy were also reported but not used for the comparison here.
(k) Unsure if mean or median values were reported. There seemed to be two results for the duration of physiological ripples: 12 and 18 ms.

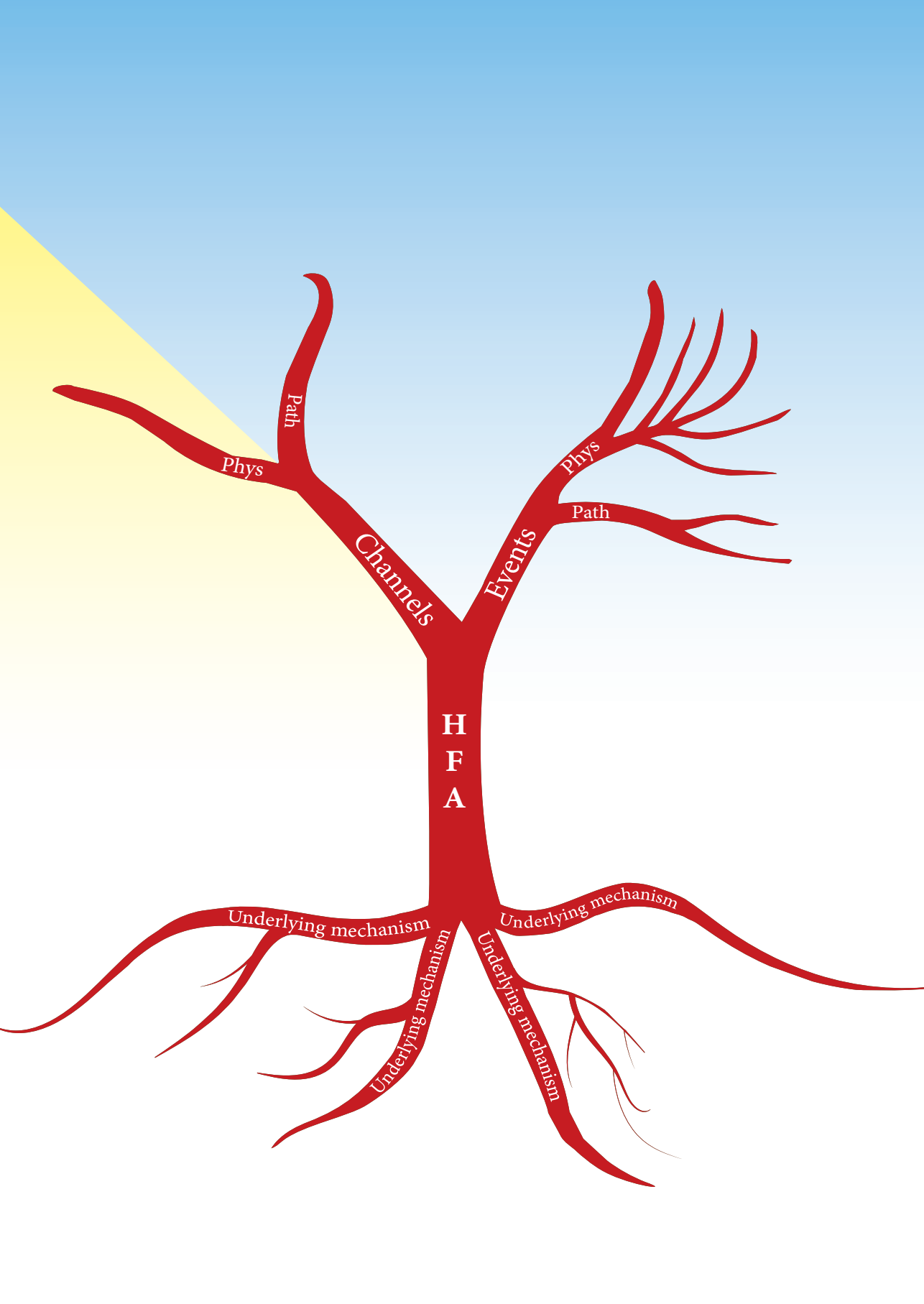
Phys
Path
Channels
Events
Phys
Path
H
F
A
Underlying mechanism
Underlying mechanism
Underlying mechanism
Underlying mechanism

Chapter 8

General discussion

Different perspectives

In this chapter, I will discuss the different perspectives that were introduced in the general introduction. It is not my intention to provide a review of all the possible aspects of the different perspectives. Instead, I will focus on topics that are directly related to results of this thesis as described in the previous chapters.

1. Clinical utility versus basic neurophysiology

In this thesis, the difference between clinical utility and basic neurophysiology is mostly characterized by a difference in how these two topics are approached: we zoomed out when clinical utility was the aim, and we zoomed in on details for basic neurophysiological research.

Zooming out

High-gamma mapping versus electrocortical simulation mapping (ESM)

High-gamma language mapping has been studied for almost 20 years, but it remains not more than a promising alternative for ESM. Why is it so difficult to draw a conclusion on the clinical utility of high-gamma mapping? The answer probably is: because of the many methodological differences between studies. We showed in part 1 that there are at least three ways in which high-gamma mapping and ESM results have been compared. We demonstrated that these different ways of comparing high-gamma mapping and ESM result in different sensitivity and specificity (part 1, chapters 2 and 3). This comparison is the last step in a study, taken after it has already been established whether the electrode or channel is considered high-gamma positive or negative. Many methodological choices need to be made before such a result is obtained. Each research group uses its own methods, which may be defendable but which make a comparison with other studies even more complicated. For example, studies use different language tasks and different ESM protocols.[12,13] As to high-gamma mapping: studies differ in terms of frequency band of choice, type of time-frequency transform used for obtaining power in that frequency band, statistical methods used to determine if there is significant task-induced high-gamma activity, etc.

Some recommendations for evaluating the performance of high-gamma language mapping compared to ESM that may help to determine whether high-gamma mapping can replace ESM:

- Study groups can use language tasks of their own choice, but at least one task should be used by all groups, and results of this task should be reported independently of the results of other tasks. In this way, results of different groups can more easily be compared. Visual object naming seems to be the best candidate for this 'standard test', because it is already the most frequently used task.[12]

- Optimal settings for high-gamma mapping should be investigated using the same language tasks as ESM, including the 'standard test', so that ESM and high-gamma mapping results can truly be compared.
- Extra tests that are only applied during high-gamma mapping *or* ESM can provide valuable information but should not be used in the comparison of the two techniques, because doing so leads to results that cannot be interpreted. For example, if an extra language test used for high-gamma mapping results in an extra language site that was not identified with ESM, should this site be considered a false positive? It may be a true positive language site that was missed by ESM because it was not tested using ESM. If an extra task is used during either mapping technique, the results should be evaluated with respect to surgery outcome.
- Sensitivity and specificity should be calculated according to methods A and B as described in part 1, (see Figure 3.1, page 38). Method C is not valid, because it makes high-gamma mapping the gold standard to which ESM is compared.

These recommendations will hopefully help to make a meaningful comparison of study results possible, which will facilitate the optimization of settings for high-gamma mapping, such as an optimal frequency band within the high-gamma range of 60-200 Hz.

A last note that needs to be made here is that our own study, as presented in chapter 2, does not fulfill the requirement of using the same task for high-gamma mapping and ESM. We compared picture naming during ESM and listening to speech and music during high-gamma mapping. The results of this study can therefore not be used to help decide if high-gamma language mapping can replace ESM. I think the significance of the language and music task is rather that we found ESM language sites not only with high-gamma activity that was induced while listening to speech, but also with high-gamma that was induced by listening to music. Music is a phenomenon that is found in every culture in the world and the evolution of language and music is thought to be related.[37,38] Language areas are spared because quality of life suffers from impairment of language functions. It is an interesting question whether we should consider if music should be given the same consideration, either for its own sake or because of its relation to language.

Interictal epileptic events

The question that needs to be answered when using invasive recording techniques in the pre-surgical work-up of epilepsy is: Does the brain area located beneath (in the case of ECoG) or around (iEEG) an electrode need to be preserved or resected? As long as this question is answered efficiently and accurately, the details of the activity that was recorded in the electrode are not relevant. In other words: in clinical practice, the simplest way of getting the answer may be the best way, provided that the simple way has the same accuracy as a method that focusses on details. Part 2, chapter 4, follows this line of thinking.

Spikes and HFOs are biomarkers for the epileptogenic zone,[15,17] but identifying these events remains challenging.[18] We therefore sought a way to use the presence of these events without the need to mark or detect them. The results of the 'skew method', reported in part 2, are promising but need confirmation in other iEEG data sets before we can conclude if the method is clinically useful.

Zooming in on neurophysiological details

Part 3 of this thesis is about a basic neurophysiological finding, namely that physiological ripples can be recorded with scalp EEG. In such a case, it is important to study the details of the newly observed phenomenon, i.e., zoom in on its characteristics, which we have done in chapters 5 and 6.

This discovery has currently no clinical use, but it opens the field of HFO research to new research possibilities. For example, if these physiological ripples are involved in memory consolidation, as was speculated in part 3 and which has become more likely since the publication of more papers on neocortical ripples in animals and humans,[7,96] they may in the future be used as biomarker for memory function, for example in children with epilepsy and memory problems. Physiological ripples may also become relevant for research on memory disorders, like different types of dementia, provided that they can be recorded in adults.

2. Invasive versus non-invasive recordings

Place versus time

The discovery that ripples and even fast ripples can be recorded with scalp EEG means that HFO research and the potential use of HFOs in clinical practice are not limited to candidates for epilepsy surgery who undergo invasive recordings. The main goal of using invasive recordings is to locate the epileptogenic zone and eloquent areas, i.e., it is focused on 'place'. In contrast, scalp EEG can also be used in healthy people, or in patients after a first seizure who may be far away from, or may never develop chronic epilepsy. This makes it possible to investigate if HFOs are also a prognostic biomarker, i.e., a biomarker of the time course of epilepsy. Examples of this idea are two studies that showed that the number of ripples co-occurring with Rolandic spikes is correlated to the number of seizures in children with Rolandic epilepsy.[129,130]

The possibility to study HFOs from the first seizure onwards also allows including them in research on changes in neurophysiological activity during epileptogenesis (i.e., the development of epilepsy). In one of the studies presented in this thesis, we found a potential example of this.

When studying ripples co-occurring with vertex waves or IEDs (part 4, chapter 7), there was one EEG in which we found two ripples that co-occurred with IEDs, but also a ripple in the same channel that co-occurred with an event that was probably a vertex wave, but the possibility that it was an IED could not definitely be excluded. The potential vertex wave had a short duration (total duration 100

ms, while the total duration of a vertex wave is usually about 200 ms or, especially in children, longer, with a maximum duration of 500 ms.[113,124]) The ripple had a duration (78.6 ms), frequency (101.8 Hz), and root mean square amplitude (1.0 μV) that were similar to the duration, frequency, and amplitude of physiological ripples (see part 4, chapter 7). However, the start of the ripple relative to the start of the co-occurring event was more like that of a pathological ripple: it started only 6 ms after the start of the dubious vertex wave.

It is impossible to draw conclusions based on one ripple, but the finding that the dubious vertex wave and the co-occurring ripple had physiological and pathological characteristics reminds me of a phenomenon reviewed by Halasz et al. (2019).[69] He described how physiological events can transform into pathological ones, taking spindles in absence epilepsy and sharp-wave ripples in mesio-temporal epilepsy as examples. Halasz also discussed Rolandic epilepsy and Panayiotopoulos syndrome and stated that in these cases: "we cannot point out a physiological sleep oscillation transforming to an epileptic variant. These conditions are featured by centro-temporal spikes, not representing a pathological transformation of any sleep oscillation,…".[69] I wonder if vertex waves could be the physiological sleep-specific transient that evolves into a pathological phenomenon in these childhood epilepsies. Halasz (2019) also mentioned that the infantile version of centro-temporal spikes behaves as an augmented evoked potential,[69] responding to acoustic and tactile stimuli, which is also a characteristic of vertex waves.[1,113] Moreover, Rolandic spikes show a greater increase in the number of occurrences with drowsiness than other IEDs[124] and drowsiness is the sleep stage in which vertex waves are the most prominent sleep-specific transient.

Testing the hypothesis that vertex waves can transform into spikes in Rolandic epilepsy and Panayiotopoulos syndrome requires a study in which ripples co-occurring with vertex waves and spikes are marked in a larger cohort of children with these diagnoses. Ripples should be divided in three categories: ripples with pathological characteristics and 'pathological' phase relation to spikes, ripples with physiological characteristics and 'physiological' phase relation to vertex waves, and ripples co-occurring with events that could be spike or vertex wave, and that have characteristics or phase relations that are expected of physiological or pathological ripples. It should then be tested if the number of ripples in each category is correlated to the duration and severity of the disease (i.e. time since diagnoses, number of seizures). Ideally this should be done in several EEGs per child that are recorded during different stages of the disease.

Physiological ripples in scalp EEGs of children and adults?

The discovery that physiological ripples can be seen in scalp EEGs of children, raises the question whether they can also be found in scalp EEGs of adults. Every new step in HFO research, from micro- to macroelectrodes, from macroelectrodes to pathological ripples co-occurring with spikes in scalp EEG, and finally to fast ripples in scalp EEG, has been cause for surprise.[131] Ever since the first descriptions of pathological ripples that were observed in scalp EEG,[23,24]

researchers have attempted to explain how these events, which are thought to be generated in a smaller area than is considered necessary for visibility on scalp EEG, can nonetheless be seen on scalp EEG. Two possible answers are:

- HFOs have a low amplitude, but they are still visible because background activity decreases with increasing frequency.[132] (Note that the background activity in Figure 1.1 (page 10) is lower in the scalp EEG traces than in the iEEG traces.)
- Ripples that are visible on scalp EEG might represent a summation of simultaneous but asynchronous ripples that are generated over a more widespread region.[133]

The skull has long been thought to filter out high-frequency activity. This is not the case, however, at least not for frequencies in the ripple or fast ripple range.[134] The resistivity of the skull does cause an attenuation of the electrical activity that passes through it, but it does so equally for low- and high-frequency activity. The skull has a further influence on activity recorded on the scalp by increasing the distance between the source of the activity and the electrode that records it, because the amplitude of a signal decreases with increasing distance from its source.[5]

We found that physiological ripples have a lower amplitude than pathological ripples (part 4, chapter 7), and even these low-amplitude physiological ripples were visible on scalp EEG. However, these physiological ripples were recorded in children, and the skull becomes thicker when children grow. Thus, it may be possible that the resistivity and the distance between the scalp electrode and the source of ripple activity may become too large for the ripples to be visible on scalp EEGs of adults. To get an impression if this might be the case, we made boxplots of the root means square (RMS) amplitude of physiological ripples recorded in children and plotted them in order of increasing age (Figure 8.1). This figure shows no trend of decreasing amplitude with increasing age. This is an encouraging sign, but based on the findings in only nine children with a maximum age of 8.9 years. The finding that even such low amplitude events as fast ripples can be seen on scalp EEGs of children (Bernardo et al., 2018,[25] and own observations (unpublished)), provides further hope for recording physiological ripples in scalp EEG of adults. Future research needs to prove if this hope is justified.

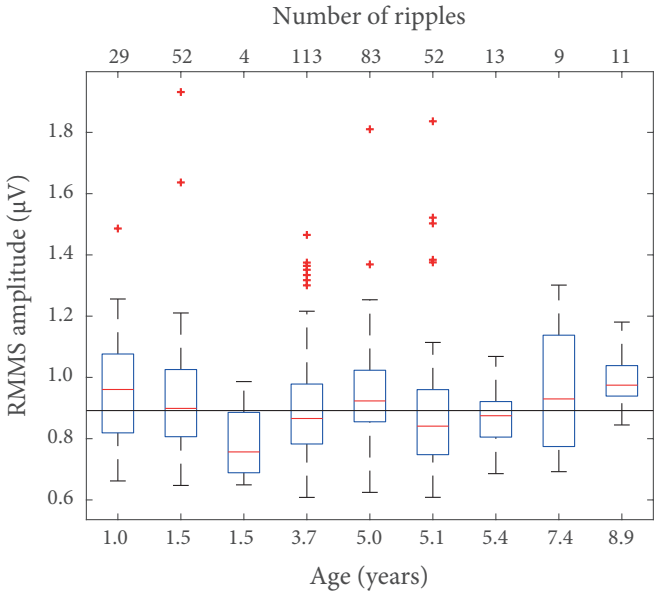

Figure 8.1 Boxplots of root mean square (RMS) amplitude of physiological ripples recorded in children without a brain disorder included in part 3. Boxes are sorted in order of increasing age. Number of ripples per child is provided at the top of the figure. The red line within each box is the median RMS amplitude per child; the horizontal black line is the mean of the medians of the nine children. Note that there is no visible trend towards decreasing ripple amplitude with increasing age.

3. Wake versus sleep

In this thesis, the high-gamma activity that was recorded in part 1, chapter 2 was induced by a listening task in patients who were awake, while the HFOs that were recorded in parts 2, 3, and 4 occurred spontaneously in patients who were sleeping. This could raise two questions:

1) Is wakefulness needed for inducing task-related high-gamma activity, and is sleep needed for recording ripples?
2) Has high-gamma activity also been recorded when occurring spontaneously, and can HFOs also be induced?

Is wakefulness needed for inducing task-related high-gamma activity, and is sleep needed for recording ripples?

I could not find papers reporting induced high-gamma activity recorded during sleep, suggesting that induced high-gamma has only been observed in awake participants. Sleep, however, is not necessary for recording ripples, but using sleep data can make finding and recognizing ripples easier.

Finding pathological ripples in sleep is easier because there are more of them: pathological ripples and fast ripple occur most often during non-rapid eye movement (NREM) sleep.[62,64,70] However, pathological HFOs can also be recorded during wakefulness.[62,64,70]

Recognizing ripples in scalp EEG can be challenging because filtering sharp artifacts can result in spurious ripples. Physiological ripples occurring in scalp EEG had not been described before, so we needed to be completely sure that the events that we marked as ripples were indeed ripples. This is much easier if there are fewer artifacts, as is the case during sleep, because there is less movement and less activity of the scalp muscles. Nonetheless, presumably physiological ripples, recorded with invasive techniques, can also occur spontaneously during wakefulness,[135,136] and may even occur more often during quiet wakefulness than during sleep.[99]

Has high-gamma activity also been recorded when occurring spontaneously, and can HFOs also be induced?

Activity in the high-gamma band was visible on time-frequency plots shown in studies on scalp EEGs of healthy sleeping adults (up to 125 Hz) and healthy sleeping children (up to 95 Hz).[89,90] Physiological HFOs can be induced by a visual task,[101] visual or motor tasks,[86] visual and cognitive task,[137] and cognitive tasks.[135,136] Inducing physiological ripples has been proposed as a way to differentiate invasively recorded physiological from pathological ripples in people with chronic epilepsy,[86,138] because a task is thought to exclusively induce physiological ripples. However, the challenge of differentiating physiological and pathological ripples lies in spontaneously occurring ripples: spontaneously occurring physiological ripples that are mistaken for pathological ones reduce the specificity of ripples for the epileptogenic zone. Since inducing ripples will not stop the spontaneous ripples from occurring, it seems unlikely that it will promote the correct differentiation of spontaneous physiological and pathological ripples. Nonetheless, inducing physiological ripples or high-gamma activity is a valuable approach when studying cognitive functioning.

Selectively evoking pathological HFOs could be another way to improve the specificity of ripples for the epileptic zone. Pathological HFOs can be evoked with single pulse electrical stimulation (SPES),[139] but SPES results are not good enough to make efforts to differentiate spontaneous physiological and pathological ripples unnecessary. In one study, fast ripples could be evoked with good specificity (84%), but sensitivity was not sufficient: only about half (52%) of the channels inside the seizure onset zone (SOZ) contained evoked fast ripples. Sensitivity of evoked ripples was higher (86%), but the specificity was poor (46%), indicating that 54% of channels outside the SOZ also contained evoked ripples.[140] Thus, evoking events is not the solution, at least not yet. Evoking fast ripples can be helpful, however, for example by strengthening the hypothesis of the location of the epileptogenic zone in patients whose recordings do not contain spontaneously occurring fast ripples.[140]

Perspectives not studied in this thesis

There are more ways to study high-frequency EEG activity than were presented in this thesis. I do not intend to provide a list of all possible ways in which HFA can be studied, but I will mention a few other examples that often occur in the HFA literature.

- Interictal versus ictal HFOs. In this thesis, all HFOs occurred in interictal recordings, but HFOs occurring during seizures have also been reported.[21]
- Visually marked versus automatically detected. In this thesis HFOs were either visually marked (parts 3 and 4) or we aimed to select channels with events without marking or detecting them (part 2).
- The field of cognitive neuroscience often studies coupling of slow and fast oscillations, for example how the amplitude of fast oscillations is modulated by the phase of a slower oscillation.[141] We also studied co-occurrence of ripples with events in the low (0-70 Hz) frequency band (chapters 6 and 7), but not using measures of phase-amplitude coupling. An advantage of phase-amplitude coupling seems to be that it can be used to describe coupling between slow and fast oscillations that occur in the same brain regions, but also between oscillations occurring in different brain regions.[142–145]

Roots of the tree

A tree cannot exist without roots. In case of the tree of HFA (Figure 1.2), the roots represent mechanisms underlying the generation of HFA. These underlying mechanisms were not investigated in this thesis, but I will briefly summarize reviews about the underlying mechanisms of gamma activity and of physiological and pathological HFOs.

- Two models have been proposed for the generation of gamma activity: a) a model based on synchrony through mutual inhibition of interneurons (the inhibitory-inhibitory or I-I model) and b) a model based on synchrony through an excitatory-inhibitory loop (E-I model), in which interneurons and pyramidal neurons interact. The two models may also work together.[146]

Complexity increases with the suggestion that there are distinct types of gamma activity, namely slow gamma (30-50 Hz), mid-frequency gamma (50-90 Hz), and fast gamma or epsilon band (90-140 Hz).[146] The fast gamma band is thought to have different underlying mechanisms than the lower frequency gamma bands.[147]

Most research groups studied a sub-band within the 60-200 Hz high-gamma band, but high-gamma activity can also appear as broadband activity which can span the above-mentioned mid-frequency and fast gamma bands. The underlying mechanisms of such broadband gamma activity are unclear. One proposed explanation is that multiple neuronal populations oscillate at different (high-gamma) frequencies, which add up to a broad band,[14] but this hypothesis has not been proven.[5]

- Physiological ripples seem to represent a summation of extracellularly recorded, synchronous, inhibitory, postsynaptic potentials (IPSPs) on the membranes of pyramidal cells.[121,123] It is not clear to me how the IPSPS relate to the I-I model that was mentioned above, but it seems likely that a brief burst of high- or fast-gamma activity of about 100 Hz is the same neurophysiological phenomenon as a physiological ripple with that frequency.
- Pathological ripples are generated by synchronization of action potential firing within groups of interconnected pyramidal neurons.[120–122] Synchronization is mediated not only through synaptic transmission, but also through gap junctions or ephaptic coupling.[121]
- Fast ripples are also generated by synchronization of action potential firing within groups of pyramidal neurons. However, the frequencies of fast ripple oscillations (250-500 Hz) exceed the maximum firing frequency of pyramidal neurons, which is thought to be about 300 Hz. Fast ripple frequencies are reached because subpopulations of neurons fire asynchronously at lower (ripple) frequencies; this out-of-phase firing can result in a doubling of the frequency.[121]

Conclusion

The work presented in the first two parts of this thesis may facilitate the clinical utility of HFA analysis. The results reported in the last two parts expand the knowledge of scalp-EEG recorded ripples. The finding that physiological ripples can be recorded with scalp EEG is the most remarkable result, because it opens up a new field for HFO research. The next step in physiological ripple research should be to investigate if physiological ripples can be found in scalp EEGs of adults and in scalp EEGs recorded during wakefulness. The most pressing question is about the neurophysiological relevance of these ripples: are they involved in memory consolidation?

Addendum

References

1. Schomer DL, Lopes da Silva FH. Niedermeyer's Electroencephalography. 7th ed. New York, NY, Oxford University Press; 2018.
2. Fisher RS, Acevedo C, Arzimanoglou A, et al. ILAE Official Report: A practical clinical definition of epilepsy. *Epilepsia*. 2014;55:475-482.
3. Ventola CL. Epilepsy Management: Newer Agents, Unmet Needs, and Future Treatment Strategies. *P T*. 2014;39:776-785.
4. Crone NE, Sinai A, Korzeniewska A. High-frequency gamma oscillations and human brain mapping with electrocorticography. *Prog Brain Res*. 2006;159:275-295.
5. Gotman J, Crone NE. High-Frequency EEG Activity. In: Schomer DL, Lopes da Silva FH. Niedermeyer's Electroencephalography, 7th ed. New York, NY, Oxford University Press; 2018;809-832.
6. Buzsáki G. Memory consolidation during sleep: a neurophysiological perspective. *J Sleep Res*. 1998;7 Suppl 1:17-23.
7. Vaz AP, Inati SK, Brunel N, Zaghloul KA. Coupled Ripple Oscillations Between the MTL and Neocortex Retrieve Human Memory. *Science*. 2019;363:975-985.
8. Zijlmans M, Jiruska P, Zelmann R, Leijten FSS, Jefferys JGR, Gotman J. High-frequency oscillations as a new biomarker in epilepsy. *Ann Neurol*. 2012;71:169-178.
9. Frauscher B, Bartolomei F, Kobayashi K, et al. High-frequency oscillations: The state of clinical research. *Epilepsia*. 2017;58:1316-1329.
10. Wilcox KS, Dixon-Salazar T, Sills GJ, et al. Issues related to development of new antiseizure treatments. *Epilepsia*. 2013;54(SUPPL.4):24-34.
11. Ryvlin P, Cross JH, Rheims S. Epilepsy surgery in children and adults. *Lancet Neurol*. 2014;13:1114-1126.
12. Hamberger MJ. Cortical Language Mapping in Epilepsy: A Critical Review. *Neuropsychol Rev*. 2007;17:477-489.
13. Hamberger MJ, Williams AC, Schevon CA. Extraoperative neurostimulation mapping: Results from an international survey of epilepsy surgery programs. *Epilepsia*. 2014;55:933-939.
14. Crone NE, Boatman D, Gordon B, Hao L. Induced electrocorticographic gamma activity during auditory perception. *Clin Neurophysiol*. 2001;112:565-582.
15. Lüders HO, Najm I, Nair D, Widdess-Walsh P. The epileptogenic zone: general principles. *Epileptic Disord*. 2006;8:S1-9.
16. Worrell G, Gotman J. Biomarkers of Epilepsy: Clinical Studies. *Biomark Med*. 2011;5:557-566.
17. Thomschewski A, Hincapié AS, Frauscher B. Localization of the epileptogenic zone using high frequency oscillations. *Front Neurol*. 2019;10:94.
18. Zijlmans M, Worrell GA, Dümpelmann M, et al. How to record high-frequency oscillations in epilepsy: A practical guideline. *Epilepsia*. 2017;58:1305-1315.
19. Buzsaki G, Horvath Z, Urioste R. High-Frequency Network Oscillation in the Hippocampus. *Science*. 1992;256:1025-1027.
20. Bragin A, Engel J, Wilson CL, Fried I, Buzsáki G. High-frequency oscillations in human brain. *Hippocampus*. 1999;9:137-142.

21. Jirsch JD, Urrestarazu E, LeVan P, Olivier A, Dubeau F, Gotman J. High-frequency oscillations during human focal seizures. *Brain*. 2006;129:1593-1608.
22. Urrestarazu E, Chander R, Dubeau F, Gotman J. Interictal high-frequency oscillations (10-500 Hz) in the intracerebral EEG of epileptic patients. *Brain*. 2007;130:2354-2366.
23. Kobayashi K, Watanabe Y, Inoue T, Oka M, Yoshinaga H, Ohtsuka Y. Scalp-recorded high-frequency oscillations in childhood sleep-induced electrical status epilepticus. *Epilepsia*. 2010;51:2190-2194.
24. Andrade-Valenca LP, Dubeau F, Mari F, Zelmann R, Gotman J. Interictal scalp fast oscillations as a marker of the seizure onset zone. *Neurology*. 2011;77:524-531.
25. Bernardo D, Nariai H, Hussain SA, et al. Visual and semi-automatic non-invasive detection of interictal fast ripples: A potential biomarker of epilepsy in children with tuberous sclerosis complex. *Clin Neurophysiol*. 2018;129:1458-1466.
26. Berry RB, Brooks R, Garnaldo CE, Harding SM, Marcus CL, Vaughn B V. The AASM Manual for the Scoring of Sleep and Associated Events: Rules, Terminology and Technical Specifications, Version 2.0. *Am Acad Sleep Med.* Darien, IL. 2012.
27. Diekelmann S, Born J. The memory function of sleep. *Nat Rev Neurosci*. 2010;11:114-126.
28. Frauscher B, Gotman J. Sleep, oscillations, interictal discharges, and seizures in human focal epilepsy. *Neurobiol Dis*. 2019;127:545-553.
29. Wu M, Wisneski K, Schalk G, et al. Electrocorticographic frequency alteration mapping for extraoperative localization of speech cortex. *Neurosurgery*. 2010;66:E407-9.
30. Kojima K, Brown EC, Rothermel R, et al. Multimodality language mapping in patients with left-hemispheric language dominance on Wada test. *Clin Neurophysiol*. 2012;123:1917-1924.
31. Sinai A, Bowers CW, Crainiceanu CM, et al. Electrocorticographic high gamma activity versus electrical cortical stimulation mapping of naming. *Brain*. 2005;128:1556-1570.
32. Brown EC, Rothermel R, Nishida M, et al. In vivo animation of auditory-language-induced gamma-oscillations in children with intractable focal epilepsy. *Neuroimage*. 2008;41:1120-1131.
33. Towle VL, Yoon H-A, Castelle M, et al. ECoG gamma activity during a language task: differentiating expressive and receptive speech areas. *Brain*. 2008;131:2013-2027.
34. Miller KJ, Abel TJ, Hebb AO, Ojemann JG. Rapid online language mapping with electrocorticography. *J Neurosurg Pediatr*. 2011;7:482-490.
35. Bauer PR, Vansteensel MJ, Bleichner MG, et al. Mismatch between electrocortical stimulation and electrocorticography frequency mapping of language. *Brain Stimul*. 2013;6:524-531.
36. Arya R, Wilson JA, Vannest J, et al. Electrocorticographic language mapping in children by high-gamma synchronization during spontaneous conversation: Comparison with conventional electrical cortical stimulation. *Epilepsy Res*. 2015;110:78-87.
37. Besson M, Schön D. Comparison between language and music. *Ann N Y Acad Sci*. 2001;930:232-258.
38. Zatorre R, Belin P, Penhune V. Structure and function of auditory cortex: music and speech. *Trends Cogn Sci*. 2002;6613:37-46.

39. Noordmans HJ, van Rijen PC, van Veelen CW, Viergever MA, Hoekema R. Localization of implanted EEG electrodes in a virtual-reality environment. *Comput Aided Surg*. 2001;6:241-258.
40. Delorme A, Makeig S. EEGLAB: an open source toolbox for analysis of single-trial EEG dynamics including independent component analysis. *J Neurosci Methods*. 2004;134:9-21.
41. Koelsch S, Gunter TC, v. Cramon DY, et al. Bach Speaks: A Cortical "Language-Network" Serves the Processing of Music. *NeuroImage.* 2002;17:956–966.
42. Asaridou SS, McQueen JM. Speech and music shape the listening brain: evidence for shared domain-general mechanisms. *Front Psychol*. 2013;4:1-14.
43. Sammler D, Koelsch S, Ball T, et al. Co-localizing linguistic and musical syntax with intracranial EEG. *Neuroimage*. 2013;64:134-146.
44. Kojima K, Brown EC, Matsuzaki N, et al. Clinical Neurophysiology Gamma activity modulated by picture and auditory naming tasks: Intracranial recording in patients with focal epilepsy. *Clin Neurophysiol*. 2013;124:1737-1744.
45. Arya R, Horn PS, Crone NE. ECoG high-gamma modulation versus electrical stimulation for presurgical language mapping. *Epilepsy Behav*. 2018;79:26-33.
46. Mooij AH, Huiskamp GJM, Gosselaar PH, Ferrier CH. Electrocorticographic language mapping with a listening task consisting of alternating speech and music phrases. *Clin Neurophysiol*. 2016;127:1113-1119.
47. Ogawa H, Kamada K, Kapeller C, et al. Clinical Impact and Implication of Real-Time Oscillation Analysis for Language Mapping. *World Neurosurg*. 2017;97:2-5.
48. Ruescher J, Iljina O, Altenmüller DM, Aertsen A, Schulze-Bonhage A, Ball T. Somatotopic mapping of natural upper- and lower-extremity movements and speech production with high gamma electrocorticography. *Neuroimage*. 2013;81:164-177.
49. Wang Y, Fifer MS, Flinker A, et al. Spatial-temporal functional mapping of language at the bedside with electrocorticography. *Neurology*. 2016;86:1181-1189.
50. Arya R, Wilson JA, Fujiwara H, et al. Presurgical language localization with visual naming associated ECoG high- gamma modulation in pediatric drug-resistant epilepsy. *Epilepsia*. 2017;58:663-673.
51. Babajani-Feremi A, Narayana S, Rezaie R, et al. Language mapping using high gamma electrocorticography, fMRI, and TMS versus electrocortical stimulation. *Clin Neurophysiol*. 2016;127:1822-1836.
52. Genetti M, Tyrand R, Grouiller F, et al. Comparison of high gamma electrocorticography and fMRI with electrocortical stimulation for localization of somatosensory and language cortex. *Clin Neurophysiol*. 2015;126:121-130.
53. Korostenskaja M, Chen P. Real-time functional mapping: potential tool for improving language outcome in pediatric epilepsy surgery. *J Neurosurg Pediatr*. 2014;14:287-295.
54. Lin J, Zuo H, Hong B, et al. Mapping language area in the frontal lobe of the left-dominant hemisphere with high gamma electrocorticography. *J Neurolinguistics*. 2015;35:85-95.
55. Ogawa H, Hiroshima S, Kamada K. Left hippocampectomy in an epilepsy patient with right hemisphere language dominance. *Cogent Med*. 2017;4:1-9.

56. Ogawa H, Kamada K, Kapeller C, Hiroshima S, Prueckl R, Guger C. Rapid and minimum invasive functional brain mapping by real-time visualization of high gamma activity during awake craniotomy. *World Neurosurg*. 2014;82:912.e1-912.e10.
57. Tamura Y, Ogawa H, Kapeller C, et al. Passive language mapping combining real-time oscillation analysis with cortico-cortical evoked potentials for awake craniotomy. *J Neurosurg*. 2016;125:1580-1588.
58. Derix J, Iljina O, Weiske J, Schulze-Bonhage A, Aertsen A, Ball T. From speech to thought: the neuronal basis of cognitive units in non-experimental, real-life communication investigated using ECoG. *Front Hum Neurosci*. 2014;8:1-17.
59. Akiyama T, Osada M, Isowa M, et al. High kurtosis of intracranial electroencephalogram as a marker of ictogenicity in pediatric epilepsy surgery. *Clin Neurophysiol*. 2012;123:93-99.
60. Geertsema EE, Visser GH, Velis DN, Claus SP, Zijlmans M, Kalitzin SN. Automated Seizure Onset Zone Approximation Based on Nonharmonic High-Frequency Oscillations in Human Interictal Intracranial EEGs. *Int J Neural Syst*. 2015;25:1550015.
61. Motoi H, Miyakoshi M, Abel TJ, et al. Phase-amplitude coupling between interictal high-frequency activity and slow waves in epilepsy surgery. *Epilepsia*. 2018;59:1954-1965.
62. Bagshaw AP, Jacobs J, Levan P, Dubeau F, Gotman J. Effect of sleep stage on interictal high-frequency oscillations recorded from depth macroelectrodes in patients with focal epilepsy. *Epilepsia*. 2009;50:617-628.
63. Wang S, Wang IZ, Bulacio JC, et al. Ripple classification helps to localize the seizure-onset zone in neocortical epilepsy. *Epilepsia*. 2013;54:370-376.
64. Dümpelmann M, Jacobs J, Schulze-Bonhage A. Temporal and spatial characteristics of high frequency oscillations as a new biomarker in epilepsy. *Epilepsia*. 2015;56:197-206.
65. von Ellenrieder N, Frauscher B, Dubeau F, Gotman J. Interaction with slow waves during sleep improves discrimination of physiologic and pathologic high-frequency oscillations (80-500 Hz). *Epilepsia*. 2016;57:869-878.
66. Gigli GL, Valente M. Sleep and EEG interictal epileptiform abnormalities in partial epilepsy. *Clin Neurophysiol*. 2000;111(SUPPL. 2):S60-S64.
67. Foldvary-Schaefer N, Grigg-Damberger M. Sleep and epilepsy: What we know, don't know, and need to know. *J Clin Neurophysiol*. 2006;23:4-20.
68. Ng M, Pavlova M. Why Are Seizures Rare in Rapid Eye Movement Sleep? Review of the Frequency of Seizures in Different Sleep Stages. *Epilepsy Res Treat*. 2013;2013:1-10.
69. Halász P, Bódizs R, Ujma PP, Fabó D, Szűcs A. Strong relationship between NREM sleep, epilepsy and plastic functions — A conceptual review on the neurophysiology background. *Epilepsy Res*. 2019;150:95-105.
70. Staba RJ, Wilson CL, Bragin A, Jhung D, Fried I, Engel J. High-frequency oscillations recorded in human medial temporal lobe during sleep. *Ann Neurol*. 2004;56:108-115.
71. von Ellenrieder N, Dubeau F, Gotman J, Frauscher B. Physiological and pathological high-frequency oscillations have distinct sleep-homeostatic properties. *NeuroImage Clin*. 2017;14:566-573.

72. Zelmann R, Zijlmans M, Jacobs J, Châtillon CE, Gotman J. Improving the identification of High Frequency Oscillations. *Clin Neurophysiol*. 2009;120:1457-1464.
73. Châtillon CE, Zelmann R, Hall JA, Olivier A, Dubeau F, Gotman J. Influence of contact size on the detection of HFOs in human intracerebral EEG recordings. *Clin Neurophysiol*. 2013;124:1541-1546.
74. Stockwell RG, Mansinha L, Lowe RP. Localization of the complex spectrum: The S transform. *IEEE Trans Signal Process*. 1996;44:998-1001.
75. Singer W. Synchronization of Cortical Activity and its Putative Role in Information Processing and Learning. *Annu Rev Physiol*. 1993;55:349-374.
76. Spanedda F, Cendes F, Gotman J. Relations between EEG seizure morphology, interhemispheric spread, and mesial temporal atrophy in bitemporal epilepsy. *Epilepsia*. 1997;38:1300-1314.
77. Frauscher B, von Ellenrieder N, Ferrari-Marinho T, Avoli M, Dubeau F, Gotman J. Facilitation of epileptic activity during sleep is mediated by high amplitude slow waves. *Brain*. 2015;138:1629-1641.
78. Buzsáki G, Lopes da Silva F. High frequency oscillations in the intact brain. *Prog Neurobiol*. 2012;98:241-249.
79. Jacobs J, LeVan P, Chander R, Hall J, Dubeau F, Gotman J. Interictal high-frequency oscillations (80-500 Hz) are an indicator of seizure onset areas independent of spikes in the human epileptic brain. *Epilepsia*. 2008;49:1893-1907.
80. Roehri N, Pizzo F, Lagarde S, et al. High-frequency oscillations are not better biomarkers of epileptogenic tissues than spikes. *Ann Neurol*. 2018;83:84-97.
81. Kirsch HE, Robinson SE, Mantle M, Nagarajan S. Automated localization of magnetoencephalographic interictal spikes by adaptive spatial filtering. *Clin Neurophysiol*. 2006;117:2264-2271.
82. Quitadamo LR, Mai R, Gozzo F, Pelliccia V, Cardinale F, Seri S. Kurtosis-Based Detection of Intracranial High-Frequency Oscillations for the Identification of the Seizure Onset Zone. *Int J Neural Syst*. 2018;28:1850001.
83. Cimbalnik J, Kucewicz MT, Worrell G. Interictal high-frequency oscillations in focal human epilepsy. *Curr Opin Neurol*. 2016;29:175-181.
84. Staba RJ, Stead M, Worrell GA. Electrophysiological biomarkers of epilepsy. *Neurotherapeutics*. 2014;11:334-346.
85. Maingret N, Girardeau G, Todorova R, Goutierre M, Zugaro M. Hippocampo-cortical coupling mediates memory consolidation during sleep. *Nat Neurosci*. 2016;19:959-964.
86. Matsumoto A, Brinkmann BH, Matthew Stead S, et al. Pathological and physiological high-frequency oscillations in focal human epilepsy. *J Neurophysiol*. 2013;110:1958-1964.
87. Alkawadri R, Gaspard N, Goncharova II, et al. The spatial and signal characteristics of physiologic high frequency oscillations. *Epilepsia*. 2014;55:1986-1995.
88. Melani F, Zelmann R, Dubeau F, Gotman J. Occurrence of scalp-fast oscillations among patients with different spiking rate and their role as epileptogenicity marker. *Epilepsy Res*. 2013;106:345-356.
89. Menicucci D, Piarulli A, Allegrini P, et al. Fragments of wake-like activity frame down-states of sleep slow oscillations in humans: New vistas for studying homeostatic processes during sleep. *Int J Psychophysiol*. 2013;89:151-157.

90. Chu C, Leahy J, Pathmanathan J, Kramer M, Cash S. The maturation of cortical sleep rhythms and networks over early development. *Clin Neurophysiol*. 2014;125:1360-1370.
91. Grenier F, Timofeev I, Steriade M. Focal synchronization of ripples (80-200 Hz) in neocortex and their neuronal correlates. *J Neurophysiol*. 2001;86:1884-1898.
92. Averkin RG, Szemenyei V, Bordé S, Tamás G. Identified Cellular Correlates of Neocortical Ripple and High-Gamma Oscillations during Spindles of Natural Sleep. *Neuron*. 2016;92:916-928.
93. Nonoda Y, Miyakoshi M, Ojeda A, et al. Interictal high-frequency oscillations generated by seizure onset and eloquent areas may be differentially coupled with different slow waves. *Clin Neurophysiol*. 2016;127:2489-2499.
94. Gelinas J, Khodagholy D, Thesen T, Devinsky O, Buzsáki G. Interictal epileptiform discharges induce hippocampal– cortical coupling in temporal lobe epilepsy. *Nat Med*. 2016;22:641-648.
95. Buzsáki G. Hippocampal sharp wave-ripple: A cognitive biomarker for episodic memory and planning. *Hippocampus*. 2015;25:1073-1188.
96. Khodagholy D, Gelinas JN, Buzsáki G. Learning-enhanced coupling between ripple oscillations in association cortices and hippocampus. *Science*. 2017;358:369-372.
97. Le Van Quyen M, Bragin A, Staba R, Crépon B, Wilson CL, Engel J. Cell type-specific firing during ripple oscillations in the hippocampal formation of humans. *J Neurosci*. 2008;28:6104-6110.
98. Staresina BP, Bergmann TO, Bonnefond M, et al. Hierarchical nesting of slow oscillations, spindles and ripples in the human hippocampus during sleep. *Nat Neurosci*. 2015;18:1679-1686.
99. Axmacher N, Elger CE, Fell J. Ripples in the medial temporal lobe are relevant for human memory consolidation. *Brain*. 2008;131:1806-1817.
100. Bruder JC, Dümpelmann M, Piza DL, Mader M, Schulze - Bonhage A, Jacobs - Le Van J. Physiological Ripples Associated with Sleep Spindles Differ in Waveform Morphology from Epileptic Ripples. *Int J Neural Syst*. 2016;27:1750011.
101. Nagasawa T, Juhász C, Rothermel R, Hoechstetter K, Sood S, Asano E. Spontaneous and visually driven high-frequency oscillations in the occipital cortex: Intracranial recording in epileptic patients. *Hum Brain Mapp*. 2012;33:569-583.
102. Song I, Orosz I, Chervoneva I, et al. Bimodal coupling of ripples and slower oscillations during sleep in patients with focal epilepsy. *Epilepsia*. 2017;58:1972-1984.
103. Pail M, Řehulka P, Cimbálník J, Doležalová I, Chrastina J, Brázdil M. Frequency-independent characteristics of high-frequency oscillations in epileptic and non-epileptic regions. *Clin Neurophysiol*. 2017;128:106-114.
104. Blanco JA, Stead M, Krieger A, et al. Data mining neocortical high-frequency oscillations in epilepsy and controls. *Brain*. 2011;134:2948-2959.
105. Molle M. Hippocampal Sharp Wave-Ripples Linked to Slow Oscillations in Rat Slow-Wave Sleep. *J Neurophysiol*. 2006;96:62-70.
106. Latchoumane CF V., Ngo HV V., Born J, Shin HS. Thalamic Spindles Promote Memory Formation during Sleep through Triple Phase-Locking of Cortical, Thalamic, and Hippocampal Rhythms. *Neuron*. 2017;95:424-435.e6.

107. Rothschild G, Eban E, Frank LM. A cortical-hippocampal-cortical loop of information processing during memory consolidation. *Nat Neurosci*. 2017;20:251-259.
108. Mooij AH, Raijmann RCMA, Jansen FE, Braun KPJ, Zijlmans M. Physiological Ripples (± 100 Hz) in Spike-Free Scalp EEGs of Children With and Without Epilepsy. *Brain Topogr*. 2017;30:739-746.
109. Mizrahi EM. Avoiding the pitfalls of EEG interpretation in childhood epilepsy. *Epilepsia*. 1996;37 Suppl 1:S41-51.
110. Pinto ALR, Fernández IS, Peters JM, et al. Localization of sleep spindles, K-complexes, and vertex waves with subdural electrodes in children. *J Clin Neurophysiol*. 2014;31:367-374.
111. Kurth S, Ringli M, Geiger A, LeBourgeois M, Jenni OG, Huber R. Mapping of Cortical Activity in the First Two Decades of Life: A High-Density Sleep Electroencephalogram Study. *J Neurosci*. 2010;30:13211-13219.
112. Halász P. The K-complex as a special reactive sleep slow wave - A theoretical update. *Sleep Med Rev*. 2016;29:34-40.
113. Kane N, Acharya J, Benickzy S, et al. A revised glossary of terms most commonly used by clinical electroencephalographers and updated proposal for the report format of the EEG findings. Revision 2017. *Clin Neurophysiol Pract*. 2017;2:170-185.
114. Malinowska U, Bergey GK, Harezlak J, Jouny CC. Identification of seizure onset zone and preictal state based on characteristics of high frequency oscillations. *Clin Neurophysiol*. 2015;126:1505-1513.
115. Cimbalnik J, Brinkmann B, Kremen V, et al. Physiological and pathological high frequency oscillations in focal epilepsy. *Ann Clin Transl Neurol*. 2018;5:1062-1076.
116. Mooij AH, Frauscher B, Goemans SAM, Huiskamp GJM, Braun KPJ, Zijlmans M. Ripples in scalp EEGs of children: Co-occurrence with sleep-specific transients and occurrence across sleep stages. *Sleep*. 2018;41:1-9.
117. van Klink N, Frauscher B, Zijlmans M, Gotman J. Relationships between interictal epileptic spikes and ripples in surface EEG. *Clin Neurophysiol*. 2016;127:143-149.
118. Clemens Z, Mölle M, Eross L, Barsi P, Halász P, Born J. Temporal coupling of parahippocampal ripples, sleep spindles and slow oscillations in humans. *Brain*. 2007;130:2868-2878.
119. Staley KJ, Dudek FE. Interictal Spikes and Epileptogenesis. *Epilepsy Curr*. 2006;6:199-202.
120. Gulyas AI, Freund TT. Generation of physiological and pathological high frequency oscillations: the role of perisomatic inhibition in sharp-wave ripple and interictal spike generation. *Curr Opin Neurobiol*. 2015;31:26-32.
121. Jiruska P, Alvarado-Rojas C, Schevon CA, et al. Update on the mechanisms and roles of high-frequency oscillations in seizures and epileptic disorders. *Epilepsia*. 2017;58:1330-1339.
122. Staba R, Bragin A. High-frequency oscillations and other electrophysiological biomarkers of epilepsy: underlying mechanisms. *Biomark Med*. 2012;5:545-556.
123. Staba RJ. Normal and Pathologic High Frequency Oscillations. In: Jasper's Basic mechanisms of the epilepsies, 2nd ed. Oxford University Press, 2012
124. Stern JM. Atlas of EEG patterns, 2nd ed. Lippincot Williams & Wilkins; 2013

125. Kobayashi K, Yoshinaga H, Toda Y, Inoue T, Oka M, Ohtsuka Y. High-frequency oscillations in idiopathic partial epilepsy of childhood. *Epilepsia*. 2011;52:1812-1819.
126. Ikemoto S, Hamano S ichiro, Yokota S, Koichihara R, Hirata Y, Matsuura R. Enhancement and bilateral synchronization of ripples in atypical benign epilepsy of childhood with centrotemporal spikes. *Clin Neurophysiol*. 2018;129:1920-1925.
127. Ohuchi Y, Akiyama T, Matsuhashi M, Kobayashi K. Clinical Neurophysiology High-frequency oscillations in a spectrum of pediatric epilepsies characterized by sleep-activated spikes in scalp EEG. *Clin Neurophysiol*. 2019;130:1971-1980.
128. Shibata T, Yoshinaga H, Akiyama T, Kobayashi K. A study on spike focus dependence of high-frequency activity in idiopathic focal epilepsy in childhood. *Epilepsia open*. 2016;1:121-129.
129. van Klink NEC, van 't Klooster MA, Leijten FSS, Jacobs J, Braun KPJ, Zijlmans M. Ripples on rolandic spikes: A marker of epilepsy severity. *Epilepsia*. 2016;57:1179-1189.
130. Kramer MA, Ostrowski LM, Song DY, et al. Scalp recorded spike ripples predict seizure risk in childhood epilepsy better than spikes. *Brain*. 2019;142:1296-1309.
131. Gotman J. Oh surprise! Fast ripples on scalp EEG. *Clin Neurophys*iol. 2018; 129: 1449-1450.
132. von Ellenrieder N, Beltrachini L, Perucca P, Gotman J. Size of cortical generators of epileptic interictal events and visibility on scalp EEG. *Neuroimage*. 2014;94:47-54.
133. von Ellenrieder N, Dan J, Frauscher B, Gotman J. Sparse asynchronous cortical generators can produce measurable scalp EEG signals. *Neuroimage*. 2016;138:123-133.
134. Oostendorp TF, Delbeke J, Stegeman DF. The conductivity of the human skull: Results of in vivo and in vitro measurements. *IEEE Trans Biomed Eng*. 2000;47:1487-1492.
135. Brázdil M, Cimbálník J, Roman R, et al. Impact of cognitive stimulation on ripples within human epileptic and non-epileptic hippocampus. *BMC Neurosci*. 2015;16:47.
136. Billeke P, Ossandon T, Stockle M, et al. Brain state-dependent recruitment of high-frequency oscillations in the human hippocampus. *Cortex*. 2017;94:87-99.
137. Kucewicz MT, Cimbalnik J, Matsumoto JY, et al. High frequency oscillations are associated with cognitive processing in human recognition memory. *Brain*. 2014;137:2231-2244.
138. Stacey W. Abby…Normal? A New Gold Standard for Identifying Normal High Frequency Oscillations. *Epilepsy Curr*. 2015;15:211-212.
139. van 't Klooster MA, Zijlmans M, Leijten FSS, Ferrier CH, van Putten MJ, Huiskamp GJM. Time-frequency analysis of single pulse electrical stimulation to assist delineation of epileptogenic cortex. *Brain*. 2011;134:2855-2866.
140. van 't Klooster MA, van Klink NEC, van Blooijs D, et al. Evoked versus spontaneous high frequency oscillations in the chronic electrocorticogram in focal epilepsy. *Clin Neurophysiol*. 2017;128:858-866.
141. Hülsemann MJ, Naumann E, Rasch B. Quantification of Phase-Amplitude Coupling in Neuronal Oscillations: Comparison of Phase-Locking Value, Mean Vector Length, Modulation Index, and Generalized-Linear-Modeling-Cross-Frequency-Coupling. *Front Neurosci*. 2019;13:1-15.

142. Canolty RT, Edwards E, Dalal SS, et al. High Gamma Power Is Phase-Locked to Theta Oscillations in Human Neocortex. *Science*. 2006;313:1626-1628.
143. Jensen O, Colgin LL. Cross-frequency coupling between neuronal oscillations. *Trends Cogn Sci*. 2007;11:267-269.
144. Sirota A, Montgomery S, Fujisawa S, Isomura Y, Zugaro M, Buzsáki G. Entrainment of Neocortical Neurons and Gamma Oscillations by the Hippocampal Theta Rhythm. *Neuron*. 2008;60:683-697.
145. Bonnefond M, Kastner S, Jensen O. Communication between Brain Areas Based on Nested Oscillations. *Eneuro*. 2017;4:ENEURO.0153-16.2017.
146. Buzsáki G, Wang X-J. Mechanisms of Gamma Oscillations. *Annu Rev Neurosci*. 2012; 35:203-225.
147. Belluscio MA, Mizuseki K, Schmidt R, Kempter R, Buzsáki G. Cross-frequency phase-phase coupling between theta and gamma oscillations in the hippocampus. *J Neurosci*. 2012;32:423-435.

Summary

Electrical activity generated by the brain can be recorded with electroencephalography (EEG). The electrical activity is recorded with electrodes, also called EEG channels. EEG recordings were first limited to activity below 70 Hz, but from the ninety-nineties, technical advances in EEG equipment made it possible to record frequencies beyond 70 Hz. Such high-frequency activity (HFA)[1] can by physiological, i.e., reflecting normal brain function, or pathological, in which case it reflects abnormal brain function, such as can occur in people with epilepsy.

Epilepsy is a brain disorder characterized by the occurrence of epileptic seizures. It affects about 70 million people worldwide. Most patients can effectively be treated with anti-epileptic drugs, but about 30% does not sufficiently respond to anti-epileptic drugs. For such patients, epilepsy surgery may be a good treatment option. Before epilepsy surgery can be performed, it must become clear what needs to be preserved, and what needs to be removed.

Areas that would result in major functional deficits if they were removed, so called eloquent areas, need to be preserved. Language areas are an example of such eloquent areas. Locating language areas is the topic of **Part 1** of this thesis. In patients who are candidates for epilepsy surgery, language areas are located using electrocortical stimulation mapping (ESM). During ESM, electrical stimulation, delivered through electrodes that are placed directly on the brain surface (i.e., inside the skull, the recording technique is called electrocorticography (ECoG)) results in a temporary block of function of the stimulated part of the brain. This block of function is thought to reflect the functional deficit that would occur if that area would be surgically removed. ESM is the standard procedure for language mapping, but it has several disadvantages. It requires a lot of patient cooperation and there is a risk that the electrical stimulation causes seizures. Researchers have therefore sought alternative methods for locating eloquent areas. Inducing a type of HFA called high-gamma (60-200 Hz) by a language task seems to be a promising alternative method for locating language areas. In **chapter 2**, we induced high-gamma activity in nine patients while they listened to an audio fragment consisting of alternating speech and music phrases. High-gamma activity was recorded with the ECoG electrodes that were also used for ESM. We determined which electrodes showed induced high-gamma activity during the listening task and compared these to the language sites identified with ESM. We found that the listening task could identify language sites with 95% specificity (i.e., sites identified by our listening task were almost certainly also identified as language sites by ESM), but low sensitivity (32%, i.e., we found only one third of language sites that were identified with ESM). We concluded that our test could not replace ESM, but it may help to quickly identify sites that are involved in language, for example as a starting point for ESM.

1 For examples of the underlined terms, see Figure 1.1, page 10

Several other research groups have compared results of high-gamma language mapping and ESM. Almost twenty years since the first report of auditory task-induced high-gamma activity there have been many papers claiming promising results, but the results differ considerably between studies. It is therefore not clear if high-gamma mapping can be used as alternative for ESM. One of the main issues that prevents comparing the results of different studies is that high-gamma mapping results are obtained *per* electrode, while ESM is performed on *pairs* of electrodes. Before high-gamma mapping and ESM results can be compared, ESM results need to be translated to results per electrode. This can be done in several ways, and sensitivity and specificity differ with each approach. We mention this point in **chapter 2**, and discuss it more in depth in **chapter 3**.

The question of what needs to be removed during epilepsy surgery is relevant for **part 2**. The goal of epilepsy surgery is to remove the epileptogenic zone. The epileptogenic zone is defined as the "area that needs to be removed to obtain seizure freedom". Epileptic spikes, which are sharp transients with durations of 20-70 ms that stand out from the background EEG signal, have for many years been used as markers of the epileptogenic zone. High-frequency oscillations (HFOs), which are at least four successive high-frequency oscillations that stand out from the background signal, are increasingly recognized as additional biomarkers for the epileptogenic zone. HFOs are divided in ripples (80-250 Hz) and fast ripples (250-500 Hz). Ripples can be physiological or pathological; only pathological ripples are biomarkers for epilepsy.

Identifying spikes and HFOs in an electrographic recording can be challenging. In **chapter 4** we developed a method that identifies channels with interictal (i.e., occurring between seizures) spikes and HFOs without the need to visually mark or automatically detect these events. The method we present is based on the skew of the distribution of power values from short fragments of data recorded with intracerebral EEG (iEEG, i.e., electrodes in the brain). We used five minutes sleep data in total, and determined the skew of the power distribution for the 5-80 Hz, 80-250 Hz (ripple), and 250-500 Hz (fast ripple) bands. We then compared the skew of the distribution of epileptic and non-epileptic channels. Epileptic channels were defined as recording from the area in which seizures start (the seizure onset zone, SOZ) or the area in which spikes occur, (the irritative zone, IZ, which often partially overlaps with the SOZ). We optimized settings for this method in a selection of 120 channels from 10 patients, compared the results to 120 channels from another 10 patients, and applied the method to data of 12 individual patients. The main result of this study was that the distribution of power values was more skewed in epileptic than in non-epileptic channels in de three frequency bands and that these differences in skew were correlated with the presence of spikes, ripples, and fast ripples. When classifying epileptic and non-epileptic channels, the sensitivity (i.e., the proportion of epileptic channels that was identified as such by the skew method) was 76% and the specificity (the proportion of non-epileptic channels that were identified as non-epileptic) was 91%. These results are promising, but the skew method should be tested in other

iEEG datasets before we can estimate its clinical utility.

Recording HFOs was for many years thought to be only possible using invasive techniques such as ECoG or iEEG (described above). This limited HFO research to people who require such invasive procedures in the work-up before for brain surgery. However, it turned out to be possible to record HFOs with scalp EEG as well. The main challenges for studying HFOs in scalp EEG are that the amplitude of HFOs is low and that scalp EEG often contains artifacts, which arise, for example, when the participant moves his or her head. The first studies on ripples in scalp EEG focused on pathological ripples that co-occur with the epileptic spikes, because spikes are relatively easy to recognize and could therefore be used as a starting point in the search for scalp-EEG recorded ripples. In **part 3, chapter 5**, we went a step further: we looked for HFOs in spike-free scalp EEGs. We studied sleep EEGs, because these contain fewer artifacts, which makes searching for ripples easier. We found ripples in EEGs of 20 out of 23 children (4 with, 16 without epilepsy). Ripples had a regular shape and occurred mostly on central and midline channels. Mean frequency was 102 Hz, mean duration 70 ms, mean root mean square amplitude 0.95 μV. We concluded that the ripples occurring in normal EEGs of children without epilepsy were physiological ripples. The similarity in their characteristics and the fact that they occurred in normal EEG (i.e., without epileptic spikes) suggested that the ripples occurring in the four children with epilepsy were also physiological. This study is the first report of physiological ripples recorded with scalp EEG.

In **part 3, chapter** 6, we investigated if the occurrence of these physiological ripples was related to sleep. Sleep consists of cycles of different phases which can be recognized in EEG, partly because of the occurrence of sleep-specific EEG transients. We discovered that 74.4 % of ripples co-occurred with sleep-specific transients and that they occurred most often during the lighter sleep stages (called non-rapid eye movement (NREM) sleep stage 1 and 2) than during deep sleep (NREM 3). Ripples co-occurred most often with vertex waves.

Vertex waves are physiological sleep-specific transients, but they resemble pathological interictal epileptiform discharges (IEDs: the previously mentioned spikes of 20-70 ms and sharp waves of 70-200 ms) in several ways: they are short, sharp transients that clearly stand out from the background EEG. In **part 4, chapter 7**, we compared several characteristics of ripples that co-occurred with vertex waves or IEDs. We looked at the timing of the start of ripples relative to the start of the co-occurring event (vertex wave or IED), and duration, frequency, and amplitude of vertex wave- and IED-associated ripples. We found that physiological ripples started on average about 100 ms after the start of the vertex wave, while pathological ripples and IEDs started approximately at the same time. Vertex wave -associated ripples had a longer duration, lower frequency, and lower amplitude than ripples co-occurring with IEDs. This is the first study on characteristics of physiological and pathological ripples in scalp EEGs.

The title of this thesis is 'High-frequency EEG activity from different perspectives'. The different perspectives, which are described in more detail in

the general introduction **(chapter 1),** all appear in the above summary: clinical utility **(parts 1 and 2)** versus basic neurophysiology **(parts 3 and 4)**; different recording techniques: invasive, i.e., inside the skull and on the brain **(part 1),** or in the brain **(part 2)**, or non-invasive, i.e., on the scalp (**parts 3 and 4**); and recording high-frequency activity during wakefulness **(part 1)** or sleep **(parts 2, 3, and 4)**. The general discussion **(chapter 8)** explores additional aspects of these perspectives and provides suggestions for future research. For example, the next step in physiological ripple research could be to investigate if physiological ripples can be found in scalp EEGs of adults. Another important question is about the neurophysiological relevance of these ripples: are they involved in memory consolidation?

Samenvatting

Elektro-encefalografie (EEG) registreert elektrische activiteit die gegenereerd wordt door de hersenen. De elektrische activiteit wordt gemeten met elektroden, ook wel EEG kanalen genoemd. EEG metingen waren voorheen beperkt tot activiteit onder de 70 Hz (d.w.z.: 70 oscillaties per seconde), maar vanaf de jaren negentig is het door technische vooruitgang in EEG apparatuur mogelijk geworden om ook activiteit met frequenties boven de 70 Hz te registreren. Deze activiteit wordt hoogfrequente activiteit (HFA)[1] genoemd. HFA kan fysiologisch zijn, d.w.z. een afspiegeling van normale hersenactiviteit, of pathologisch, dan is het een afspiegeling van abnormaal functioneren van de hersenen, zoals het geval kan zijn bij mensen met epilepsie.

Epilepsie is een hersenaandoening die gekenmerkt wordt door het optreden van epileptische aanvallen. Ongeveer 70 miljoen mensen wereldwijd hebben epilepsie. De meeste epilepsiepatiënten kunnen afdoende behandeld worden met medicatie, maar ongeveer 30% van de epilepsiepatiënten reageert hier niet voldoende op. Voor dit soort patiënten kan epilepsiechirurgie een goede optie zijn. Voor epilepsiechirurgie uitgevoerd kan worden, moet duidelijk worden wat onaangetast moet blijven en wat chirurgisch verwijderd moet worden.

Gebieden die bij verwijdering zouden resulteren in ernstige functionele beperkingen moeten onaangetast blijven. Deze gebieden worden eloquente gebieden genoemd. Taalgebieden zijn hier een voorbeeld van. Bepalen waar precies in de hersenen zich de taalgebieden bevinden, is het onderwerp van het **deel 1** van dit proefschrift. Dit wordt in patiënten die waarschijnlijk een epilepsieoperatie zullen ondergaan gedaan door middel van een methode die in het Engels electrocortical stimulation mapping (ESM) heet. Tijdens ESM wordt de functie van kleine stukjes van de hersenschors tijdelijk geblokkeerd door elektrische stroompjes die het hersenweefsel bereiken via elektroden die direct op de hersenschors liggen (d.w.z.: binnen de schedel, de meetmethode heet elektrocorticografie (ECoG)). Deze tijdelijke functionele blokkade wordt gezien als een afspiegeling van de functionele schade die zou optreden als het geblokkeerde stukje verwijderd zou worden. ESM is de standaardprocedure voor het lokaliseren van taalgebieden, maar het heeft een aantal nadelen: de methode vraagt veel van de patiënt en het risico bestaat dat door de elektrische stimulatie epileptische aanvallen uitgelokt worden. Er wordt daarom gezocht naar andere methoden om eloquente gebieden te lokaliseren. Tijdens het uitvoeren van een taaltest wordt een type hoogfrequente activiteit opgewekt die hoogfrequente gamma activiteit (60-200 Hz) genoemd wordt. Het registreren van zulke opgewekte hoogfrequente gamma activiteit lijkt een veelbelovende alternatieve methode voor het lokaliseren van taalgebieden. In **hoofdstuk 2** hebben wij hoogfrequente gamma activiteit opgewekt door negen patiënten naar een audiofragment te laten luisteren waarin taal- en muziekfragmenten elkaar afwisselden. De hoogfrequente gamma

1 Voor voorbeelden van de onderstreepte termen, zie Figuur 1.1 op pagina 10

activiteit werd geregistreerd met dezelfde ECoG elektroden die gebruikt waren om ESM uit te voeren. We vergeleken de gebieden waarin door de luistertaak hoogfrequente gamma activiteit was opgewekt met door ESM vastgestelde locaties van taalgebieden. De door de luistertaak opgewekte hoogfrequente gamma activiteit bleek taalgebieden met 95% specificiteit te lokaliseren (d.w.z.: gebiedjes die door de luistertaak aangewezen werden, waren vrijwel zeker ook als taalgebied aangewezen met ESM), maar de sensitiviteit was slechts 32% (d.w.z.: met onze luistertest werd slechts een derde van de door ESM aangewezen taalgebieden gevonden). Onze conclusie was dat de luistertest ESM niet kon vervangen, maar dat deze test kan helpen om snel gebieden te vinden die betrokken zijn bij taal. Deze plekken zouden dan als startpunt voor ESM gebruikt kunnen worden.

Meerdere andere onderzoeksgroepen hebben resultaten van taallokalisatie met behulp van hoogfrequente gamma vergeleken met ESM. Bijna twintig jaar sinds het eerste artikel over het induceren van hoogfrequente gamma activiteit door een luistertaak zijn er veel artikelen die rapporteren dat de resultaten veelbelovend zijn. De uitkomsten verschillen echter sterk per studie, waardoor het niet duidelijk is of het induceren van hoogfrequente gamma activiteit gebruikt kan worden als alternatief voor ESM. Dat resultaten van verschillende studies moeilijk te vergelijken zijn, komt mede doordat hoogfrequente gamma resultaten verkregen worden *per* elektrode, terwijl ESM gedaan wordt in elektrode *paren.* Voordat hoogfrequente gamma resultaten vergeleken kunnen worden met ESM resultaten, moeten de ESM resultaten eerst 'vertaald' worden naar resultaten per elektrode. Dit vertalen kan op verschillende manier gebeuren, en de sensitiviteit en specificiteit veranderen per vertaalmethode. We noemen dit punt in **hoofdstuk 2**, en gaan hier in **hoofdstuk 3** dieper op in.

De vraag wat er verwijderd moet worden tijdens epilepsiechirurgie is relevant voor **deel 2**. Het doel in epilepsiechirurgie is het verwijderen van de epileptogene zone. De epileptogene zone is "het gebied dat verwijderd moet worden om aanvalsvrij te worden". Epileptische pieken, korte (20-70 ms) scherpe EEG fenomenen die opvallen ten opzichte van het achtergrond EEG signaal, zijn jarenlang de belangrijkste biomarker van de epileptogene zone geweest. Hoogfrequente oscillaties (HFOs), dat zijn minstens vier opeenvolgende hoogfrequente golfjes die duidelijk opvallen t.o.v. het achtergrondsignaal, worden steeds meer gezien als biomarkers die van toegevoegde waarde zijn bij het lokaliseren van de epileptogene zone. HFOs worden verdeeld in 'ripples' (80-250 Hz) en 'fast ripples' (250-500 Hz). Ripples kunnen fysiologisch of pathologisch zijn; alleen pathologische ripples zijn biomarkers voor epilepsie.

Het kan lastig zijn om pieken en HFOs in een elektrografische opname te herkennen. In **hoofdstuk 4** hebben we daarom een methode ontwikkeld die kanalen met pieken en HFOs kan selecteren zonder dat deze EEG fenomenen individueel gemarkeerd of gedetecteerd hoeven te worden. De methode die wij voorstellen is gebaseerd op de scheefheid van de verdeling van de power van stukjes signaal gemeten met intracerebraal EEG (iEEG, d.w.z. elektroden in de hersenen). We gebruikten in totaal 5 minuten iEEG signaal, opgenomen tijdens slaap. We

bekeken de scheefheid van de power verdeling voor drie frequentiebanden: de 5-80 Hz band, 80-250 Hz (ripple) band, en 250-500 Hz (fast ripple) band. We vergeleken de scheefheid van de verdelingen in epileptische kanalen en niet-epileptische kanalen. Kanalen werden geclassificeerd als epileptisch als ze registreerden in het gebied waar epileptisch aanvallen ontstonden (de 'seizure onset zone', SOZ), en/of het gebied waarin epileptische pieken voorkomen (de 'irritative zone', IZ). We optimaliseerden de instellingen voor deze methode in een selectie van kanalen van 10 patiënten (120 kanalen in totaal), vergeleken de verkregen uitkomsten met 120 kanalen van 10 andere patiënten, en gebruikten de methode vervolgens om bij 12 afzonderlijke patiënten epileptische en niet epileptische kanalen te onderscheiden. De belangrijkste uitkomst van de studie was dat de verdeling van de power uitkomsten schever was in epileptische dan in niet epileptische kanalen in de drie frequentie banden, en dat deze bevinding gecorreleerd was aan het voorkomen van pieken, ripples en fast ripples in de epileptisch kanalen. De methode kon 76% van de epileptische kanalen als zodanig herkennen (sensitiviteit = 76%), en 91% van de niet-epileptische kanalen werd correct als niet-epileptisch geclassificeerd werd (specificiteit = 91%). Deze resultaten zijn veelbelovend, maar de methode moet getest worden in iEEG data van meer patiënten voor we kunnen inschatten hoe nuttig de methode voor de klinische praktijk kan worden.

Het registreren van HFOs leek jarenlang alleen mogelijk met invasieve technieken zoals ECoG en iEEG (hierboven beschreven). Hierdoor was onderzoek naar HFOs beperkt tot mensen die waarschijnlijk een hersenoperatie zouden ondergaan en in voorbereiding daarop zo'n invasieve registratie ondergingen. HFOs blijken echter ook geregistreerd te kunnen worden met oppervlakte EEG, waarbij de elektroden op de hoofdhuid geplaatst worden. Het lastige bij het bestuderen van HFOs in oppervlakte EEG is dat de amplitudes van HFOs laag zijn en dat oppervlakte EEG vaak artefacten (storingen) bevat, die bijvoorbeeld ontstaan doordat het hoofd bewogen wordt. De eerste studies die ripples in oppervlakte EEG zochten, keken daarom alleen naar ripples die tegelijk met epileptische pieken voorkomen. Pieken zijn relatief eenvoudig te herkennen en kunnen daardoor als startpunt dienen voor de zoektocht naar ripples geregistreerd met oppervlakte EEG. In **deel 3, hoofdstuk 5**, gingen wij een stap verder: we gingen op zoek naar HFOs in normale EEGs, waarin dus geen pieken voorkwamen. Om het zoeken naar ripples makkelijker te maken, onderzochten we slaap EEGs, omdat daar minder artefacten in voorkomen. We vonden ripples in 20 van de 23 onderzochte EEGs, van 4 kinderen met en 16 kinderen zonder epilepsie. De ripples hadden een regelmatige vorm en werden het meest midden op het hoofd gemeten. Ze hadden een gemiddelde frequentie van 102 Hz, een gemiddelde duur van 70 ms, en een gemiddelde root mean square (RMS, de wortel van het gemiddelde van het kwadraat) amplitude van 0.95 μV. We concludeerden dat de ripples die voorkwamen in normale EEGs van kinderen zonder epilepsie fysiologische ripples moesten zijn. Ripples die voorkwamen in de vier EEGs van kinderen met epilepsie waren waarschijnlijk ook fysiologisch, omdat ze voorkwamen in normale EEGs en omdat ze dezelfde eigenschappen

hadden als ripples die voorkwamen in de EEGs van gezonde kinderen. Dit is de eerste beschrijving van fysiologische ripples geregistreerd met oppervlakte EEG.

In **deel 3, hoofdstuk** 6, hebben wij onderzocht of het voorkomen van deze fysiologische ripples samenhangt met slaap. Slaap bestaat uit cycli van verschillende slaapfases die herkend kunnen worden in het EEG, deels vanwege het voorkomen van specifieke slaap-EEG-fenomenen. We ontdekten dat 74,4% van deze ripples voorkwamen tijdens een specifiek slaap-EEG-fenomeen en dat ze vaker optraden tijdens de lichtere fases van slaap (de eerste twee fases van slaap zonder snelle oogbewegingen, NREM 1 en 2 geheten) dan tijdens diepe slaap (NREM 3). Ripples kwamen het vaakst samen voor met vertex golven.

Vertex golven zijn fysiologische slaap-EEG-fenomenen, maar ze lijken op Interictale (d.w.z.: optredend tussen epileptische aanvallen) Epileptiforme ontladingen ('Discharges' in het Engels, daarom afgekort tot IEDs). Naast de eerdergenoemde epileptische pieken (met een duur van 20-70 ms) worden ook scherpe golven (met een wat langere duur, 70-200 ms) IEDs genoemd. Zowel vertex golven als IEDs zijn scherpe, korte EEG fenomenen die opvallen ten opzichte van het achtergrondsignaal. In **deel 4, hoofdstuk 7**, hebben we verschillende kenmerken vergeleken van ripples die samen met vertex golven of IEDs voorkwamen. We keken naar de start van de ripple ten opzichte van de start van de vertex golf of IED, en naar duur, frequentie en amplitude van de ripples die voorkwamen met beide type scherpe EEG fenomenen. We vonden dat fysiologische ripples ongeveer 100 ms na de start van de vertex golven begonnen, terwijl pathologische ripples en IEDs ongeveer gelijk begonnen. Ripples die met vertex golven voorkwamen hadden een langere duur, lagere frequentie en lagere amplitude dan ripples die met IEDs voorkwamen. Deze studie is de eerste waarin kenmerken van fysiologische en pathologische ripples die geregistreerd waren met oppervlakte EEG vergeleken worden.

De titel van dit proefschrift is 'Hoogfrequente EEG oscillaties vanuit verschillende perspectieven'. De verschillende perspectieven, die meer in detail worden toegelicht in de algemene introductie in **hoofdstuk 1**, komen allemaal voor in bovenstaande samenvatting: klinisch nut **(deel 1 en 2)** versus basale neurofysiologie **(deel 3 en 4)**; verschillende manieren van registreren: invasief (binnen de schedel, op **(deel 1)** of in **(deel 2)** de hersenen), of niet-invasief (oppervlakte EEG, **deel 3 en 4**); en het registreren van hoogfrequente activiteit tijdens waak **(deel 1)** of slaap **(deel 2, 3 en 4)**. In de algemene discussie **(hoofdstuk 8)** worden extra aspecten van deze perspectieven besproken. Ook bevat de algemene discussie suggesties voor vervolgonderzoek. Zo zou een volgende stap in onderzoek naar fysiologische ripples kunnen zijn om te onderzoeken of deze ripples ook in het oppervlakte EEG van volwassenen gevonden kunnen worden. Een andere belangrijke vraag gaat over de neurofysiologische relevantie van deze ripples: zijn ze betrokken bij het consolideren van herinneringen?

List of publications presented in this thesis

Anne H. Mooij, Geertjan J.M. Huiskamp, Peter H. Gosselaar, Cyrille H. Ferrier. Electrocorticographic language mapping with a listening task consisting of alternating speech and music phrases. Clinical Neurophysiology 2016; 127:1113-1119. doi: 10.1016/j.clinph.2015.08.005

A.H. Mooij, R.C.M.A. Raijmann, F.E. Jansen, K.P.J. Braun, M. Zijlmans. Physiological ripples (± 100 Hz) in spike-free scalp EEGs of children with and without epilepsy; Brain Topography, 2017; 30:739-746. doi: 10.1007/s10548-017-0590-y

Anne H. Mooij, Laura C.M. Sterkman, Maeike Zijlmans, Geertjan J.M. Huiskamp. Electrocorticographic high-gamma language mapping: Mind the pitfalls of comparison with electrocortical stimulation. Epilepsy & Behavior 2018; 82:196-199. doi: 10.1016/j.yebeh.2018.02.001

Anne H. Mooij, Birgit Frauscher, Sophie A.M. Goemans, Geertjan J.M. Huiskamp, Kees P.J. Braun, Maeike Zijlmans. Ripples in scalp EEGs of children: co-occurrence with sleep-specific transients and occurrence across sleep stages SLEEP 2018; 41:1-9. doi: 10.1093/sleep/zsy169

Anne H. Mooij, Birgit Frauscher, Jean Gotman, Geertjan J.M. Huiskamp. A skew-based method for identifying iEEG channels with epileptic activity without detecting spikes, ripples, or fast ripples. Clinical Neurophysiology 2020; 131:183-192. doi: 10.1016/j.clinph.2019.10.025

Anne H. Mooij, Geertjan J.M. Huiskamp, Emmeke Aarts, Cyrille H. Ferrier, Kees P.J. Braun, Maeike Zijlmans. Scalp-EEG recorded physiological and pathological ripples. In preparation

Dankwoord

Ik wil graag de beoordelingscommissie bedanken voor hun bereidwilligheid mijn proefschrift te beoordelen. I would like to thank my supervisors, Prof. Kees Braun, Prof. Jean Gotman, Dr. Maeike Zijlmans, and Dr. Geertjan Huiskamp for all that they have done to enable me to start and to complete this PhD. I have learned a lot from each of you. I am grateful to Birgit Frauscher, Cyrille Ferrier, and Emmeke Aarts for their contributions to the work presented in this thesis. Ik wil graag mevr. Henriëtte Vluggen-Hamaekers van het Prins Bernhard Cultuurfonds en mevr. Isabelle Scholten-de Vries van het Hendrik Muller's Vaderlandsch Fonds bedanken voor hun steun en vertrouwen bij de start van dit promotietraject. Ook dank ik het Epilepsiefonds, dat het grootste deel van mijn promotietraject en het drukken van dit proefschrift gefinancierd heeft. De patiënten van wie ik het EEG onderzocht ben ik dankbaar dat ze mijn onderzoek mogelijk gemaakt hebben.

De samenwerking met Laura, Renee en Sophie tijdens hun stages en ook nog lang daarna behoorde tot de leukste ervaringen tijdens mijn promotietraject. Ook heb ik genoten van de gezellige momenten met mijn collega's. Vrienden, huisgenoten en familie wil ik bedanken voor alle hulp en steun die ik de afgelopen jaren van hen gekregen heb.

Curriculum vitae

Anne Mooij was born on November 11, 1983, in Middelburg, The Netherlands. She studied medicine in Utrecht. After graduating, she worked for two years as neurology resident in Groningen. She then switched to research, and after a research internship on music and the brain in Toronto, Canada, started working on the language and music project that forms the second chapter of this thesis. She then went back to Canada to work in the lab of Prof. Jean Gotman at the Montréal Neurological Institute as part of her PhD on high-frequency EEG activity. After returning from Montreal, she continued her PhD research in Utrecht, the Netherlands, supervised by Prof. Kees Braun, Dr. Maeike Zijlmans, and Dr. Geertjan Huiskamp.

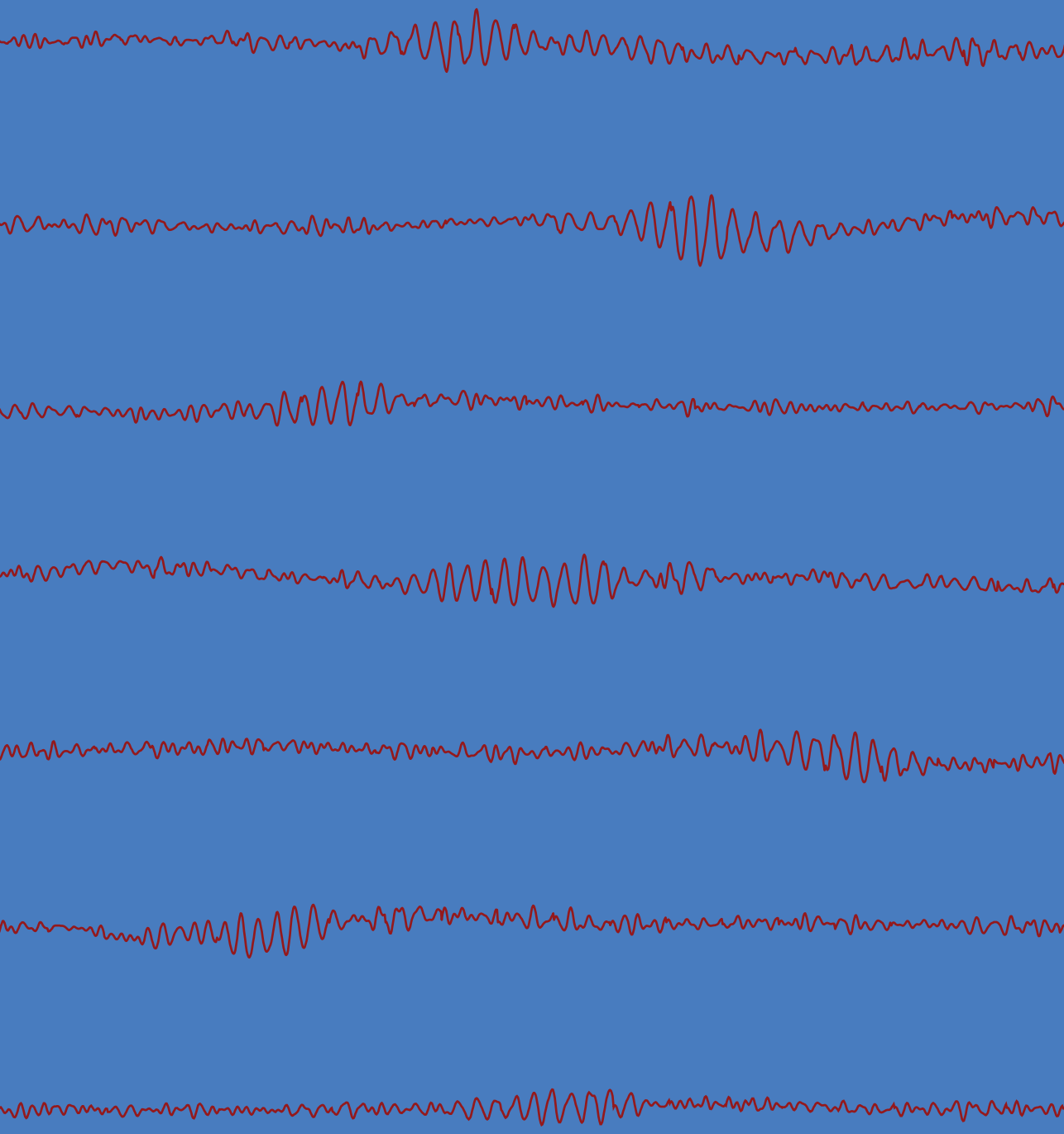

UMC Utrecht

Universiteit Utrecht

ISBN 978-90-393-7236-4